UNIVERSIDAD NACIONAL DE COLOMBIA

Viscosity reduction of heavy crude oil through the addition of nanofluids on the non-thermal process.

Esteban Alberto Taborda Acevedo

Universidad Nacional de Colombia
Facultad de Minas, Escuela de Procesos y Energía
Medellín, Colombia
2017

Viscosity reduction of heavy crude oil through the addition of nanofluids on the non-thermal process.

Esteban Alberto Taborda Acevedo

Tesis o trabajo de investigación presentada(o) como requisito parcial para optar al título de:
Doctor en Ingeniería – Sistemas Energéticos

Director:
Ph.D., M.Sc., Ingeniero Químico, Farid Bernardo Cortés Correa

Línea de Investigación:
Hidrocarburos
Grupo de Investigación:
Grupo de Investigación en Fenómenos de Superficie "Michael Polanyi"

Universidad Nacional de Colombia
Facultad de Minas, Escuela de Procesos y Energía
Medellín, Colombia
2017

DEDICATORIA

A mi hija ***Valentina***, la persona más importante de mi vida y mi motor para seguir adelante.

A mis padres ***Carlos y Amparo***, por creer en mí brindarme su apoyo en los momentos más difíciles.

A mi hermana ***Diana*** por su confianza y ayuda en toda mi vida.

A ***Mónica*** por brindarme tanto cariño durante todo este tiempo

Acknowledgments

I would like to express my sincere thanks to my Director, Professor Farid B. Cortés Correa, from which I have learned all this time, his knowledge, patience and wise leadership taught me to grow professionally and personally. I am convinced that without him it would have been impossible to carry out this work.

My sincere acknowledge to the members of the research group in surface phenomena "Michael Polanyi," and the petrophysics lab for their support and valuable advice in the development of the experimental work.

Special thanks to Dr. Vladimir Alvarado and his research group for receiving me with hospitality at the University of Wyoming. Their vast experience and invaluable help were key to the development of this research.

I also want to acknowledge Dr. Sócrates Acevedo from Universidad Central de Venezuela for sharing their expertise and their valuable contributions.

Special acknowledge to COLCIENCIAS and ECOPETROL for the support provided in the agreement 264 of 2013. I also acknowledge Universidad Nacional de Colombia for logistical and financial support.

Resumen

El crecimiento de la población mundial, la constante industrialización de los países desarrollados y un aumento considerable en el consumo energético han promovido una demanda creciente de petróleo en el mundo. Sin embargo, el declive de las reservas de crudo liviano hace atractivo la explotación de petróleo pesado y extra-pesado para suplir los requerimientos energéticos debido a la capacidad de petróleo recuperable (IEA). El crudo pesado y extrapesado (bitumen) se define como aquel con gravedad API igual o inferior a 20 e igual o inferior a 10 (más denso que el agua), respectivamente. A pesar de la importancia y los altos volúmenes de las reservas de crudo pesado, el desarrollo, la producción y el refinamiento se dificulta debido a sus propiedades físico-químicas, principalmente su alta densidad y viscosidad, baja gravedad API, y alto contenido de hidrocarburos pesados. Los crudos pesados (HO) y extrapesados (EHO) por lo general tienen un gran porcentaje de componentes pesados como resinas y asfaltenos los cuales reducen la gravedad API° y aumentan drásticamente la viscosidad del crudo. Para mejorar el transporte del crudo pesado en superficie las técnicas convencionales usadas son: el calentamiento de tuberías y estaciones de bombeo, la dilución con solventes menos viscosos, emulsificación, y reducción de fricción (flujo anular). Sin embargo estas técnicas son costosas debido principalmente a los altos consumos de materia prima, al calentamiento de grandes distancias de tubería y a la necesidad de procesos adicionales para el trasporte del crudo. Por tal motivo esta tesis se presenta con el objetivo de analizar una nueva tecnología que permita mejorar el trasporte de crudos pesados a condiciones de yacimiento y de superficie mediante la aplicación de nanofluidos en procesos no térmicos. Se espera que sea una técnica novedosa y competitiva en términos económicos, ya que el nanofluido se obtiene mediante rutas de síntesis poco complejas y su cantidad de uso en comparación con los solventes convencionales es mucho menor.

Palabras clave: Nanopartículas, Crudos Pesados, Asfaltenos, Adsorción, Viscosidad.

Abstract

The growth of the world population, the constant industrialization of developed countries and a considerable increase in energy consumption have promoted an increasing demand for oil in the world. However, the decline in light crude reserves makes it attractive to exploit heavy and extra-heavy oil to meet energy requirements due to recoverable oil capacity (IEA). Heavy and extra-heavy crude (bitumen) is defined as one with API gravity equal to or less than 20 and equal to or less than 10 (denser than water), respectively. Despite the importance and high volumes of heavy crude reserves, development, production and refinement is difficult due to its physico-chemical properties, mainly its high density and viscosity, low API gravity, and high hydrocarbon content Heavy crude (HO) and extra-heavy (EHO) crude oils usually have a large percentage of heavy components such as resins and asphaltenes which reduce API gravity and drastically increase crude viscosity. In order to improve the transportation of heavy crude oil to the surface, the conventional techniques used are heating piping and pumping stations, dilution with less viscous solvents, emulsification, and reduction of friction (annular flow). However, these techniques are costly due mainly to the high consumption of raw material, the heating of large pipe distances and the need for additional processes for the transport of crude oil. For this reason, this thesis is presented with the objective of analyzing a new technology that allows improving the transportation of heavy crude oil to reservoir and surface conditions through the application of nanofluids in non-thermal processes. It is expected to be a novel technique and competitive in economic terms since nanofluid is obtained by means of little complex synthesis routes and its quantity of use in comparison with the conventional solvents is much smaller.

Keywords: Nanoparticles, Heavy Oil, Asphaltenes, Adsorption, Viscosity.

Content

List of figures

Pág.

List of tables

Introduction

Currently, fossil fuels supply about 85% of the world's energy needs; with oil being responsible for over 40% of global energy consumption [1]. World oil demand has increased in the first years of the 21st century compared to the last years of the 20th century [2]. On this basis, it can be said that the world's oil needs will grow and remain as the main source of global energy supply [1, 2]. The growth of the world population, the constant industrialization of developed countries and a considerable increase in energy consumption have promoted an increasing demand for oil in the world. However, the decline in light crude reserves makes it attractive to exploit heavy and extra-heavy oil to meet energy requirements due to recoverable oil capacity.

Heavy and extra-heavy crudes are defined as crude with low API gravities below 20° and 10° respectively, and very high viscosities (> 1000 cP at 25°C) [3-6]. Heavy crudes have complex components of high molecular weight and highly polar, called asphaltenes. Asphaltenes are usually defined as the heaviest, most aromatic and active surface area of crude oil [7-9], being insoluble in light paraffin such as n-pentane, n-hexane, and n-heptane, but soluble in light aromatic compounds such as benzene, Toluene or pyridine [7-9]. Although the structure of asphaltenes is complex, a general description is that they have a nucleus composed of one or more poly-crosslinked aromatic hydrocarbons (PAH) attached to aliphatic chains, classified according to their configuration as island type, Continental archipelago, or rosary structures[10-12]. Asphaltenes have heteroatoms such as nitrogen, sulfur and oxygen, and metals such as vanadium, iron, and nickel, indicating the presence of functional groups such as carboxyl, ketones, aldehydes, benzothiophenes, Dibenzothiophenes, naphthenobenzothiophenes, alkyl sulphides, alkyl aryl sulphides and aryl sulphides which can be found [11, 13, 14]. High amounts of sulfur forming strong bonds CS and C=S which drastically increase the viscosity of the crude [15, 16]. In addition, because of the amphiphilic behavior of asphaltenes, they tend to self-associate and form large aggregates that also increase the viscosity of heavy crude.

The injection of naphtha or CO_2 for viscosity reduction are proven techniques to improve the production of heavy and extra-heavy oil both at the site and at the surface [17-19]. However, these

techniques could lead to serious problems due to the possibility of modifying the behavior from oil phases to reservoir conditions, leading to precipitation of asphaltenes and deposition in porous media through the production system [17, 18]. In addition, if precipitation and deposition occur in the rock, it could be reduced so much Porosity and permeability, negatively affecting the wettability of the system.

On the surface, the most commonly used method to reduce the viscosity of heavy crude is the use of thinner diluents such as light crude oil, naphtha, kerosene, among others [17]. The method consists of obtaining a mixture of lower viscosity by adding considerable amounts of diluents to achieve significant improvements in crude oil transportation. However, the high consumption of these solvents, coupled with the need to have pumping equipment, increases transportation costs and creates an environmental risk due to the production of polluting gasses, making it a not so attractive technique [17]. The second with the largest order of importance is the method of heating the crude oil [20]. The principle is to keep oil at wellhead temperature. In general, additional heating is required due to heat losses. Crude oil is heated in the pumping stations through direct heaters [21]. It is common to bury the pipes in order to insulate them thermally. These methods are widely used, but they are economically very costly, but when large distances are to be transported [18, 20, 21].

For this reason, the phenomenon of viscosity reduction to improve the mobility of heavy crude oil has been extensively studied [22-33]. Two lines of work are highlighted to improve the mobility of heavy crude: in thermal processes and in non-thermal processes. In thermal processes, the work of: Clark et al. [34, 35], Fan et al. [36] Song et al. [37], claim that the reduction of the viscosity of heavy crude is mainly due to chemical reactions, specifically by hydrolysis reactions [34, 35], acuotermolysis [36, 37] and visbreaking [37-39], there the hydrolysis of aliphatic bonds of sulfur is the main characteristic of these reactions and its main effect is the reduction of asphaltenes and resins, reducing the molecular weight of the asphaltene and the sulfur content of the crude and thus generating a reduction of viscosity [16]. Yufeng et al. [40] investigated the catalytic cracking of asphaltenes and resins by converting them into lighter molecules during acuotermolysis using nickel and iron catalysts. The best catalyst evaluated was iron naphthenate increasing the asphaltene conversion by 15%

Different authors [38, 39, 41, 42] obtained a viscosity reduction in the acuotermolysis process using metallic and bimetallic catalysts with titanium, tungsten, and molybdenum. In a more recent study, Hashemi et al. [42] used ultra-dispersive Ni-W-Mo nanocatalysts prepared in-situ within a vacuum gas oil matrix for the enhancement of Athabasca bitumen at temperature and pressure conditions.

The authors found that the nanoparticles were suitable for improving bitumen by increasing the API gravity by 17% and the reduction of the viscosity of the oil by hydrogenation reactions at 340 °C was 42%. In addition, the microcarbon residue, sulfur, and nitrogen content were reduced. This series of studies highlight the high performance of the nanoparticles as catalysts, however, each thermal process demands high amounts of energy and the use of agents necessary to carry out the reactions typical of each process.

On the other hand, there are non-thermal processes of viscosity reduction for which the following works stand out: Castro et al. [43] and the company GeoSstratos report the use of different viscosity reducing agents. Castro et al. [43] investigate the rheological behavior of solutions with terpolymers at different shear rates and temperatures. They synthesize terpolymers with different contents of styrene (S), n-butylacrylate (BA), and vinyl acetate (VA) by semicontinuous emulsion polymerization. The results confirm that the viscosity of the crude is reduced when the terpolymers have a high percentage in S and small amounts of BA or VA. The molecular weight of the terpolymers plays an important role in their performance as viscosity reducers. GeoEstratos SA offer viscosity bioreductores based on vegetable oils, reaching reductions in viscosity up to 60% at injection conditions of 3% applied to a reservoir at a temperature of 50 °C and a depth of 1280m, in emulsions with water content Of 2%

Water-oil emulsions are also used to reduce the viscosity of the heavy crude oil and facilitate transportation. Emulsions require three conditions to form: the presence of water and oil as immiscible phases, agitation and a stabilizing agent (emulsifier). Naturally, the crude-water mixtures form water-in-oil (W/O) emulsions. This is because heavy oils have high asphaltenes contents, which act as natural emulsifiers and because of their solubility in the oil form the W/O emulsion. Other components of the oil also affect the stability of emulsions, such as resins, paraffin and naphthenic acids [44, 45]. Resins help the solubilization of asphaltenes in the crude oil, which keeps them away from the interface and therefore decreases the Stability of the emulsion [45]. The paraffin, on the other hand, is co-adsorbed at the interface and improve the stability of the emulsion. Naphthenic acids are probably responsible for the dependence of emulsion stability on the pH of water [45]. In addition, the presence of wettable particles in the oil also favors the stability of emulsions [44, 45]. Different studies study the rheological behavior of emulsions W/O. It is stated that the viscosity of the emulsion depends on factors such as Volumetric fraction of the dispersed phase, viscosity of the continuous phase, shear rate (if non-Newtonian), temperature, average and drop size distribution, viscosity of the dispersed phase, nature and concentration of the emulsifying agent and the presence of solids [44, 46]. The majority of authors obtain a higher emulsion viscosity than crude oil for emulsions W/O [47-

[49]. Farah et al. [44], studied the effective viscosity of W/O emulsions using 6 different crude oils (API 19-41 °) at shear rates between 10 and 80 s^{-1}, temperatures between 8 and 50 °C and volumetric fractions of water between 0 and 40%. They obtain viscosity increases with increases in water fraction, decrease in temperature and cutting speed. In addition, they observe that the emulsions initially show a non-Newtonian behavior, but when increasing the temperature, they behave as Newtonian fluids. By increasing the volumetric fraction of water in the emulsion, the temperature increases above which the Newtonian behavior occurs. Johnsen and Ronningsen et al. [50], study the viscosity of pressurized W/O emulsions (14.5 - 1450 psi) for 7 different crudes from the North Sea (API between 19 ° and 38 °), at temperatures between 50 and 70 °C and water contents between 0 and 90%. Viscosity increases of up to 82% are obtained for an amount of water of 88%.

At the industrial level, the application of emulsions to transport the heavy crude through the Orimulsión® developed by the Venezuelan state oil company PDVSA in the eighties, this one consists of an emulsion of crude oil in water. The technology was developed with the aim of facilitating the transportation of heavy crude because the dilution with conventional diesel oil was no longer economically attractive [42, 45, 49, 51].

Another method of reducing pressure drop in pipes caused by friction in order to transport bitumen and heavy crude is the annular flow. The first report of this technique is from Isaacs and Speed [26] where it specifies the possibility of the channeling of viscous fluids through the lubrication of the walls of the tube with water. The main idea of this technique is to surround the core of the heavy crude matrix and to flow through the pipeline with a film layer of water or solvent near the wall of the pipeline, which acts as a lubricant. In this sense, the water or solvent behaves like the ring, while the heavy crude is the core in the flow through the pipe. The required water or solvent is in the range of 10-30% [32, 52]. This implies that the pressure drop across the pipe depends weakly on the viscosity of the heavy oil, but strongly on that of the water. In addition, Bensakhria et al. [23], found that with heavy oil as the center of the pipe and water near the surface of the pipe wall, the reduction in pressure drop was greater than 90% compared to crude Without lubrication. However, some of the limitations include the formation of waves that are created at the interface of the water, and the oil hinders the flow [23, 26]. In addition, when the density difference between oil and water is large, a buoyancy force will produce a radial movement of the oil core. In addition, the stability of the flow system is still under investigation [24, 26].

Many papers have been presented highlighting the different techniques available to improve the mobility of heavy crude oil with its advantages and limitations. In search of new methods to optimize

the flow process of heavy crude, nanotechnology emerges as an alternative technique to reduce the viscosity of heavy crude. An extensive search converges on scarce jobs involving nanotechnology for this purpose.

The usual techniques for the transport of heavy and extra-heavy oil are expensive and dangerous, and nanotechnology appears as a complementary technique capable of competing economically and technically because it exhibits a high potential, improving the mobility of heavy crude due to Reduction of viscosity through the interaction of minute particles with asphaltenes present in the crude. When the particles are added to nano size, they have high adsorptive capacity since their A/V ratio is very high. In addition, its nanometric size does not represent a problem to plug the pore grooves of conventional crude oil deposits, its surface has high affinity for the asphaltenes present in the crude, much larger than the affinity between own asphaltene aggregates, it is expected that when this occurs, the molecular weight of these aggregates also decreases and thus a considerable reduction of viscosity is obtained.

Hence, the main objective of this study is synthesized nanofluids of different chemical nature that allow reducing the viscosity of the heavy crude by reducing the size of the asphaltene aggregate.

For this reason, this document is divided into five main chapters that include: 1) Synthesis and characterizations of nanoparticles/nanofluids and its interactions with asphaltenes of heavy crude oil, 2) Viscosity reduction of heavy crude oil through the addition of nanoparticles/nanofluids by steady state rheology measurements, 3) Changes in internal structure of heavy oil with dynamic rheology measurements, 4) Transport conditions optimization with the addition of nanofluids, and 5) Increase of mobility at reservoir conditions on a porous media through coreflooding tests.

References

1. Franco, C.; Flórez, A.; Ochoa, M., Análisis de la cadena de suministros de biocombustibles en Colombia. *Revista de Dinámica de Sistemas* **2008,** 4, (2), 109-133.
2. Martinius, A. W.; Hegner, J.; Kaas, I.; Bejarano, C.; Mathieu, X.; Mjøs, R., Sedimentology and depositional model for the Early Miocene Oficina Formation in the Petrocedeño Field (Orinoco heavy-oil belt, Venezuela). *Marine and Petroleum Geology* **2012,** 35, (1), 354-380.
3. Chew, K. J., The future of oil: unconventional fossil fuels. *Philosophical Transactions of the Royal Society of London A: Mathematical, Physical and Engineering Sciences* **2014,** 372, (2006), 20120324.
4. Meyer, R. F.; Attanasi, E. D., Heavy oil and natural bitumen-strategic petroleum resources. *World* **2003,** 434, 650-7.

5. Rana, M. S.; Samano, V.; Ancheyta, J.; Diaz, J., A review of recent advances on process technologies for upgrading of heavy oils and residua. *Fuel* **2007,** 86, (9), 1216-1231.
6. Shah, A.; Fishwick, R.; Wood, J.; Leeke, G.; Rigby, S.; Greaves, M., A review of novel techniques for heavy oil and bitumen extraction and upgrading. *Energy & Environmental Science* **2010,** 3, (6), 700-714.
7. Abdel-Raouf, M., Factors affecting the stability of crude oil emulsions. *Crude oil emulsions–composition, stability and characterization. Croatia: Intech* **2012**, 183-204.
8. Auflem, I. H. Influence of asphaltene aggregation and pressure on crude oil emulsion stability. Norwegian University of Science and Technology Trondheim, 2002.
9. Tharanivasan, A. K. Asphaltene Precipitation from Crude Oil Blends, Conventional Oils, and Oils with Emulsified Water. UNIVERSITY OF CALGARY, 2012.
10. Acevedo, S.; Castro, A.; Negrin, J. G.; Fernández, A.; Escobar, G.; Piscitelli, V.; Delolme, F.; Dessalces, G., Relations between asphaltene structures and their physical and chemical properties: The rosary-type structure. *Energy & fuels* **2007,** 21, (4), 2165-2175.
11. Groenzin, H.; Mullins, O. C., Asphaltene molecular size and structure. *The Journal of Physical Chemistry A* **1999,** 103, (50), 11237-11245.
12. Mullins, O. C., The asphaltenes. *Annual Review of Analytical Chemistry* **2011,** 4, 393-418.
13. Mullins, O. C.; Sabbah, H.; Eyssautier, J. l.; Pomerantz, A. E.; Barré, L.; Andrews, A. B.; Ruiz-Morales, Y.; Mostowfi, F.; McFarlane, R.; Goual, L., Advances in asphaltene science and the Yen–Mullins model. *Energy & Fuels* **2012,** 26, (7), 3986-4003.
14. Speight, J. G., *The chemistry and technology of petroleum*. CRC press: 2014.
15. Chuan, W.; Guang-Lun, L.; YAO, C.-j.; SUN, K.-j.; Gai, P.-y.; CAO, Y.-b., Mechanism for reducing the viscosity of extra-heavy oil by aquathermolysis with an amphiphilic catalyst. *Journal of Fuel Chemistry and Technology* **2010,** 38, (6), 684-690.
16. Ghanavati, M.; Shojaei, M.-J.; SA, A. R., Effects of asphaltene content and temperature on viscosity of Iranian heavy crude oil: experimental and modeling study. *Energy & Fuels* **2013,** 27, (12), 7217-7232.
17. Al-Maamari, R. S.; Buckley, J. S., Asphaltene precipitation and alteration of wetting: the potential for wettability changes during oil production. *SPE Reservoir Evaluation & Engineering* **2003,** 6, (04), 210-214.
18. Gharfeh, S.; Yen, A.; Asomaning, S.; Blumer, D., Asphaltene flocculation onset determinations for heavy crude oil and its implications. *Petroleum science and technology* **2004,** 22, (7-8), 1055-1072.
19. Oskui, G.; Reza, P.; Jumaa, M. A.; Folad, E. G.; Rashed, A.; Patil, S. In *Systematic Approach for Prevention and Remediation of Asphaltene Problems During CO2/Hydrocarbon Injection Project*, The Twenty-first International Offshore and Polar Engineering Conference, 2011; International Society of Offshore and Polar Engineers: 2011.
20. Hart, A., A review of technologies for transporting heavy crude oil and bitumen via pipelines. *Journal of Petroleum Exploration and Production Technology* **2014,** 4, (3), 327-336.
21. Perry, G., Method of shear heating of heavy oil transmission pipelines. In Google Patents: 2005.
22. Al-Roomi, Y.; George, R.; Elgibaly, A.; Elkamel, A., Use of a novel surfactant for improving the transportability/transportation of heavy/viscous crude oils. *Journal of Petroleum Science and Engineering* **2004,** 42, (2), 235-243.
23. Bensakhria, A.; Peysson, Y.; Antonini, G., Experimental study of the pipeline lubrication for heavy oil transport. *Oil & Gas Science and Technology* **2004,** 59, (5), 523-533.
24. Chang, C.; Nguyen, Q. D.; Rønningsen, H. P., Isothermal start-up of pipeline transporting waxy crude oil. *Journal of non-newtonian fluid mechanics* **1999,** 87, (2), 127-154.
25. Gateau, P.; Hénaut, I.; Barré, L.; Argillier, J., Heavy oil dilution. *Oil & gas science and technology* **2004,** 59, (5), 503-509.
26. Isaac, J. D.; Speed, J. B. Method of piping fluids. 1904.

27. Joseph, D. D.; Bai, R.; Mata, C.; Sury, K.; Grant, C., Self-lubricated transport of bitumen froth. *Journal of fluid mechanics* **1999,** 386, 127-148.
28. Kessick, M. A.; Denis, C. E. S., Pipeline transportation of heavy crude oil. In Google Patents: 1982.
29. Khan, M. R., Rheological properties of heavy oils and heavy oil emulsions. *Energy Sources* **1996,** 18, (4), 385-391.
30. McKibben, M. J.; Gillies, R. G.; Shook, C. A., A laboratory investigation of horizontal well heavy oil—water flows. *The Canadian Journal of Chemical Engineering* **2000,** 78, (4), 743-751.
31. Olivera, M.; Zuleta, L. A.; Aguilar, T. L.; Osorio, A., Impacto del sector de servicios petroleros en la economía colombiana. **2011**.
32. Saniere, A.; Hénaut, I.; Argillier, J., Pipeline transportation of heavy oils, a strategic, economic and technological challenge. *Oil & Gas Science and Technology* **2004,** 59, (5), 455-466.
33. Zhang, Z. Experimental Study of In-Situ Upgrading for Heavy Oil Using Hydrogen Donors and Catalyst under Steam Injection Condition. Texas A&M University, 2011.
34. Clark, P.; Hyne, J., Studies on the chemical reactions of heavy oils under steam stimulation condition. *Aostra J Res* **1990,** 29, (6), 29-39.
35. Clark, P. D.; Clarke, R. A.; Hyne, J. B.; Lesage, K. L., Studies on the effect of metal species on oil sands undergoing steam treatments. *Aostra J Res* **1990,** 6, (1), 53-64.
36. Fan, H.; Zhang, Y.; Lin, Y., The catalytic effects of minerals on aquathermolysis of heavy oils. *Fuel* **2004,** 83, (14), 2035-2039.
37. Song, K.-W.; Kim, Y.-S.; Chang, G.-S., Rheology of concentrated xanthan gum solutions: Steady shear flow behavior. *Fibers and Polymers* **2006,** 7, (2), 129-138.
38. Hassanzadeh, H.; Galarraga, C.; Abedi, J.; Scott, C.; Chen, Z.; Pereira-Almao, P. In *Modelling of bitumen ultradispersed catalytic upgrading experiments in a batch reactor*, Canadian International Petroleum Conference, 2009; Petroleum Society of Canada: 2009.
39. Loria, H.; Trujillo-Ferrer, G.; Sosa-Stull, C.; Pereira-Almao, P., Kinetic modeling of bitumen hydroprocessing at in-reservoir conditions employing ultradispersed catalysts. *Energy & Fuels* **2011,** 25, (4), 1364-1372.
40. Yi, Y.; Li, S.; Ding, F.; Yu, H., Change of asphaltene and resin properties after catalytic aquathermolysis. *Petroleum Science* **2009,** 6, (2), 194-200.
41. Chen, Y.; Wang, Y.; Lu, J.; Wu, C., The viscosity reduction of nano-keggin-K 3 PMo 12 O 40 in catalytic aquathermolysis of heavy oil. *Fuel* **2009,** 88, (8), 1426-1434.
42. Hashemi, R.; Nassar, N. N.; Pereira Almao, P., Enhanced heavy oil recovery by in situ prepared ultradispersed multimetallic nanoparticles: A study of hot fluid flooding for Athabasca bitumen recovery. *Energy & Fuels* **2013,** 27, (4), 2194-2201.
43. Castro, L. V.; Flores, E. A.; Vazquez, F., Terpolymers as Flow Improvers for Mexican Crude Oils†. *Energy & Fuels* **2011,** 25, (2), 539-544.
44. Farah, M. A.; Oliveira, R. C.; Caldas, J. N.; Rajagopal, K., Viscosity of water-in-oil emulsions: Variation with temperature and water volume fraction. *Journal of Petroleum Science and Engineering* **2005,** 48, (3), 169-184.
45. Langevin, D.; Argillier, J.-F., Interfacial behavior of asphaltenes. *Advances in colloid and interface science* **2015**.
46. Johnson, E.; Bossler, D.; Bossler, V., Calculation of relative permeability from displacement experiments. **1959**.
47. Ahmed, N. S.; Nassar, A. M.; Zaki, N. N.; Gharieb, H. K., Formation of fluid heavy oil-in-water emulsions for pipeline transportation. *Fuel* **1999,** 78, (5), 593-600.
48. Arhuoma, M.; Dong, M.; Yang, D.; Idem, R., Determination of water-in-oil emulsion viscosity in porous media. *Industrial & Engineering Chemistry Research* **2009,** 48, (15), 7092-7102.
49. Martínez-Palou, R.; de Lourdes Mosqueira, M.; Zapata-Rendón, B.; Mar-Juárez, E.; Bernal-Huicochea, C.; de la Cruz Clavel-López, J.; Aburto, J., Transportation of heavy and extra-heavy

crude oil by pipeline: A review. *Journal of Petroleum Science and Engineering* **2011,** 75, (3), 274-282.
50. Johnsen, E. E.; Rønningsen, H. P., Viscosity of 'live'water-in-crude-oil emulsions: experimental work and validation of correlations. *Journal of Petroleum Science and Engineering* **2003,** 38, (1), 23-36.
51. Salager, J.-L.; Briceño, M. I.; Bracho, C. L., Heavy hydrocarbon emulsions. Making use of the state of the art in formulation engineering. *Encyclopedic Handbook of Emulsion Technology* **2001,** 20, 455-495.
52. Wylde, J.; Leinweber, D.; Low, D.; Botthof, G.; Oliveira, A.; Royle, C.; Kayser, C. In *Heavy oil transportation: advances in water-continuous emulsion methods*, Proceedings of the world heavy oil congress, Aberdeen, 2012; 2012.

1. Synthesis and characterizations of nanoparticles/nanofluids and its interactions with asphaltenes of heavy crude

By definition a nanoparticle is a "*Microscopic particle whose size is measured in nanometers, often restricted to so-called nanosized particles (NSPs; <100 nm in aerodynamic diameter), also called ultrafine particles"*.[1] Nanotechnology has been developing in the last years applying to all type of industry: Food industry,[2, 3] biotechnology,[4] medicine,[5-7] energy,[8-10] textiles,[11] construction,[12] environments,[13] and obviously the oil and gas industry.[14] Nanoparticles have been used by the oil industry for formation damage inhibition,[15-18] HO, and EHO upgrading,[19] enhanced (EOR) and improve recovery (IOR) processes,[17, 20] and wastewater remediation.[21] Due to their particle sizes, between 1 and 100 nm, large available surface area, high dispersibility and tunable physicochemical characteristics, nanoparticles are prone to selectively adsorb asphaltenes and inhibit their self-association. [22] In a previous study, [17, 20, 23] our research group focused on using silica, γ-alumina and magnetite nanoparticles to inhibit the aggregation of asphaltenes under varying temperature, solvent ratios and asphaltene concentration. Hence, the characterization of the nanoparticles is of paramount importance to the understanding of the nanoparticle's role in the heavy oil and extra-heavy oil viscosity reduction. Nanoparticle's size is a key parameter to take into account when considering these materials for an *in-situ* application. It has to be ensured that the material available for injection into the reservoir meets the size constraints to ensure that nanoparticles would not cause a further damage into the reservoir due to pore throat bridging or blockage. According to the one-third to one-seventh arch principles, the particle size could contribute to the bridging/blockage as follows: i) particles larger than 1/3 of pore size are prone to generate pore blocking, ii) particles in the range 1/7 – 1/3 of pore size would generate a bridge in the pore throat that further will generate pore blockage and iii) particles with size lower than 1/7 of pore size are able to pass through the pore throat.[24-26] It is expected that nanoparticles employed for injection into the reservoir would accomplish the third aforementioned scenario.[22] Because of their unique and exceptional properties, such as large surface area and size-and shape-dependent catalytic properties, nanoparticles can also

be employed as adsorbents and/or catalysts for removal of heavy waste polar hydrocarbons from crude oil, like asphaltenes. The adsorption and subsequent catalytic thermal decomposition of asphaltenes onto different surfaces of nanoparticles were first introduced by Nassar and coworkers.[22, 27-34]. In his earlier study,[34] Nassar investigated the kinetics and thermodynamic of the asphaltene adsorption on γ-Al_2O_3 nanoparticles. The author reported that adsorption was fast as adsorption equilibrium was achieved in less than 2 h. This was attributed to the non-porous character of the material, where the external adsorption is dominated. More recently, Cortés et al...[35] and Franco et al...[16] have developed several studies on the adsorption of *n*-C_7 asphaltenes extracted from Colombian crude oils using NiO nanoparticles supported onto nanoparticles of silica and alumina,[16, 17, 35] respectively. Authors found that the selected nanoparticles have high adsorptive capacities and the adsorption equilibrium time was very short (i.e., about two minutes).[16] In this order, this chapter describes the synthesis and characterization of the selected nanoparticles and nanofluids, and the adsorption of the asphaltenes onto nanoparticles. Silica nanoparticles were synthesized by the sol-gel method, respectively. Magnetite, Silica, and Alumina were purchased. Additionally, the surface of a nanoparticle was modified using basic and acid agents. Nanoparticles were characterized trough, particle size, and surface area measurements.

1.1 Experimental

1.1.1 Materials

Commercial nanoparticles of fumed silica (S8, S12, and S285), magnetite (F97), γ-alumina (Al35), and in-house synthesized nanoparticles of silica (S97, S8A, and S8B) were used as viscosity reducers agents. The commercial nanoparticles of fumed silica and γ-alumina were obtained from Sigma-Aldrich (St. Louis, MO) and commercial magnetite nanoparticles from Nanostructured & Amorphous Materials (Houston, TX).

Tetraethyl orthosilicate (TEOS, > 99%), ethanol (99.9%) and NH_4OH (28%) were used to synthesize the silica nanoparticles. All reactants employed for the synthesis were purchased from Sigma-Aldrich (St. Louis, MO). For SiO_2 nanoparticles surface modification, H2SO4 (95-97%, Merck KGaA, Germany) and NH4OH (28%, Sigma-Aldrich, St. Louis, MO) was used.

Two Colombian oils were used as heavy oil (HO) and extra heavy oil (EHO). The properties of the selected HO and EHO are presented in Table 1.1. Four nanofluids were prepared with different diluents. Toluene (99.5%, Merck KGaA, Germany), biodiesel, and naphtha were used as diluents;

these two last were provided by the Ecopetrol S.A (Colombia). Cetyltrimethylammonium Bromide CTAB (98%, PanReac, Spain) and non-ionic surfactant Tween 80 (Sigma-Aldrich, St. Louis, MO) were employed for nanofluids preparation.

Table 1.1 HO and EHO characterization

Material	API (°)	Viscosity at 298 K (cP)	C (wt%)	H (wt%)	N (wt%)	O (wt%)
HO	13	1.2×10^5	80.4	9.46	2.3	7.84
EHO	6.4	2.2×10^6	84.8	7.5	0.88	6.82

- **Silica nanoparticles synthesis and surface modification.**

The S97 nanoparticles were synthesized using the sol-gel method following a basic route, based on the procedure initially proposed by Stöber et al...[36, 37] The sol-gel method consists in a sol preparation, its further gelation, and solvent removal and could be produced from inorganic or organic precursors. Here, silica nanoparticles were obtained by forming a 3-D structure of interconnected siloxane bridges (Si–O–Si) achieved through simultaneous and repeated hydrolysis and polycondensation of determined precursor such as TEOS.[38] NH_4OH and ethanol are used, respectively, as catalyst of the hydrolysis reaction and as mutual solvent between water and TEOS.[36] Route A consisted in stirring the previously mixed reactants at 300 rpm for 4 hours. Then, the solution is centrifuged at 4500 rpm for 30 min using a Hermle Z 306 Universal Centrifuge (Labnet, NJ) and left to stand overnight. Finally, the result is washed with ethanol and deionized water and dried overnight at 120°C. The quantities TEOS:H2O:NH4OH:ethanol molar ratios of 1:6:1:0.25 were used. In this document, SiO_2 nanoparticles are nomenclated according to the size. For instance, S97 nanoparticles, are SiO_2 nanoparticles of 97 nm o diameter size. The commercial nanomaterial of 8 nm was selected for acidification and basification of the surface, which consisted of mixing nanoparticles and sulfuric acid at 0.3 wt% to obtain a solution at pH = 4, and NaOH at 0.3wt% to obtain a solution at pH=11. A Horiba Navih pH meter was used for pH measurements. The solution was sonicated for 2 hours at room temperature, then further stirred magnetically at 100 rpm for 12 hours and subsequently centrifuged at 4500 rpm for 15 minutes. The nanoparticles were dried at 393 K for 4 hours.

- **Nanofluids preparation**

The nanofluid is prepared using four different types of carrier fluid namely: toluene, biodiesel, biodiesel + Tween 80, and biodiesel + CTAB. In the addition of surfactants to the biodiesel, 1 wt% of the respective surfactant is mixed with the biodiesel at 300 rpm and 298 K. A fixed nanoparticles dosage of 1000 mg/L regarding the oil volume was selected for nanofluids preparation. This nanoparticles concentration was chosen based on the experimental results of our previous work.[39] Nanoparticles were added to the carrier fluid using a magnetic stirrer at 300 rpm for 1 h at 298 K and subsequently sonicated for 30 min for guarantying the correct dispersion of the nanoparticles in the liquid medium. The properties of the prepared nanofluids are summarized in Table 1.2. In this document, the obtained nanofluids are named after the initial letter of the base fluid and the surfactant employed. For instance, biodiesel-based nanofluid with 1 wt% of Tween 80 is named as BTWNF.

Table 1.2 Properties of the prepared nanofluids at 298 K.

Nanofluid	Diluent	Surfactant	Density at 298 K (g/mL)	Viscosity at 298 K (cP)
TNF	Toluene	-	0.87 ± 0.02	0.61 ± 0.01
BNF	Biodiesel	-	0.88 ± 0.02	4.4 ± 0.2
BTWNF	Biodiesel	1 wt% Tween 80	0.91 ± 0.03	4.9 ± 0.4
BCNF	Biodiesel	1 wt% CTAB	0.92 ± 0.03	4.8 ± 0.5

1.1.2 Nanoparticles characterization

Commercial, synthesized and modified nanoparticles were characterized trough particles size and surface area. Particle or crystallite size of nanoparticles was determined using field emission scanning electron microscopy (FESEM) and dynamic light scattering (DLS) measurements. The surface areas (S_{BET}) of the selected nanoparticles were measured following the Brunauer−Emmett−Teller (BET) [40, 41] method and was compared to the geometrical surface area according to the estimated particle size.

- **Particle size measurements**

The size of the evaluated nanoparticles (*dp*) was determined by FESEM, DLS, and XRD. A JSM-6701F (JEOL, Japan) field emission scanning electron microscope was used to obtain images of the selected materials with their particle size distribution. The sample was prepared by dispersing the material on ethanol in a concentration of 100 mg/L and sonicated for 3 h at room temperature. Then, a drop of the dispersion was carefully placed in a graphite tape previously stuck in the apparatus sampler. Finally, the sample is gold-plated and further introduced to the microscope.

DLS measurements were performed using a nanoplus-3 from Micromeritics (Norcross, ATL) set at room temperature and equipped with a 0.9 mL glass cell.[42-44] The solid sample was dispersed in water in a relation of 0.5 mg/10 mL and sonicated for four hours. Then, an aliquot of the sonicated sample was placed in the glass cell. The scattering angle varies according to the solvent used to optimize the intensity of the flocculation of scattering light. The mean particle diameter (hydrodynamic diameter) is obtained from the Stokes-Einstein equation, as follows: [45]

$$dp = \frac{k_B T}{3\pi\eta D_a} \tag{1.1}$$

where k_B (1.38 x 10^{-23} $m^2 kg \cdot s^{-2} K^{-1}$) is the Boltzmann constant, T (K) is temperature, η (cP) is the viscosity of the medium, and D_a ($m^2 \cdot s^{-1}$) is the diffusion coefficient of the particles.

- **Surface area estimation**

The S_{BET} of the selected nanoparticles were measured following the BET method.[40, 41] This was achieved by performing nitrogen adsorption−desorption at 196°C, using an Autosorb-1 from Quantacrome. The samples were degassed at 140°C under N_2 flow overnight before analysis. Surface areas were calculated using the BET equation.

Additionally, assuming non-porous spheres with sphericity = 1, the geometrical surface area (*SA*, m^2/g) of the nanoparticles was calculated according to Eq. 1.2: [46, 47]

$$SA = \frac{6000}{dp \cdot \rho} \tag{1.2}$$

where ρ (g/cm^3) is the true material density taken as 2.65, 3.95, and 4.95 g/cm^3 for SiO_2, Al_2O_3, and Fe_3O_4, respectively.

1.1.3 Methods

- ***n*-C_7 asphaltenes isolation protocol**

Asphaltenes were precipitated from Akacias and Suria crude oil following a standard procedure.[16] In brief, an excess amount of n-heptane was added to the crude oil in a volume ratio of 40:1. The mixture was then sonicated for 2 h at 298 K and further stirred at 300 rpm for 20 h. Black precipitates formed at the bottom. The precipitated asphaltenes were collected after decanting the supernatant. Then, asphaltenes were washed with fresh n-heptane at a ratio 1:4 (g/mL), centrifuged at 5000 rpm for 15 min and left to rest for 24 h. The asphaltenes were separated from the final solution by filtration using an 8 µm Whatman filter paper. The cake was washed with n-heptane several times until the color of the asphaltenes became shiny black. Finally, the obtained asphaltenes were homogenized and fined using pestle and mortar and left to dry at 298 K in a vacuum oven for 12 h.

- ***n*-C_7 asphaltenes adsorption**

Adsorption isotherms for n-C7 asphaltenes on the nanoparticles were collected at 303 K, in a concentration (Ci) range of 100-1500 mg/L and at a ratio of nanoparticle-to-solution of 100 mg per 10 mL.[19, 48] An UV-vis spectrophotometer Genesys 10S (Thermo Scientific, Waltham, MA) was used to determine the asphaltene concentration in solution before and after the adsorption process. Hence, a number of n-C7 asphaltenes adsorbed (Nads) onto the selected nanoparticles could be estimated by a mass balance analysis once adsorption equilibrium is reached.[34] Additional information on the procedure can be found in previous publications.[16, 17, 48]

- ***n*-C_7 asphaltenes aggregation experiments.**

DLS measurements of heavy oil model solutions in the presence and absence of nanoparticles were performed to evaluate the average aggregate size of n-C7 asphaltenes as a function of nanoparticle addition. n-C7 asphaltenes were dissolved in a mixture n-heptane/toluene (Heptol) 40% v/v at a concentration of 1000 mg/L. The mixture was magnetically stirred at 300 rpm, and aliquots were taken to obtain the mean asphaltene aggregate size as a function of time. The dosage of nanoparticles was fixed at 10 g/L to guarantee total decantation of the nanoparticles and thus obtain an accurate estimate of the n-C7 asphaltenes aggregate size.[20]

1.2 Modeling

The solid-liquid equilibrium model (SLE) is used for describing the adsorption isotherms of asphaltenes on nanoparticles and for estimating the thermodynamic properties of adsorption.

1.2.1 Solid-Liquid equilibrium model (SLE)

The adsorption isotherm of *n*-C_7 asphaltenes onto nanoparticles is described by using the association theory suggested by Talu and Meunier[49] for the adsorption of associating molecules in micropores and further developed by Montoya et al...[50] for describing the adsorption isotherms of self-assemble asphaltenes onto non-porous surfaces. The model is expressed as follows:[50]

$$C_E = \frac{\psi H}{1+K\psi}\exp\left(\frac{\psi}{q_m \cdot A}\right) \tag{1.3}$$

where q_m (mg/m^2) is the maximum adsorption capacity, H is the measured Henry's law constant, which is only a function of temperature, and an indicator of the adsorption affinity (i.e., the strength of interactions for adsorption) of asphaltenes onto nanoparticle surface. The lower the H value (i.e., higher Henry's constant) is the higher the affinity (i.e., the active sites are in locations which are easily accessible by asphaltenes). K is constant and an indicator of rapid association of asphaltenes molecules once the primary sites are occupied. A (m^2/mg) is the measured surface area per mass of nanoparticles and C_E (mg/g) is the equilibrium concentration of asphaltenes. The other parameters are defined as follows:

$$K = \frac{K_T RT}{A} \tag{1.4}$$

$$\psi = \frac{-1+\sqrt{1+4K\xi}}{2K} \tag{1.5}$$

where, ξ is a constant defined as

$$\xi = \left(\frac{q_m \cdot q}{q_m - q}\right) A \tag{1.6}$$

q is the amount adsorbed (mg/m^2), and K_T is the reaction constant for dimer formation. For describing the thermodynamic properties of asphaltene adsorption, a five-parameter-temperature independent SLE model is used. In this case, H and K parameters in Eq. 2.2 are replaced by the following correlations:[50]

$$H = \exp\left(H_o + \frac{H_1}{T} \right) \tag{1.7}$$

$$K = \exp\left(K_o + \frac{K_1}{T} \right) \tag{1.8}$$

where K_0 and K_1 are related to the reaction entropy, and a reaction enthalpy of asphaltenes adsorption on the nanoparticles surface and T is the absolute temperature. Accordingly, the change in standard entropy (ΔS^o_{ads}) and standard enthalpy (ΔH^o_{ads}) are calculated as follows

$$\Delta S^0_{ads} = K_0 R \tag{1.9}$$

$$\Delta H^0_{ads} = K_1 R \tag{1.10}$$

Using the Gibbs equation,[51] the change in Gibbs free energy can be estimated as follows:

$$\Delta G^o_{ads} = -RT \ln K \tag{1.11}$$

The accuracy of the model was evaluated through the root-mean-square error (RMSE%) using the excel package:[52]

1.3 Results

1.3.1 Particle size

Panels a− j from Figure 1.1 show the FESEM images and the corresponding particle size probability distribution for the nanoparticles (a and b) S8, (c and d) S12, (e and f) S97, (g and h) S285, (i and j) F97, and (k and l) Al35. Additionally, Table 1.3 shows the estimated values of the mean particle size and surface areas of the selected nanoparticles obtained by the methods previously described. As observed in Figure 1.1 all materials, synthesized and commercials, except S298, have a mean particle diameter in the nano-scale according to the definition of nanotechnology. Results are in excellent agreement with Dabbaghian et al.,[53] who synthesized silica nanoparticles trough the sol-gel method using TEOS as the precursor and NH_4OH as a catalyst and found that for molar ratios NH_4OH/H_2O < 2 the particle size increased as the NH_4OH/H_2O molar ratio increased. Figure 1.2 shows the DLS results for the synthesized and commercial nanoparticles. As seen in Figure 1.2 and Table 1.3, the mean particle of nanoparticles has the same trend than the one observed trough FESEM. This could be due to great van der Waals attractive forces between nanoparticles in the aqueous medium because of Brownian motion.[46, 54]

The S285 nanoparticles are larger than the one acceptable for classifying them as nanoparticles. However, the sample will be considered for asphaltenes adsorption and subsequent viscosity reduction tests due to two main reasons: i) nanoparticles could be sufficiently small for neglecting the possibility of blockage or bridging in an HO reservoir formation[55, 56] and ii) about the 15% of the particles are in the nanoscale range. For example, Pachón[25] evaluated the petrophysic properties of the K1 and K2 units from the Gacheta and Une formations in the Castilla field (HO) placed in the Meta department, the central region of Colombia. The author found that for depths between 6417 and 6911 ft the predominant mean pore diameter was about 204 μm. Hence, according to the bridge arch principle, bridging due to particle intrusion in the pore throats would happen for particles with an average size between 29 and 68 μm, values much higher than that of the mean particle size of S285.

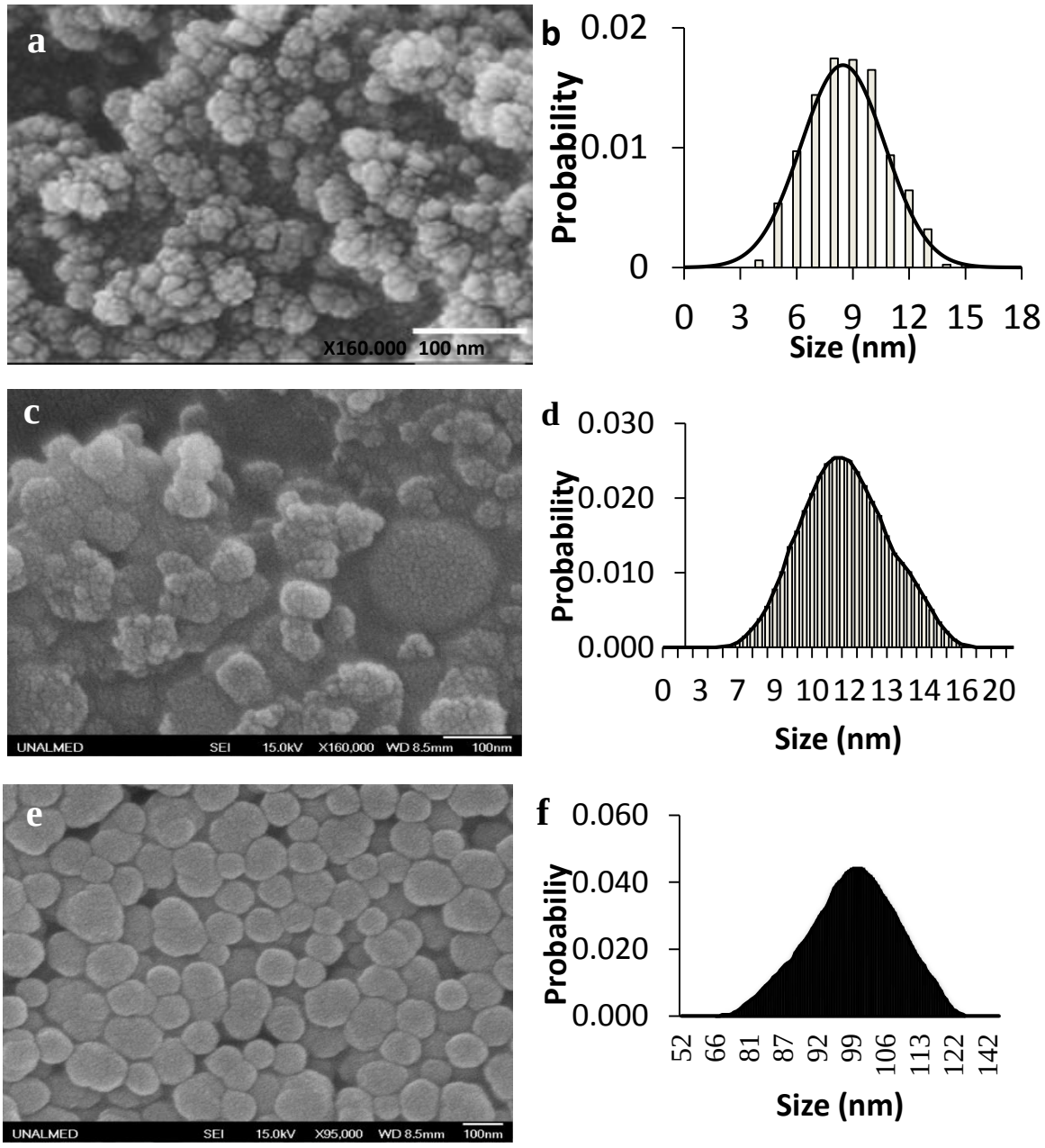
a
X160.000 100 nm
b
0.02
0.01
0
Probability
0 3 6 9 12 15 18
Size (nm)
c
UNALMED SEI 15.0kV X160,000 WD 8.5mm 100nm
d
0.030
0.020
0.010
0.000
Probability
0 3 7 9 10 12 13 14 16 20
Size (nm)
e
UNALMED SEI 15.0kV X95,000 WD 8.5mm 100nm
f
0.060
0.040
0.020
0.000
Probabiliy
52 66 81 87 92 99 106 113 122 142
Size (nm)

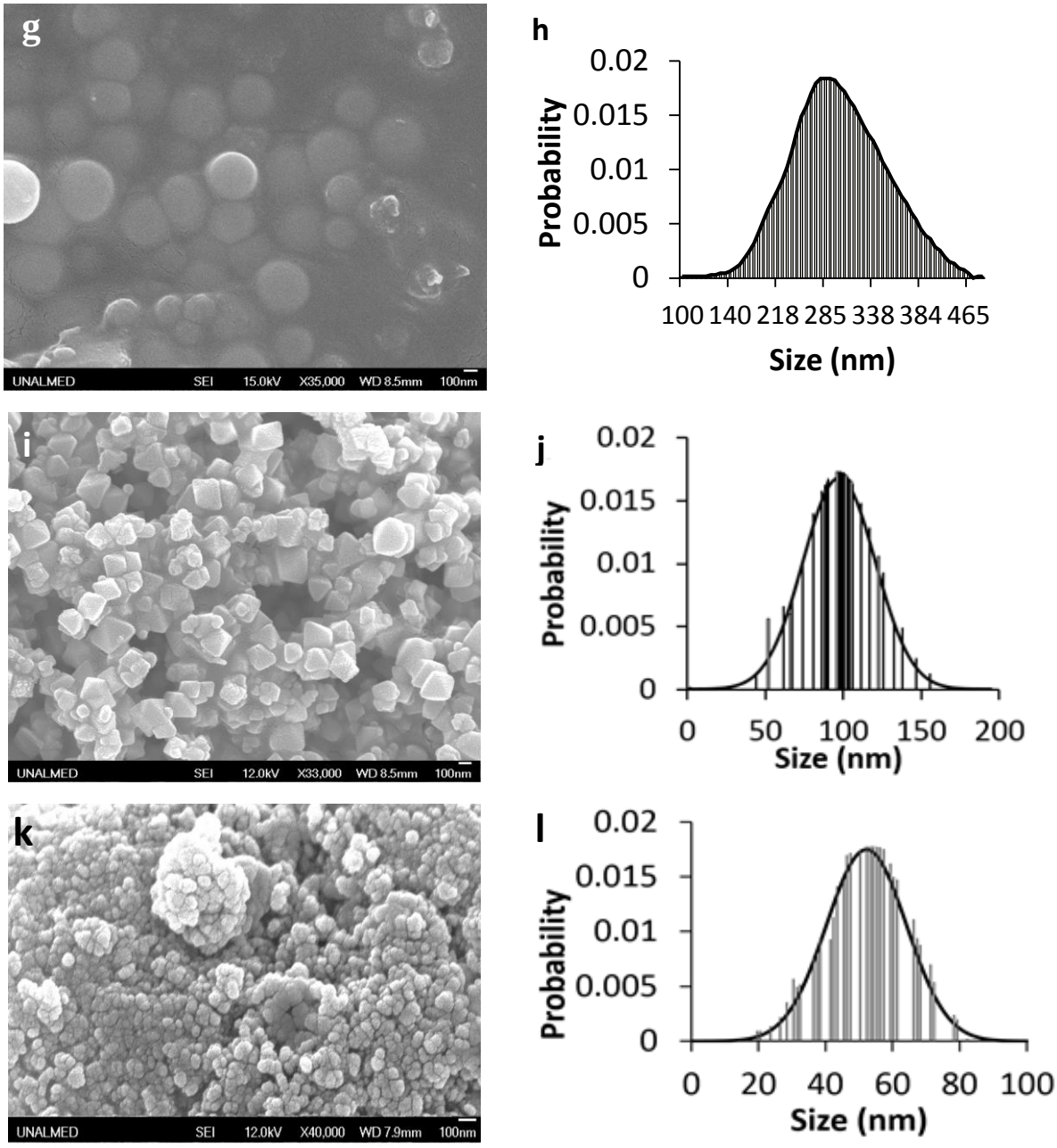

Figure 1.1. ¡Error! No se encuentra el origen de la referencia.

Table 1.3 Estimated surface area and particle size of the selected nanoparticles.

Material	Particle size (nm)		Surface Area (m^2/g)
	$dp50_{FESEM}$	$dp50_{DLS}$	S_{BET}
S8	9	8	389.1
S8A	9	8	239.7
S8B	9	8	138.1
S11	11	12	210
S97	95	97	26
S285	300	292	14
F97	92	97	102.2
Al35	29	35	123

1.3.2 Surface area

- **Synthesized and commercial nanoparticles**

The S_{BET} of the nanoparticles was determined through N_2 physisorption at -196°C. Table 1.3 shows the estimated values of the surface areas obtained by the BET method. Among the nanoparticles, it can be observed that as expected, for the same nature chemistry of nanoparticle, the surface area increases as the size of the particle decreases. The trend followed by the surface area is S8 > S12 > S97 > S285. It is worth noting that the surface area of the surface modified silica tends to decrease because the acid or base molecules possibly cover the pores of the virgin nanoparticle. For this reason, the value for S8A and S8B is lower than for S8

1.3.3 Adsorption isotherms.

In this section, we present the interaction between the nanoparticles selected in this thesis and the asphaltenes of the two types of crudes used throughout this research.

The process of extracting asphaltenes and preparation of the solution models was previously explained in the methodology of the chapter.

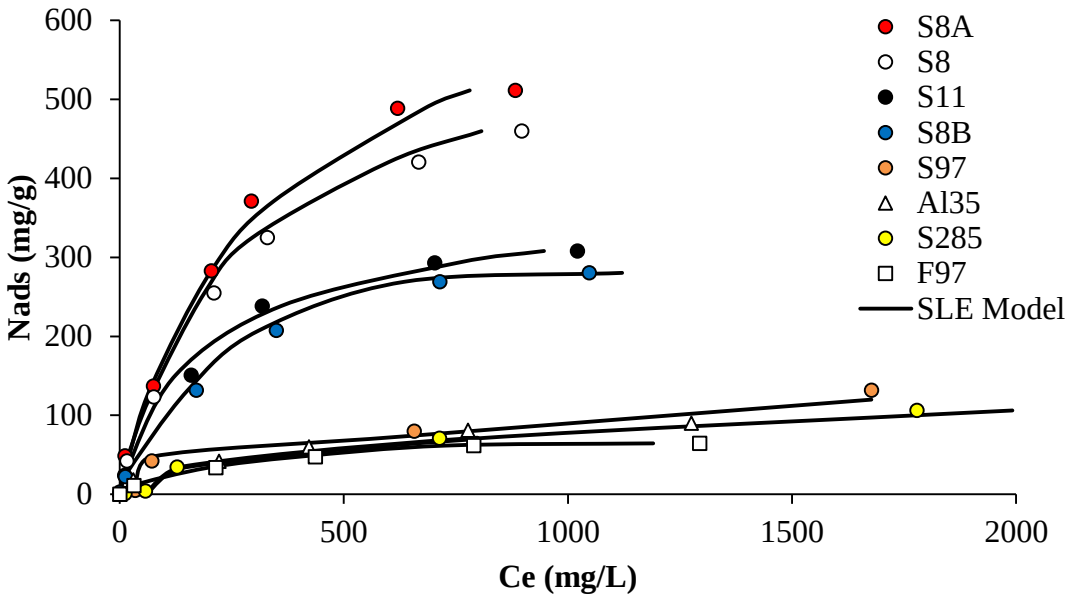

Figure 1.2 Adsorption isotherms of EHO *n*-C_7 asphaltenes onto nanoparticles of S8, S8A, S8B, S11, S97, S285, Al35, and F97 at 298 K.

Figure 1.2 shows the experimental adsorption isotherms of EHO n-C7 asphaltenes onto nanoparticles evaluated at 298 K along with the solid-liquid-equilibrium (SLE) model. Figure 1.2 shows that the n-C7 asphaltene adsorption isotherms follow a Type I behavior according to the International Union of Pure and Applied Chemistry (IUPAC) classification. Indeed, it can be clearly seen that the adsorptive capacity of the S8A nanoparticles is greater than that of the other nanoparticles evaluated. The results indicate that the adsorption ability to capture n-C7 asphaltenes by nanoparticles follows the order S8A > S8 > S11 > S8B > S97 > Al35 > S285 > F97, which is supported by the parameters values obtained from the SLE model, mainly the maximum adsorbed uptake (Table 1.4). It is noted that the adsorptive capacity of nanoparticles of acidic silica is greater than the rest, especially at low concentrations (Henry´s Region) wherein the affinity of the nanoparticles is greater than for others. This is confirmed by the values of the H parameter of the SLE model in increasing order S8A < S8 < S11 < S8B < S97 < Al35 < S285 < F97, showing the lower affinity for the F97 sample in comparison to the other ones. These results are in agreement with Nassar et al.,[34] and Montoya et al..[57] This could be explained by the increased surface acidity of the nanoparticles and is in agreement with those reported by Nassar et al..[58] and Guzmán et al.,[59] who found that the n-C7 asphaltenes adsorption increased concomitantly with the surface increased acidity [88]. It was found that the Al35 has affinity for asphaltenes, possibly due to the molecular interactions between aluminol group and O-, N. or S-containing functional groups of the n-C7 asphaltenes.[60] However, besides of

presenting lower surface area than those of S8 and S8A nanoparticles, the interaction between the hydroxyl links of n-C7 asphaltenes and the silanol groups on the silica surface are stronger than the affinity for alumina, and favors adsorption [60]. As the nanoparticle is acidified, the content of silanol groups on its surface is increased, promoting greater adsorption.[61, 62]

Table 1.4 Parameters estimated from the SLE model for EHO *n*-C_7 asphaltene adsorption on nanoparticles.

Sample	H (mg/g)	K x 10^{-4} (g/g)	$N_{ads,m}$ (mg/g)	R^2	RSME
S8A	0.44	2.2	1172.1	0.96	6.84
S8	0.45	2.4	963.2	0.98	4.29
S11	0.47	3.1	563.2	0.97	5.79
S8B	0.49	3.3	512.2	0.98	4.12
S97	2.75	7.8	223.4	0.95	7.86
Al35	3.39	9.0	188.6	0.99	4.99
S285	3.64	9.4	175.6	0.95	8.43
F97	3.66	9.3	174.3	0.96	6.78

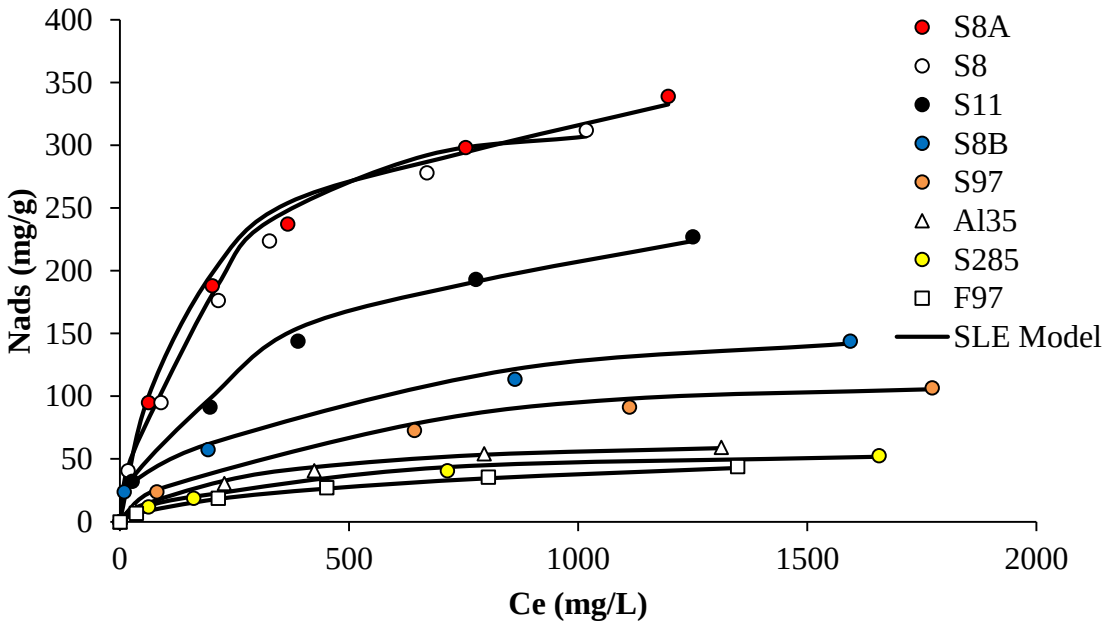

Figure 1.3 Adsorption isotherms of HO *n*-C_7 asphaltenes onto nanoparticles of S8, S8A, S8B, S11, S97, S285, Al35, and F97 at 298 K.

Figure 1.3 shows the experimental adsorption isotherms of HO n-C7 asphaltenes onto nanoparticles evaluated at 298 K along with the solid-liquid-equilibrium (SLE) model. Figure 1.3 shows that the HO n-C7 asphaltene adsorption isotherms follow a Type I behavior according to the International Union of Pure and Applied Chemistry (IUPAC) classification. Indeed, it can be clearly seen that the adsorptive capacity of the S8A nanoparticles is greater than that of the other nanoparticles evaluated. The results indicate that the adsorption ability to capture n-C7 asphaltenes by nanoparticles follows the order S8A > S8 > S11 > S8B > S97 > Al35 > S285 > F97, which is supported by the parameters values obtained from the SLE model, mainly the maximum adsorbed uptake (Table 1.5). It is noted that the adsorptive capacity of nanoparticles of acidic silica is greater than the rest, especially at low concentrations (Henry´s Region) wherein the affinity of the nanoparticles is greater than for others. This is confirmed by the values of the H parameter of the SLE model in increasing order S8A < S8 < S11 < S8B < S97 < Al35 < S285 < F97, showing the lower affinity for the F97 sample in comparison to the other ones.

Compared with the isotherms obtained with extra-heavy crude asphaltenes (Figure 1.2), the trend is similar, however, the adsorbed amount is different. Adsorption of n-C7 asphaltenes depends on many factors, and relevant to this work are among others, structure, and composition, the capacity of the sample to pack at the interface, concentration, aggregation in solution and time.[63] Thus any attempt to account for the differences shown in Figure 1.3 would be speculative. Hence, we speculate that such a difference could in part be due to differences in aggregation trends. As described earlier,[63] aggregation in solution hinder the adsorption, and this would be consistent with a higher aggregation trend for the HO n-C7 asphaltenes. These arguments are consistent with the higher hydrodynamic radii found for HO n-C7 asphaltenes when compared with the EHO n-C7 asphaltenes.

Table 1.5 Parameters estimated from the SLE model for HO *n*-C_7 asphaltene adsorption on nanoparticles.

Sample	H (mg/g)	K x 10^{-4} (g/g)	$N_{ads,m}$ (mg/g)	R^2	RSME
S8A	0.42	1.9	672.1	0.98	4.84
S8	0.41	2.1	573.2	0.98	5.29
S11	0.46	2.7	295.2	0.98	4.79
S8B	0.49	3.5	225.2	0.97	6.45
S97	1.95	5.8	185.4	0.98	4.86
Al35	2.89	8.1	178.6	0.99	3.19

S285	3.24	8.4	175.6	0.95	8.43
F97	3.29	8.1	174.3	0.96	6.78

1.2.4. Asphaltene kinetic aggregation

The affinity between nanoparticles and *n*-C_7 asphaltenes of extra-heavy crude oil was demonstrated by the results of adsorption isotherms. However, the nanoparticles evaluated also must have the ability to reduce the mean size of asphaltene aggregates (d_{asp}) in the fluid with the objective of impacting the configuration and distribution of them in the oil matrix. In heavy crude oils with asphaltene content above 5 wt%, the configuration of asphaltenes is generally formed by a series of clusters of nanoaggregates, forming a viscoelastic network of large size.[43, 64] For this reason, it is expected for the nanoparticles to have the ability to break the attachment points within the viscoelastic network and greatly reduce the size of the aggregates of asphaltenes, resulting in the reduction of the crude oil viscosity. Figure 1.4 shows the mean aggregate size of EHO *n*-C_7 asphaltenes in heptol 40 in the presence and absence of nanoparticles evaluated at 298 K. In Figure 1.4, the curve of *n*-C_7 asphaltenes in the absence of nanoparticles initially reflects a growth in d_{asp} as a function of time, followed by a reduction in this value until stabilization after approximately 300 min. This likely occurs due to aggregation-fragmentation forces that exist under certain shear conditions, which in turn have a direct influence on the mean asphaltene aggregate size (growth/reduction).[20, 63, 65] The behavior of *n*-C_7 asphaltenes in the presence of a nanoparticle system is similar, but with a smaller d_{asp} and a faster stabilization after 180 min. The evaluated nanoparticles were able to successfully reduce the d_{asp} in decreasing order of effectiveness, S8A = S8 < S11 < S8B < S97 < Al35 < S285 < F97. For example, after 80 minutes, the reduction in d_{asp} is 21, 57 and 61% when using Al_{35}, S8 and S8A, respectively. Hence, higher *n*-C_7 asphaltene uptake will result in the decrease of the number of asphaltenes available in the solution for the aggregation-fragmentation process. [20, 63, 65] These results are consistent with those presented by Nassar et al., [20] who evaluated the reduction of the *n*-C_7 asphaltene mean aggregate size and found out that silica nanoparticles were more prone to reduce it as they had greater adsorption capacity.

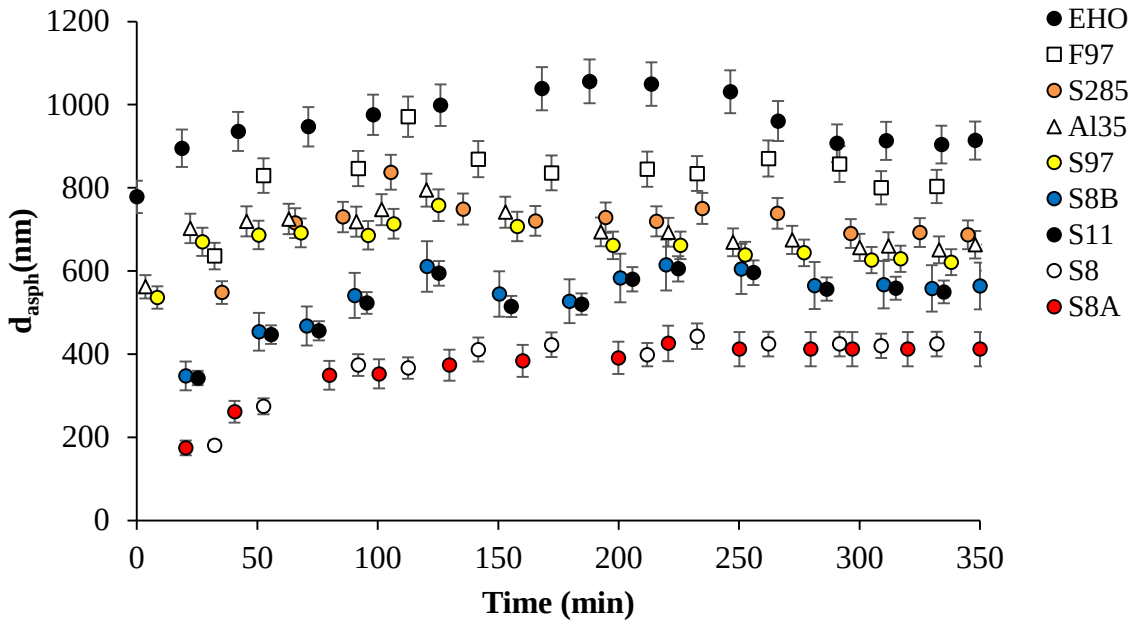

Figure 1.4 Effect of nanoparticles on the mean aggregate size of EHO *n*-C_7 asphaltene in heptol 40 solutions at 298 K.

Figure 1.4 shows the mean aggregate size of EHO n-C7 asphaltenes in heptol 40 in the presence and absence of nanoparticles evaluated at 298 K.

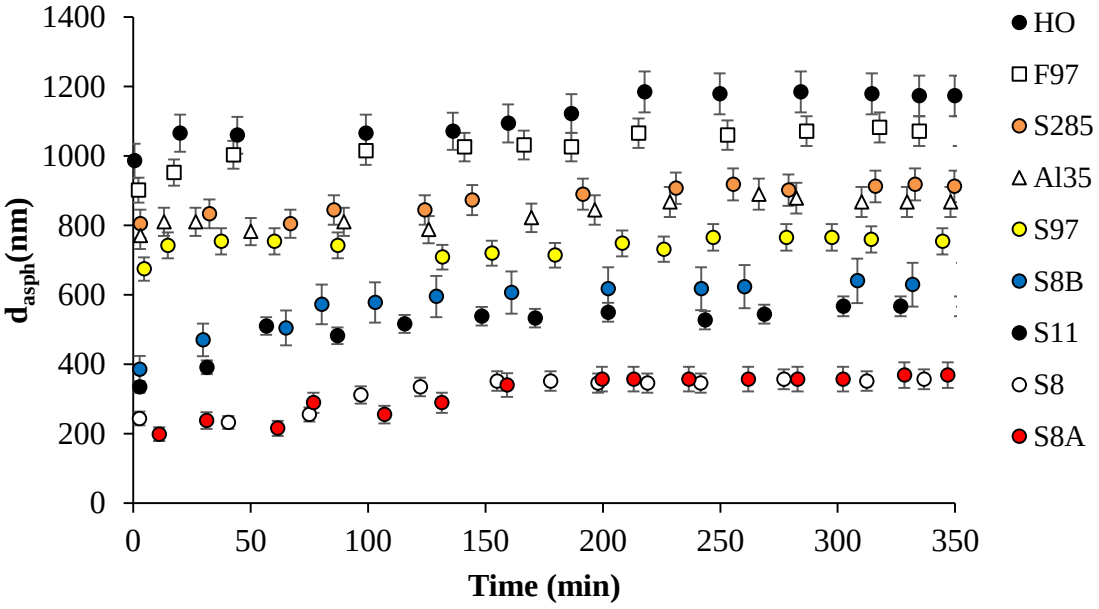

Figure 1.5 Effect of nanoparticles on the mean aggregate size of HO *n*-C_7 asphaltene in heptol 40 solutions at 298 K.

In Figure 1.4, the curve of n-C7 asphaltenes in the absence of nanoparticles initially reflects a growth in d_{asp} as a function of time, followed by a reduction in this value until stabilization after approximately 300 min. This likely occurs due to aggregation-fragmentation forces that exist under certain shear conditions, which in turn have a direct influence on the mean asphaltene aggregate size (growth/reduction).[20, 63, 65] The behavior of n-C7 asphaltenes in the presence of a nanoparticle system is similar, but with a smaller d_{asp} and a faster stabilization after 180 min.

The nanoparticles evaluated with the aim of reducing the average size of the asphaltene aggregate have the same tendency for both types of crude evaluated and follow the same trend as that determined in adsorption isotherms. In this way, it is confirmed that the way in which the nanoparticle favors the disaggregation or fragmentation of asphaltene aggregate depends mainly on its adsorption capacity. The trend is: S8A = S8 < S11 < S8B < S97 < Al35 < S285 < F97. It can be inferred that the structures of the asphaltenes of both crudes are similar because it does not present any considerable difference when interacting with nanoparticles of different chemical nature, and different sizes.

1.4 Partial conclusions

- Silica nanoparticles were successfully synthesized by the sol-gel method and. Obtained materials were characterized by particle size and surface area. Commercial Silica, Alumina and Magnetite nanoparticles were purchased and also characterized by particle size and surface area, the nanoparticles resulted in mean particle diameters in the nanoscale. The trend followed by the surface area of the nanoparticles was S8 > S8A > S11 > S8B > Al35 > F97 > S97 > S285.
- The trend found in the surface area of the nanoparticles is opposite to the average size of the nanoparticles, fulfilling the stipulated by multiple researchers who affirm that to a smaller size, the nanoparticle presents greater superficial area. This is true for all nanoparticles, except when we compare S11 with S8B, the reason the surface area of the nanoparticle S8B is reduced is due to the presence of NaOH on its surface, which blocks pores considerably reducing the surface area in comparison With the completely virgin nanoparticle (S8).

- Adsorption isotherms were constructed by extracting asphaltenes from two different sources (Ho and EHO), which were dissolved in toluene to obtain the solution models. All nanoparticles have the ability to adsorb asphaltenes, from highest to lowest the trend was: S8A > S8 > S11 > S8B > S97 > Al35 > S285 > F97, this is mainly due to the interaction between polar groups of the asphaltene and the silanol group of the silica nanoparticles.
- The average size of the asphaltenes present in a solution of Heptol 40 was measured using DLS techniques. The ability of the nanoparticles to decrease the average size was also evaluated by fragmentation phenomena. The tendency was the same one presented in adsorption isotherms: S8A > S8 > S11 > S8B > S97 > Al35 > S285 > F97.

1.5 References

1. Duffus, J. H.; Nordberg, M.; Templeton, D. M., Glossary of terms used in toxicology, (IUPAC recommendations 2007). *Pure and Applied Chemistry* **2007,** 79, (7), 1153-1344.
2. Duncan, T. V., Applications of nanotechnology in food packaging and food safety: barrier materials, antimicrobials and sensors. *Journal of colloid and interface science* **2011,** 363, (1), 1-24.
3. Rashidi, L.; Khosravi-Darani, K., The applications of nanotechnology in food industry. *Critical reviews in food science and nutrition* **2011,** 51, (8), 723-730.
4. West, J. L.; Halas, N. J., Applications of nanotechnology to biotechnology: Commentary. *Current opinion in Biotechnology* **2000,** 11, (2), 215-217.
5. Davis, S., Biomedical applications of nanotechnology—implications for drug targeting and gene therapy. *Trends in biotechnology* **1997,** 15, (6), 217-224.
6. Labhasetwar, V.; Leslie-Pelecky, D. L., *Biomedical applications of nanotechnology*. John Wiley & Sons: 2007.
7. Wilkinson, J., Nanotechnology applications in medicine. *Medical device technology* **2003,** 14, (5), 29-31.
8. Hughes, M. P., AC electrokinetics: applications for nanotechnology. *Nanotechnology* **2000,** 11, (2), 124.
9. Hussein, A. K., Applications of nanotechnology in renewable energies—A comprehensive overview and understanding. *Renewable and Sustainable Energy Reviews* **2015,** 42, 460-476.
10. Qu, X.; Alvarez, P. J.; Li, Q., Applications of nanotechnology in water and wastewater treatment. *Water research* **2013,** 47, (12), 3931-3946.
11. Wong, Y.; Yuen, C.; Leung, M.; Ku, S.; Lam, H., Selected applications of nanotechnology in textiles. *AUTEX Research Journal* **2006,** 6, (1), 1-8.
12. Ge, Z.; Gao, Z., Applications of nanotechnology and nanomaterials in construction. *First Inter. Confer. Construc. Develop. Countries* **2008**, 235-240.
13. Tratnyek, P. G.; Johnson, R. L., Nanotechnologies for environmental cleanup. *Nano today* **2006,** 1, (2), 44-48.
14. Mokhatab, S.; Fresky, M. A.; Islam, M. R., Applications of nanotechnology in oil and gas E&P. *Journal of petroleum technology* **2006,** 58, (04), 48-51.
15. Amanullah, M.; Al-Tahini, A. M. In *Nano-technology-its significance in smart fluid development for oil and gas field application*, SPE Saudi Arabia Section Technical Symposium, 2009; Society of Petroleum Engineers: 2009.

16. Franco, C.; Patiño, E.; Benjumea, P.; Ruiz, M. A.; Cortés, F. B., Kinetic and thermodynamic equilibrium of asphaltenes sorption onto nanoparticles of nickel oxide supported on nanoparticulated alumina. *Fuel* **2013,** 105, 408-414.
17. Franco, C. A.; Nassar, N. N.; Ruiz, M. A.; Pereira-Almao, P.; Cortés, F. B., Nanoparticles for inhibition of asphaltenes damage: adsorption study and displacement test on porous media. *Energy & Fuels* **2013,** 27, (6), 2899-2907.
18. Mohammadi, M.; Akbari, M.; Fakhroueian, Z.; Bahramian, A.; Azin, R.; Arya, S., Inhibition of asphaltene precipitation by TiO2, SiO2, and ZrO2 nanofluids. *Energy & Fuels* **2011,** 25, (7), 3150-3156.
19. Franco, C. A.; Montoya, T.; Nassar, N. N.; Pereira-Almao, P.; Cortés, F. B., Adsorption and subsequent oxidation of colombian asphaltenes onto Nickel and/or Palladium oxide supported on fumed silica nanoparticles. *Energy & Fuels* **2013,** 27, (12), 7336-7347.
20. Nassar, N. N.; Betancur, S.; Acevedo, S.; Franco, C. A.; Cortés, F. B., Development of a Population Balance Model to Describe the Influence of Shear and Nanoparticles on the Aggregation and Fragmentation of Asphaltene Aggregates. *Industrial & Engineering Chemistry Research* **2015,** 54, (33), 8201-8211.
21. Franco, C. A.; Martínez, M.; Benjumea, P.; Patiño, E.; Cortés, F. B., Water remediation based on oil adsorption using nanosilicates functionalized with a petroleum vacuum residue. *Adsorption Science & Technology* **2014,** 32, (2-3), 197-207.
22. Nassar, N. N.; Hassan, A.; Pereira-Almao, P., Effect of the Particle Size on Asphaltene Adsorption and Catalytic Oxidation onto Alumina Particles. *Energy & Fuels* **2011,** 25, (9), 3961-3965.
23. Zabala. R, F. C. A., Cortes. F.B., Application of Nanofluids for Improving Oil Mobility in Heavy Oil and Extra-Heavy Oil: A Field Test. *Society of Petroleum Engineers Journal* **2016**, 14.
24. Bedrikovetsky, P.; Monteiro, P.; Neto, A.; Riente, A. In *Fractional flow theory for suspension flow in petroleum reservoirs*, SPE 121822 presented at 2009 SPE Latin American and Caribbean Petroleum Engineering Conference held in Cartagena, Colombia, 2009; 2009.
25. Bratli, R. K.; Risnes, R., Stability and failure of sand arches. *Society of Petroleum Engineers Journal* **1981,** 21, (02), 236-248.
26. Yu, C.; Jingen, D.; Xianmin, G.; Qian, J., Analysis of Gravel-Sizing Optimization Method for High-Pressure Gravel-Packing Sand Control. *Petroleum Science and Technology* **2011,** 29, (12), 1257-1263.
27. Nassar, N. N.; Hassan, A.; Pereira-Almao, P., Clarifying the catalytic role of NiO nanoparticles in the oxidation of asphaltenes. *Applied Catalysis A: General* **2013,** 462–463, (0), 116-120.
28. Hassan, A.; Lopez-Linares, F.; Nassar, N. N.; Carbognani-Arambarri, L.; Pereira-Almao, P., Development of a support for a NiO catalyst for selective adsorption and post-adsorption catalytic steam gasification of thermally converted asphaltenes. *Catalysis Today* **2013,** 207, (0), 112-118.
29. Nassar, N. N.; Hassan, A.; Carbognani, L.; Lopez-Linares, F.; Pereira-Almao, P., Iron oxide nanoparticles for rapid adsorption and enhanced catalytic oxidation of thermally cracked asphaltenes. *Fuel* **2012,** 95, 257–262.
30. Nassar, N. N.; Hassan, A.; Pereira-Almao, P., Comparative oxidation of adsorbed asphaltenes onto transition metal oxide nanoparticles. *Colloids and Surfaces A: Physicochemical and Engineering Aspects* **2011,** 384, (1-3), 145-149.
31. Nassar, N. N.; Hassan, A.; Pereira-Almao, P., Effect of surface acidity and basicity of aluminas on asphaltene adsorption and oxidation. *Journal of Colloid and Interface Science* **2011,** 360 233–238.
32. Nassar, N. N.; Hassan, A.; Pereira-Almao, P., Application of Nanotechnology for Heavy Oil Upgrading: Catalytic Steam Gasification/Cracking of Asphaltenes. *Energy & Fuels* **2011,** 25, (4), 1566-1570.

33. Nassar, N. N.; Hassan, A.; Pereira-Almao, P., Metal Oxide Nanoparticles for Asphaltene Adsorption and Oxidation. *Energy & Fuels* **2011,** 25, (3), 1017-1023.
34. Nassar, N. N., Asphaltene adsorption onto alumina nanoparticles: kinetics and thermodynamic studies. *Energy & Fuels* **2010,** 24, (8), 4116-4122.
35. Cortés, F. B.; Mejía, J. M.; Ruiz, M. A.; Benjumea, P.; Riffel, D. B., Sorption of asphaltenes onto nanoparticles of nickel oxide supported on nanoparticulated silica gel. *Energy & Fuels* **2012,** 26, (3), 1725-1730.
36. Brinker, C. J.; Scherer, G. W., *Sol-gel science: the physics and chemistry of sol-gel processing*. Academic press: 2013.
37. Stöber, W.; Fink, A.; Bohn, E., Controlled growth of monodisperse silica spheres in the micron size range. *Journal of colloid and interface science* **1968,** 26, (1), 62-69.
38. Rahman, I. A.; Padavettan, V., Synthesis of silica nanoparticles by sol-gel: size-dependent properties, surface modification, and applications in silica-polymer nanocomposites—a review. *Journal of Nanomaterials* **2012,** 2012, 8.
39. Taborda, E. A.; Franco, C. A.; Lopera, S. H.; Alvarado, V.; Cortés, F. B., Effect of nanoparticles/nanofluids on the rheology of heavy crude oil and its mobility on porous media at reservoir conditions. *Fuel* **2016,** 184, 222-232.
40. Rouquerol, J.; Rouquerol, F.; Llewellyn, P.; Maurin, G.; Sing, K. S., *Adsorption by powders and porous solids: principles, methodology and applications*. Academic press: 2013.
41. Brunauer, S.; Emmett, P. H.; Teller, E., Adsorption of gases in multimolecular layers. *Journal of the American chemical society* **1938,** 60, (2), 309-319.
42. Ramalho, J. B. V.; Lechuga, F. C.; Lucas, E. F., Effect of the structure of commercial poly (ethylene oxide-b-propylene oxide) demulsifier bases on the demulsification of water-in-crude oil emulsions: elucidation of the demulsification mechanism. *Química Nova* **2010,** 33, (8), 1664-1670.
43. Yudin, I. K.; Anisimov, M. A., Dynamic light scattering monitoring of asphaltene aggregation in crude oils and hydrocarbon solutions. In *Asphaltenes, Heavy Oils, and Petroleomics*, Springer: 2007; pp 439-468.
44. Rane, J. P.; Harbottle, D.; Pauchard, V.; Couzis, A.; Banerjee, S., Adsorption kinetics of asphaltenes at the oil–water interface and nanoaggregation in the bulk. *Langmuir* **2012,** 28, (26), 9986-9995.
45. Bern, B.; Pecora, R., Dynamic Light scattering with Applications to Chemistry. *Biology and Physics (Wiley, New York, 1976). JJ Fisz et al./Two-photon-excitation fluorescence depolarization in solutions* 207.
46. Bowen, P., Particle size distribution measurement from millimeters to nanometers and from rods to platelets. *Journal of Dispersion Science and Technology* **2002,** 23, (5), 631-662.
47. Nassar, N. N.; Hassan, A.; Vitale, G., Comparing kinetics and mechanism of adsorption and thermo-oxidative decomposition of Athabasca asphaltenes onto TiO 2, ZrO 2, and CeO 2 nanoparticles. *Applied Catalysis A: General* **2014,** 484, 161-171.
48. Guzmán, J. D.; Betancur, S.; Carrasco-Marín, F.; Franco, C. A.; Nassar, N. N.; Cortés, F. B., Importance of the Adsorption Method Used for Obtaining the Nanoparticle Dosage for Asphaltene-Related Treatments. *Energy & Fuels* **2016,** 30, (3), 2052-2059.
49. Talu, O.; Meunier, F., Adsorption of associating molecules in micropores and application to water on carbon. *AIChE journal* **1996,** 42, (3), 809-819.
50. Tatiana Montoya, D. C., Camilo Franco, Nashaat Nassar, Farid Cortés, A Novel Solid-Liquid Equilibrium Model for Describing the Adsorption of Associating Asphaltene Molecules onto Non-Porous Surfaces Based on the "Chemical Theory". *Energy & Fuels* **2014**.
51. Smith, J. M.; Van Ness, H. C.; Abbott, M. M., *Introduction to chemical engineering thermodynamics*. Boston: McGraw-Hill; 7th ed.: 2005.
52. Montgomery, D. C.; Runger, G. C., *Applied statistics and probability for engineers*. John Wiley & Sons: 2010.

53. Dabbaghian, M.; Babalou, A.; Hadi, P.; Jannatdoust, E., A parametric study of the synthesis of silica nanoparticles via sol-gel precipitation method. *International Journal of Nanoscience and Nanotechnology* **2010,** 6, (2), 104-113.
54. Akbari, B.; Tavandashti, M. P.; Zandrahimi, M., Particle Size Characterization of Nanoparticles–A Practicalapproach. *Iranian Journal of Materials Science and Engineering* **2011,** 8, (2), 48-56.
55. Chopra, S.; Lines, L. R.; Schmitt, D. R.; Batzle, M. L., *Heavy oils: reservoir characterization and production monitoring*. Society of Exploration Geophysicists Tulsa, OK: 2010.
56. Pachón, Z. Determinación de las propiedades petrofísicas de rocas de yacimientos petrolíferos colombianos por métodos de relajación de resonancia magnética nuclear Universidad Industrial de Santander, 2005.
57. Montoya, T.; Coral, D.; Franco, C. A.; Nassar, N. N.; Cortés, F. B., A novel solid–liquid equilibrium model for describing the adsorption of associating asphaltene molecules onto solid surfaces based on the "Chemical Theory". *Energy & Fuels* **2014,** 28, (8), 4963-4975.
58. Nassar, N. N.; Hassan, A.; Pereira-Almao, P., Effect of surface acidity and basicity of aluminas on asphaltene adsorption and oxidation. *Journal of colloid and interface science* **2011,** 360, (1), 233-238.
59. Guzmán, J. D.; Betancur, S.; Carrasco-Marín, F.; Franco, C. A.; Nassar, N. N.; Cortés, F. B., Importance of the Adsorption Method Used for Obtaining the Nanoparticle Dosage for Asphaltene-Related Treatments. *Energy & Fuels* **2016**.
60. Adams, J. J., Asphaltene adsorption, a literature review. *Energy & Fuels* **2014,** 28, (5), 2831-2856.
61. Shayan, N. N.; Mirzayi, B., Adsorption and Removal of Asphaltene Using Synthesized Maghemite and Hematite Nanoparticles. *Energy & Fuels* **2015,** 29, (3), 1397-1406.
62. Betancur, S. Desarrollo de Nanopartículas basadas en Sílice para la Inhibición de la Precipitación/Depositación de Asfaltenos Universidad Nacional de Colombia, Medellín, Colombia, 2015.
63. Acevedo, S.; Castillo, J.; Fernández, A.; Goncalves, S.; Ranaudo, M. A., A study of multilayer adsorption of asphaltenes on glass surfaces by photothermal surface deformation. Relation of this adsorption to aggregate formation in solution. *Energy & fuels* **1998,** 12, (2), 386-390.
64. Mullins, O. C.; Betancourt, S. S.; Cribbs, M. E.; Dubost, F. X.; Creek, J. L.; Andrews, A. B.; Venkataramanan, L., The colloidal structure of crude oil and the structure of oil reservoirs. *Energy & Fuels* **2007,** 21, (5), 2785-2794.
65. Spiecker, P. M.; Gawrys, K. L.; Kilpatrick, P. K., Aggregation and solubility behavior of asphaltenes and their subfractions. *Journal of colloid and interface science* **2003,** 267, (1), 178-193.

2. Reduction of the viscosity of heavy crude by addition of nanoparticles: Steady state rheology.

Heavy (HO) and extra – heavy crude oils (EHO) are attractive for the oil and gas industry due to the existence of vast reserves. However, their main characteristics, i.e. high density and elevated viscosity that negatively impacts oil mobility at both reservoir and surface conditions, challenge HO and EHO production, transport and refining. In terms of density, HO lies in the range of 10 to 20 °API,[1-3] while EHO has a specific gravity lower than 10.[1, 3, 4] Additionally, other features of these crude oils are a high percentage of heteroatoms, mainly N, O and S,[1, 5-7] metals (features such as V, Ni)[5] and an elevated fraction of asphaltenes.[8, 9] Asphaltenes have been extensively studied,[5, 10-18] being the most polar oil fraction, with complex chemical structures with a low ratio of aliphatic/aromatic chains.[11, 14, 19, 20] Asphaltenes possess structures containing heteroatoms that allow self-aggregation, initially leading to colloidal aggregates, promoting the growth of the aggregates and consequently increasing oil viscosity.[6, 21] The increase in viscosity is mostly due to the formation of a viscoelastic network of interacting asphaltenes nanoaggregates.[14, 22] also, sulfur can form strong C-S and C=S bonds, which can also contribute to an increase in the crude oil viscosity.[6, 23]

Viscosity is a very important property in the treatment and management of HO and EHO, so improving oil mobility at reservoir or surface conditions has become a challenge for the Oil & Gas industry at present.[24] The most commonly used techniques to improve HO and EHO mobility are economically and environmentally costly,[25-27] including 1) dilution techniques with several (toxic) chemical diluents involving high volumetric consumption; this requires intensive maintenance of pipelines and storage systems as diluents tend to be corrosives[26, 28-30] and 2) thermal techniques that are highly costly due to the energy consumption.[27, 31-34] Mortazavi-Manesh and Shaw [35] studied the effect of different types of chemical compounds on rheological properties of Maya crude oil at different temperatures. The compounds used in their study were toluene, n-heptane and a 50/50 vol% mixture of toluene and butanone. The rheological evaluation was performed using steady-state methods at shear rates 0-200 s^{-1}; as expected, dilution and temperature increase reduced oil viscosity.

These mixtures exhibit a characteristic non-Newtonian shear-thinning behavior, but with increasing temperature, the Newtonian behavior becomes dominant. Diluents in decreasing viscosity reduction effectiveness for the entire range evaluated are a mixture of toluene-butanone > toluene > n-heptane. Earlier, Mortazavi-Manesh and Shaw [36] characterized Maya crude oil to investigate its thixotropic characteristics as a function of temperature to determine the influence of time on viscosity measurements. The authors demonstrated that the thixotropic behavior of this oil increases as temperature decreases. Authors performed thixotropy measurements based on three tools widely used: hysteresis loops, step-wise change in shear rate and start-up experiments. The results are useful to optimize pipeline transport conditions, mainly in processes where pressure is required to restart fluid flow.

More recently, nanotechnology has emerged as a technique able to compete economically and technically against conventional processes.[13, 37-40] One of the appealing characteristics of nanoparticles is their small size and consequently their large surface area-to-volume ratio,[37, 39, 41] dispersibility,[37, 39, 41] and high adsorption affinity due to their energy surface.[13, 39, 41-45] Several researchers have demonstrated the application of nanotechnology in several areas in the Oil & Gas industry.[13, 38, 39, 44, 46-50] Our group has pioneered the use of nanofluids for reducing the viscosity of HO and EHO, which has been tested in "huff-puff" pilot tests. [13, 38, 39, 51-55] These studies have confirmed that some nanofluids can be used to reduce the viscosity of these crude oils at surface conditions. These nanofluids may feature strong interactions with the asphaltenes and induce aggregate reduction due to their ability to adsorb them as well as other molecules present in HO and EHO. The latter properties can positively impact the viscoelastic network of nanoaggregates reducing the viscosity of these crude oils. In contrast, the specialized open literature contains no research work associated with HO and EHO viscosity reduction with the addition of solid particles of nanometric size.

On the other hand, some of the earlier use of nano or micro-particles on fluids, except in HO and EHO, led to a viscosity increase.[56-60] This can be explained by Einstein's theory on hydrodynamic viscosity,[56] which suggests that an increase in fluid viscosity should occur upon addition of solid particles that is directly proportional to the volume fraction of solids added. However, the proposed model does not fit adequately many fluids assessed, and for that reason several researchers have proposed modified mathematical models derived from Einstein's equation[56, 61] such as Money,[59] Eilers,[62] Roscoe,[63] Chong,[64] Maron and Pierce,[65] Krieger and Dougherty.[66] These models often represent a better approximation to the viscosity response of different types of suspensions than Einstein's equation.[67, 68] For applications in crude oils, some authors have studied the addition of asphaltenes in an attempt to understand the viscosity behavior of HO and EHO, which has been

shown to increase drastically as the asphaltene fraction increases. Other authors have experimentally studied and modeled the rheological behavior of emulsions W/O.[69-74] Recently, Pal and Rhodes[68] proposed a non-Newtonian shear model based on Einstein´s theory, which has been applied to explain the behavior of the viscosity of several crude oils and de-asphalted oils (DAO) varying their content of asphaltenes by the addition. The model is as follows:

$$n_r = (1 - K_o\phi)^{-2.5} \quad (1)$$

Where n_r is the relative viscosity, ϕ corresponds to the volume fraction of dispersed particles, and K_o is the solvation constant, which relates to the immobilization of the continuous phase on the dispersed particles surface, so for spherical particles, the form factor is 2.5. As can be seen in Eq. (1), the value of viscosity increases when the volume fraction of dispersed particles is large. This study relied on adding asphaltenes to crude oils and de-asphalting oils. Luo and Gu[75] developed a generalized model based on the Pal & Rhodes' model:[67, 76]

$$n_r = (1 - K_o\phi)^{-V} \quad (2)$$

Where V refers to the "shape factor," varying according to the type of particle. The other parameters, ϕ and K_o, are described by Phal and Rhodes.[75, 76] This model has been successfully applied to describe the viscosity response of crude oils (HO, EHO, and de-asphalted oil) to the addition of asphaltenes at different temperatures (293-333 K). The authors consider asphaltenes as semisolid particles, and for this reason one expects the viscosity to increase the higher the asphaltene content.[11, 14, 68, 77] Similarly, multiple authors have modeled the viscosity of heavy crude as a function of asphaltene content with conventional models derived from Einstein's equation.[68, 70, 73-75]

To the best of our knowledge, the effect of solid nanoparticles on HO & EHO properties has not yet been studied, either experimental or theoretically, thus the novelty of this paper. Here we provide a rheological characterization of heavy and extra heavy oils containing NP´s of different chemicals nature, particle size, surface acidity and concentrations of nanoparticles. These results are contrasted with measurements in the absence of NP's. In addition, a first mathematical approach based on Pal and Rhodes model for describing the viscosity reduction of crude oils containing a low concentration (ϕ) of nanoparticles (ϕ < 0.004). Our experimental and theoretical study sheds light on phenomena associated with the inclusion of nanoparticles in the crude oil matrix for futures applications in the Oil & Gas Industry.

2.1 Experimental

2.1.1 Materials

Commercial nanoparticles of fumed silica (S8, S12, and S285), magnetite (F97), γ-alumina (Al35), and in house synthesized nanoparticles of silica (S97, S8A, and S8B) were used as viscosity reducers agents. The commercial nanoparticles of fumed silica, and γ-alumina were obtained from Sigma-Aldrich (St. Louis, MO) and commercial magnetite nanoparticles from Nanostructured & Amorphous Materials (Houston, TX).

Tetraethyl orthosilicate (TEOS, > 99%), ethanol (99.9%) and NH_4OH (28%) were used to synthesize the silica nanoparticles. All reactants employed for the synthesis were purchased from Sigma-Aldrich (St. Louis, MO). For SiO_2 nanoparticles surface modification, H2SO4 (95-97%, Merck KGaA, Germany) and NH4OH (28%, Sigma-Aldrich, St. Louis, MO) was used.

Two Colombian oils were used as heavy oil (HO) and extra heavy oil (EHO). The properties of the selected HO and EHO are presented in Table 1.1.

More information about materials and characterization methods are described in chapter 1.

2.1.2 Methods

- **Evaluation of nanoparticles as viscosity reducers**

Rheological measurements were performed using a Kinexus Pro+ rotational rheometer (Malvern Instruments, Worcestershire - UK), equipped with a Peltier plate for temperature control, with a 20-mm serrated plate-plate geometry at a gap of 300 μm. To analyze the change in viscosity induced by the addition of nanoparticles, several conditions were evaluated, including the effect of concentration, particle size and the nanoparticle chemical nature. The rheological measurements were conducted at 298 K at a shear rate range of 1-75 s^{-1}. Each experimental condition set was repeated three times. Nanoparticles were mixed with the oil by stirring at 500 rpm for 30 min at room temperature until homogenization with a mixer model HP130915Q from Thermo Scientific (Waltham, Massachusetts, USA).

- *Nanoparticle concentration effect.*

The S8 sample was selected to evaluate the effect of concentration on the rheological properties of the HO matrix. In previous works[13, 39, 46, 78] we demonstrated that S8 nanoparticles had a great affinity for the asphaltenes and heavy compounds in oil, reducing the asphaltenes aggregates size present in

the HO matrix. For this reason, the addition of these particles should positively affect oil rheological properties, mainly by reducing the HO viscosity. The concentrations tested were 10, 100, 1000 and 10000 mg/L.

- *Nanoparticle size effect.*

SiO_2 nanoparticles were selected to evaluate the size effect on rheological properties. We choose a single nanoparticle concentration that yields the largest viscosity reduction, among all the evaluated cases in the previous step. The nanoparticles selected were S8, S12, S97, and S285.

- *Nanoparticle chemical nature effect.*

To study the effect of nanoparticles chemical nature on HO viscosity, S8, S8A, S8B, Al35, and F97 nanoparticles were used at a fixed concentration of 1000 mg/L, which is the optimal value determined aforementioned concentration tests.

- *Temperature and high shear rate effect.*

The S8 nanoparticle at 1000 mg/L was selected to evaluate the effect of temperature on the rheological properties of the HO matrix. The concentration of 1000 mg/L was selected according to the greatest viscosity reduction from all the measurements above. The temperatures evaluated was 298, 318, and 333 K respectively. The shear rate range of evaluation was 0 – 500 s^{-1}.

- *Effect of oil chemical nature.*

Two crude matrices were evaluated, i.e. HO and EHO. The type of nanoparticle and their concentration in these tests was selected according to the greatest viscosity reduction from all the aforementioned measurements.

2.2 Modeling

2.2.1 Pal and rhodes modified model

The model proposed by Pal and Rhodes [67, 75] allows one to calculate the viscosity of HO suspensions where asphaltene aggregates are considered semi-solid particles or colloids embedded in the matrix of the HO. In multiple works proposed by several researchers,[62, 68-70, 73, 74, 79] the model is applied to

heavy crudes with different contents of asphaltenes. The viscosity is found to increase concomitantly with the increase in asphaltene content clearly, and the model fits the experimental data well. However, in our particular case, when oil is in the presence of nanoparticles at low concentration, the viscosity decreases significantly. The nanoparticles are purported to interact with the asphaltenes aggregates, reducing their average size by reducing the interaction energy between the nanoparticles and asphaltenes, consequently changing the asphaltene colloidal structure. This, in turn, redistributes and generates a decrease in viscosity.[78, 80] Therefore, a disaggregation phenomenon is happening instead of an asphaltenes aggregation process.[78]

Based on the observed viscosity behavior of the HO and EHO, the Pal and Rhodes model is modified.[75, 76] Our approach was validated using the experimental rheological results varying the S8 nanoparticles concentration (0, 10, 100, and 1000 mg/L). These values are equivalent to volume fractions of 0, 3.7 x 10^{-6}, 3.7 x 10^{-5}, and 3.7 x 10^{-4}, correspondingly, which were estimated using a theoretical density for SiO_2 = 2.65 gr/cm3. Therefore, it is possible to obtain a mathematical approach that matches what is obtained in the laboratory for a fixed shear rate (γ). The proposed model is shown in Eq. (3):

$$n_r = (1 + K_o\phi)^{-V} \tag{3}$$

Similarly, n_r, the relative viscosity, ϕ is the volume fraction of dispersed particles, K_o is the solvation constant, K_o is the solvation constant, which relates to the immobilization of the continuous phase on the dispersed particles surface, so for spherical particles, the form factor is 2.5 and V is the "shape factor" of dispersed particles. The goodness of fit of the proposed model was evaluated through the correlation coefficient R2 and root-mean-square error (RSME%):[81]

$$RSME\% = 100\sqrt{\frac{1}{k}\left[\sum_{1}^{k}\left(\frac{\mu_{\exp} - \mu_{calc}}{\mu_{calc}}\right)^2\right]} \tag{4}$$

where k is the number of observations and $\mu_{\exp}$ and μ_{calc} are the observed and calculated values of viscosity, respectively.

2.3 Results

A group of several nanoparticles was evaluated, and for this reason, the concentration effect of nanoparticles was first tested, then the best-performing one was selected to evaluate the effect of particle size. Posteriorly, the chemical nature of nanoparticle and heavy oil effect were evaluated by testing two types of crude oils.

2.3.1 Nanoparticle concentration effect

Figure 2.1 shows the experimental rheological measurement of HO matrix in the presence of S8 nanoparticles at concentrations of 10, 100, 1000, and 10000 mg/L. It is observed that by increasing the concentration of nanoparticles in the medium, the viscosity tends to decrease. This occurs up to the optimal concentration of 1000 mg/L is reached. For a concentration of 10,000 mg/L the viscosity reduction still occurs, though smaller compared to the optimal concentration. This might be possibly due to an increase in the packing factor of the particles, which can cause nanoparticles aggregation, as such reduces the energy of interactions among asphaltenes aggregates present in the fluid.

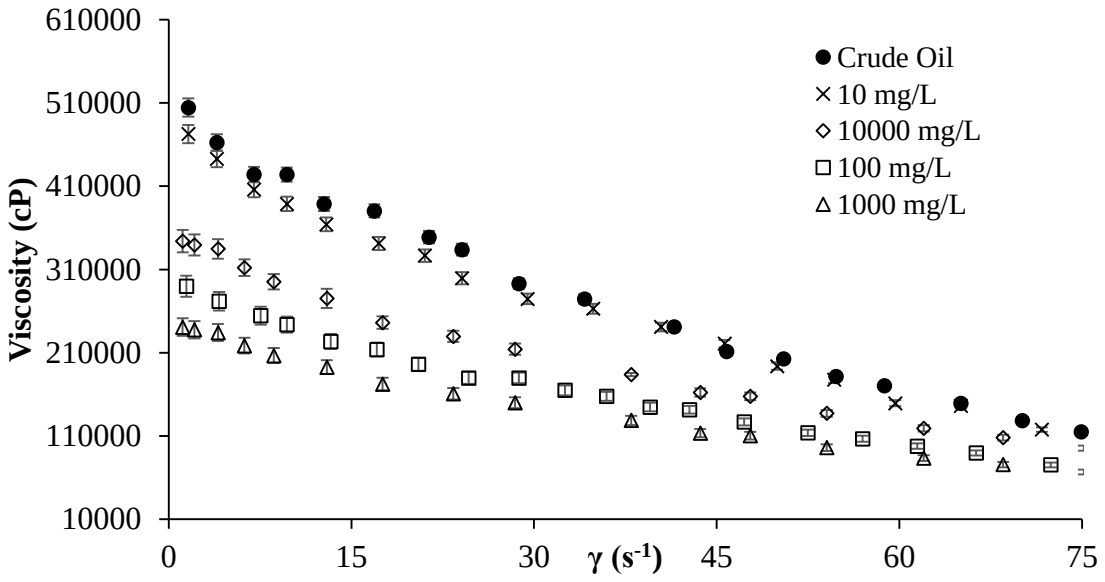

Figure 2.1 Viscosity of heavy oil in the presence of SiO_2 nanoparticles at different concentrations at 298 K and shear rate between 0 and 75 s^{-1}.

The degree of viscosity reduction (DVR), see Eq. (6)[9], is defined and calculated by:

$$DVR\% = \frac{\left(\mu_{HO} - \mu_{np}\right)}{\mu_{HO}} \times 100 \quad (6)$$

where, μ_{HO} and μ_{np} are the crude oil before and the after-nanoparticle-inclusion viscosity values, measured at shear rates between 0 and 75 s^{-1}, respectively.

In Figure 2.2 the DVR% for S8 nanoparticles at 10, 100, 1000 and 10000 mg/L for different shear rates (0 -75 s^{-1}) are shown. The values of DVR show that the optimal concentration at which the greatest change in viscosity occurs is 1000 mg/L for all shear rates. The lowest concentration tested (10 mg/L) generates average reductions in viscosity of roughly 3%. The increasing shear rate slightly decreases the DVR benefit, which is mainly due to a change in the internal structure of the fluid [8, 36] that causes a decrease in viscosity. For this reason, the oil viscosity without nanoparticles is lower at high shear rates than low shear rates, and although the nanoparticles have an effect on any shear rate, its performance is slightly lower.

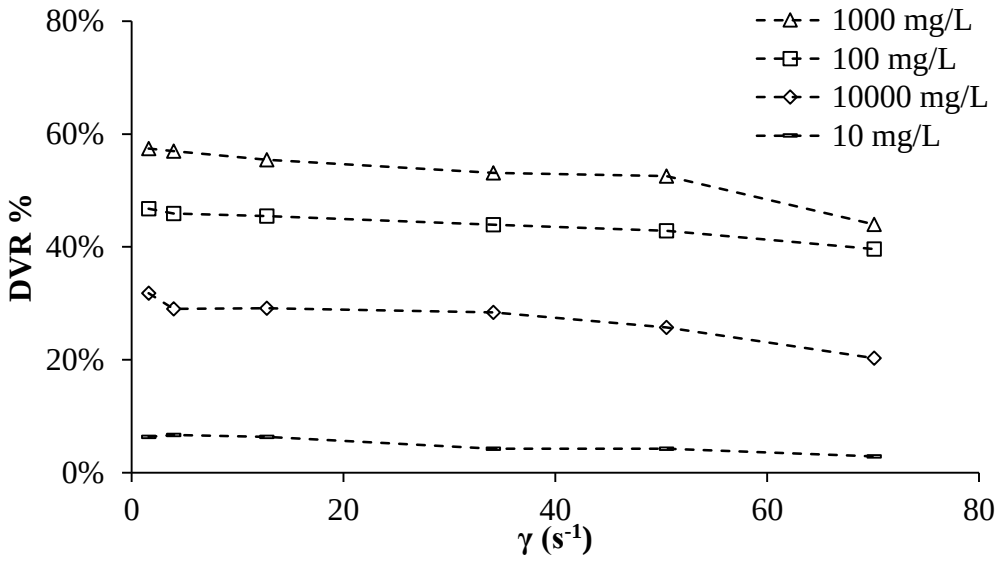

Figure 2.2 The degree of viscosity reduction of HO matrix on silica nanoparticles of different sizes presence, at 298 K and shear rate between 0-75 s^{-1}.

The modified Pal and Rhodes model were used to evaluating the experimental data for fixed shear rates. In Figure 2.3, the evaluation of model is presented for a fixed shear rate of 6 s^{-1} for all volume fractions. The modified Pal and Rhodes model have an acceptable fit to the experimental data at the shear rates evaluated. As the concentration of nanoparticles in the fluid increases, the relative viscosity decreases for the range evaluates from the minimum volumetric fraction until the optimum

point, that is a volume fraction of 3.7 X 10^{-4}, and can benefit from an interesting mathematical approach that can explain the phenomena.

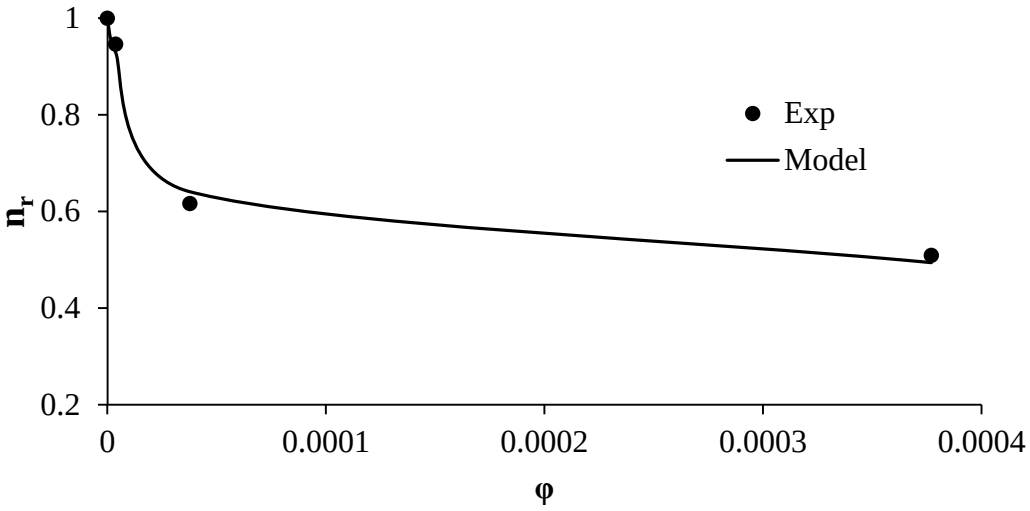

Figure 2.3 Modified Pal and Rhodes model evaluation for S8 nanoparticles at different volume fractions, at 298 K and shear rate 6 s^{-1}

The mathematical model developed here readily explains the beneficial effect of nanoparticles. In Figure 2.4, the K and V parameters are shown for all shear rates evaluated. The values of parameters are presented in Table 2.1. The model fits well, as evidenced by the RSME% value less than 10%. The solvation constant (K) decreases as the shear rate increases, due to an increase in the fluidity of crude oil as its rheological behavior is pseudo-plastic or shear thinning.[36, 82] The shape factor V depends significantly on the geometric shape of asphaltene-nanoparticle. Asphaltenes aggregate onto nanoparticles[10, 11, 80] modifying the nanoparticles apparent geometry and as the shear rate increases, the V parameter follows to slightly increased trend; this is due to the alteration of the geometry of asphaltene-nanoparticle by increased the medium turbulence.

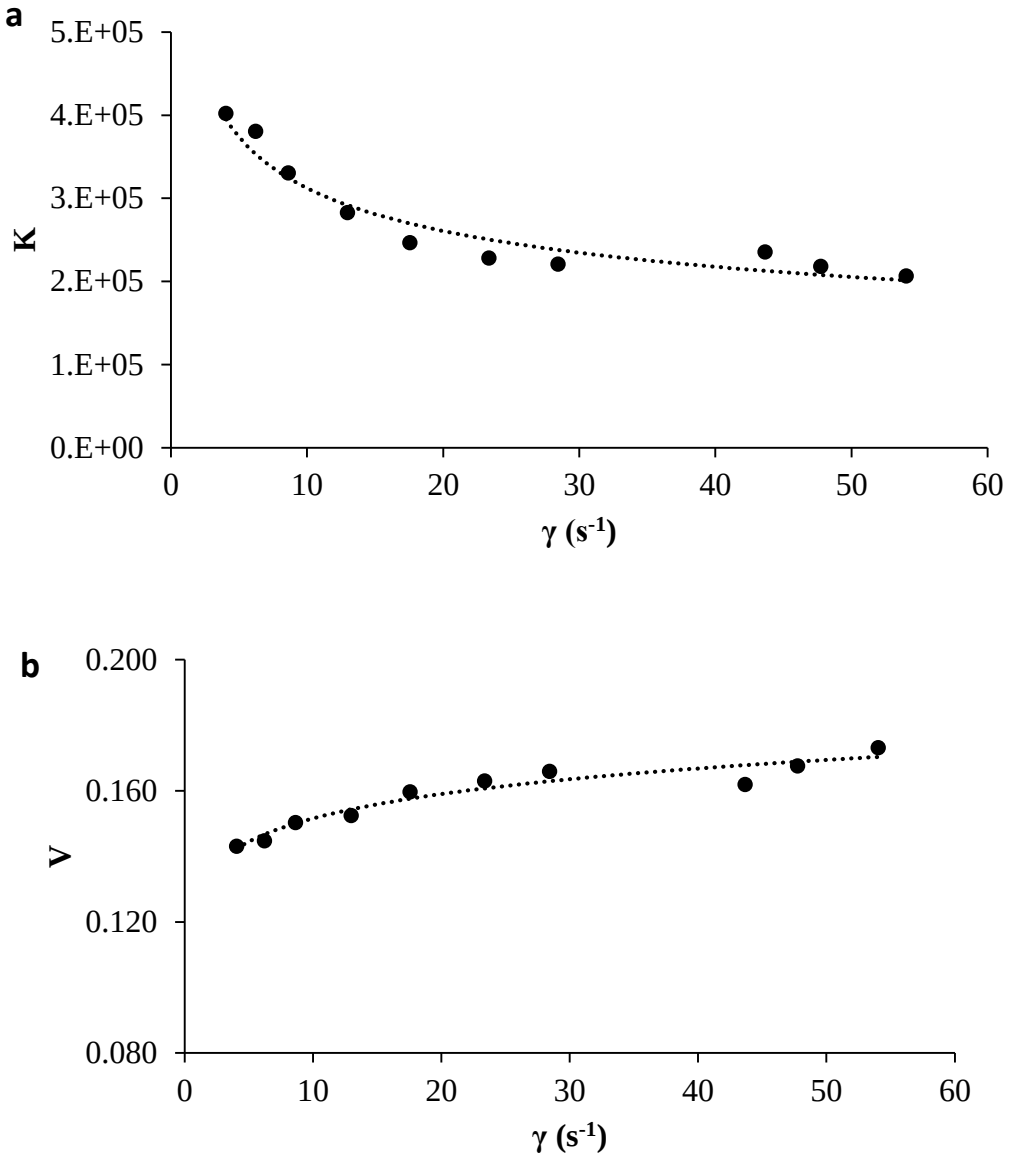

Figure 2.4 a) K and b) V parameters of Pal and Rhodes modified model for S8 nanoparticles at different volume fractions at 298 K and shear rate between 0 and 60 s^{-1}.

Table 2.1 Parameters of Pal and Rhodes modified model for S8 nanoparticles at different volume fractions, at 298 K and shear rate between 0 and 54 s^{-1}.

γ (s^{-1})	K x10^5	V	R^2	RSME (%)
4.0	4.02	0.143	0.96	8.05
6.2	3.80	0.145	0.98	6.08
8.6	3.31	0.150	0.97	7.32
13.0	2.82	0.152	0.97	8.55
17.6	2.46	0.160	0.97	8.84
23.4	2.28	0.163	0.95	9.49
28.4	2.20	0.166	0.97	8.36
43.6	2.35	0.162	0.97	8.12
47.8	2.18	0.168	0.97	7.59
54.0	2.07	0.173	0.96	8.50

2.3.2 Nanoparticle size effect

Figure 2.5 shows the experimental rheological measurements of HO in the presence of SiO_2 nanoparticles with different sizes at 1000 mg/L. For this section, four nanoparticles of different sizes ranging from 8 to 285 nm were evaluated. The viscosity reduction in the HO matrix increases as nanoparticle size decreases. At a fixed concentration or lower than that, there is a larger number of individual nanoparticles interacting with asphaltene aggregates, which increases the contact area and tends to further fragmentation of these heavy hydrocarbons. Consequently, the viscosity change may be generated by an internal redistribution with smaller aggregates.[78]

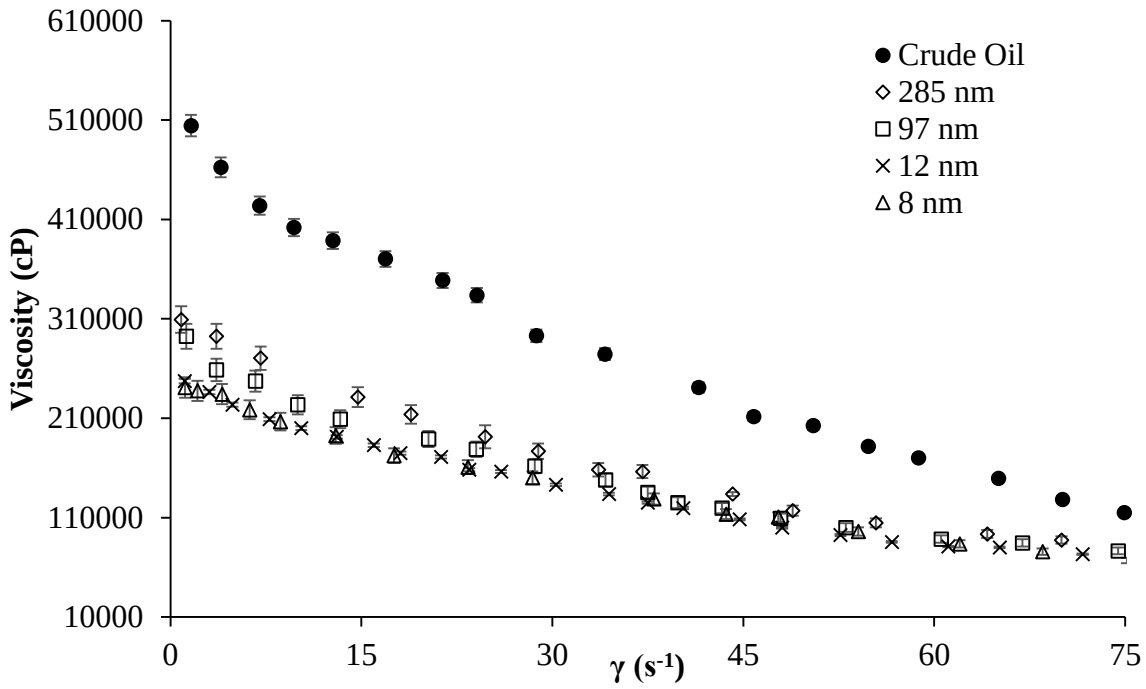

Figure 2.5 Viscosity of heavy oil in absence and presence of SiO_2 nanoparticles of different sizes at 1000 mg/L, 298 K and shear rate between 0 and 75 s^{-1}.

In Figure 2.6, the DVR% for S8, S12, S97 and S285 nanoparticles at different shear rates in the 0 - 75 s^{-1} range is shown. As the shear rates increases, the degree of viscosity reduction is lowered due to a partial breakdown of the internal structure.[9, 36, 83, 84] Despite the latter, the nanoparticles remain effective.

The S8 nanoparticle is the best-performing system among cases evaluated, allowing viscosity reductions of 42-55%. The S285 sample is the one with the lowest DVR; nevertheless, it has an acceptable performance with reductions in viscosity between 30 and 40%. As per our results, all evaluated nanoparticles produce a decrease in fluid viscosity at all shear rates. As the particle size increases, a decrease in performance is noticed. From 8 to 12 nm, the difference is very small, but as the size increases, the change in the DVR comparing with the S8 nanoparticles also increase.

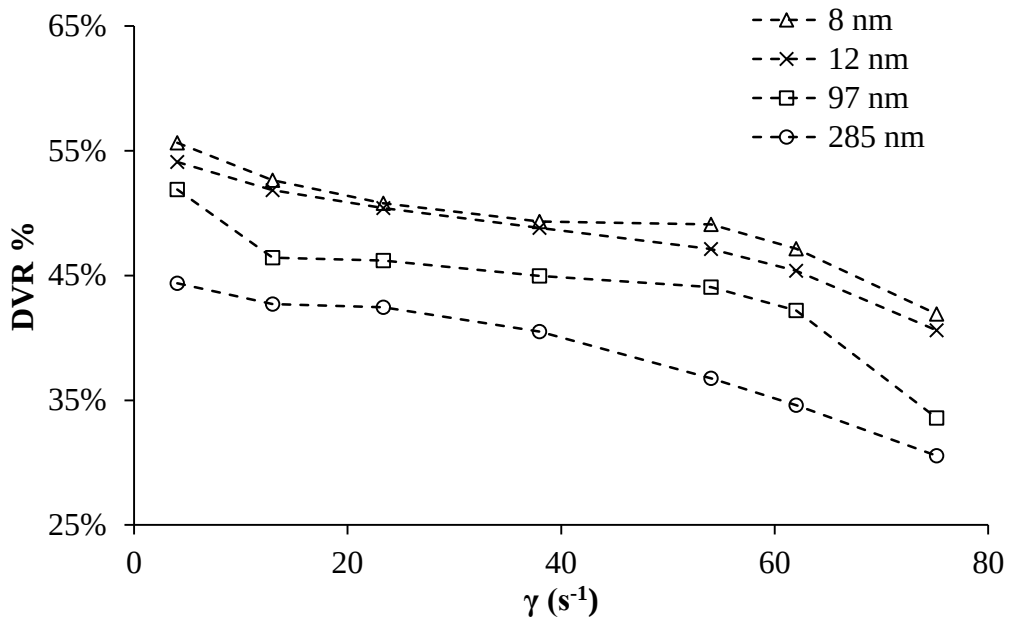

Figure 2.6 The degree of viscosity reduction of heavy oil in the presence of SiO_2 nanoparticles of different sizes at 1000 mg/L, 298 K and shear rate between 0 and 75 s^{-1}.

2.3.3 Nanoparticle chemical nature effect.

Figure 2.7 shows the experimental rheological measurements of HO in the presence of SiO_2 nanoparticles with different acidic-basic surfaces, Al_2O_3, and Fe_3O_4 nanoparticles at 1000 mg/L. For this reason, S8, S8A, S8B, Al35, and F97 were mixed in an HO matrix interacting with the heavy compounds of crude oil affecting their colloidal state.[78, 80] It is worth mentioning that asphaltenes have been proposed to exhibit a colloidal behavior with the ability to self-associate.[78, 80] By increasing asphaltene concentration in the heavy oil, aggregate size also increases, and when the concentration reaches the asphaltene critical micelle concentration (CMC), i.e. the concentration at which micelles large aggregates that directly impact viscosity form, increasing its value dramatically,[11, 85, 86] the viscosity is expected to increase significantly.[9, 14, 75, 80, 87] However, the self-association of asphaltenes can be inhibited to different degrees depending on the nanoparticles chemical nature.[78, 88] Our results indicate that all samples exhibit a viscosity reduction. The ability to reduce viscosity follows the order S8 > Al35 ≈ F35 > S8A > S8B. The attraction forces between the nanoparticles and asphaltenes are higher for S8, happening due to the formation of silanol groups (SiOH), but also because of the surface area (S_{BET}) that is the highest value of all nanoparticles evaluated. For that reason, the greatest contact area and more active centers for interacting with the *i*-mer of asphaltenes are available for these particles. The Al35 and F35 nanoparticles showed a

similar behavior and the surface area (S_{Bet}) has similar values; the interaction forces respond to the chemical interaction with the heteroatoms of asphaltene aggregates.[78] For S8A and S8B nanoparticles, the surface acid modification affects the interaction forces; this depends on the quantity of basic and acid centers of asphaltenes, and for this case, it has a better impact on a nanoparticle neutral surface. On previous works the affinity of the nanoparticles evaluated produced a fragmentation of the asphaltenes aggregates[78] affecting their colloidal structure and the internal structure of the crude oil, generating an HO viscosity reduction.

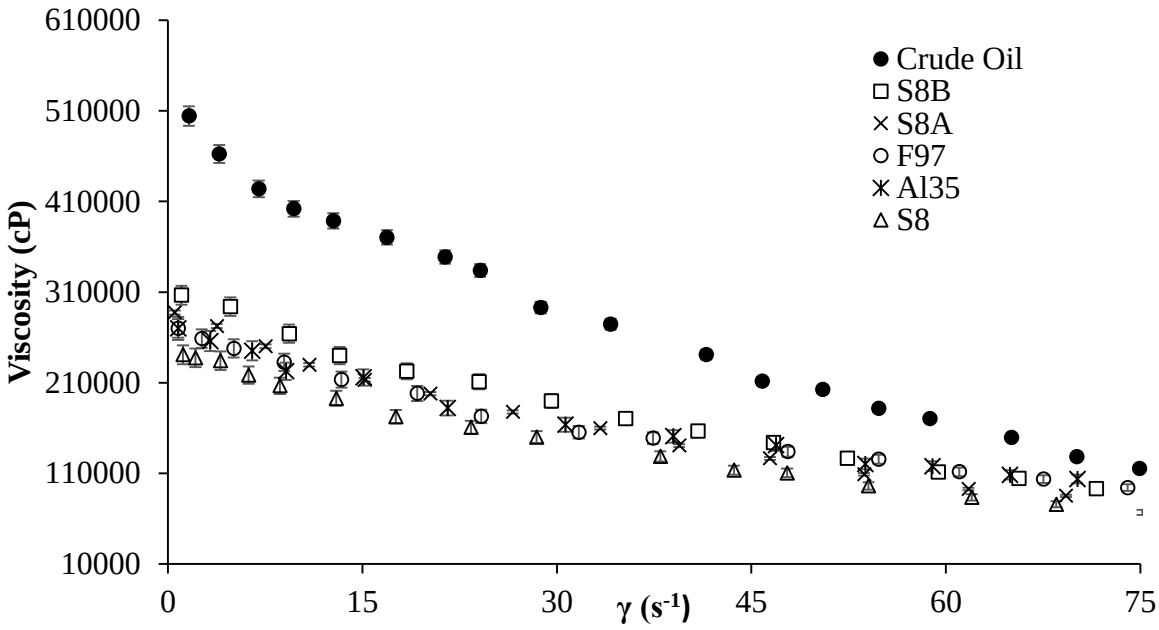

Figure 2.7 Viscosity of heavy oil in absence and presence of S8, S8A, S8B, Al35 and F97 nanoparticles at 1000 mg/L, 298 K and shear rate between 0 and 75 s^{-1}.

According to the results, the S8 nanoparticle has the best performance on the HO viscosity reduction. For this reason, this sample was selected to evaluate the effect of oil chemical nature.

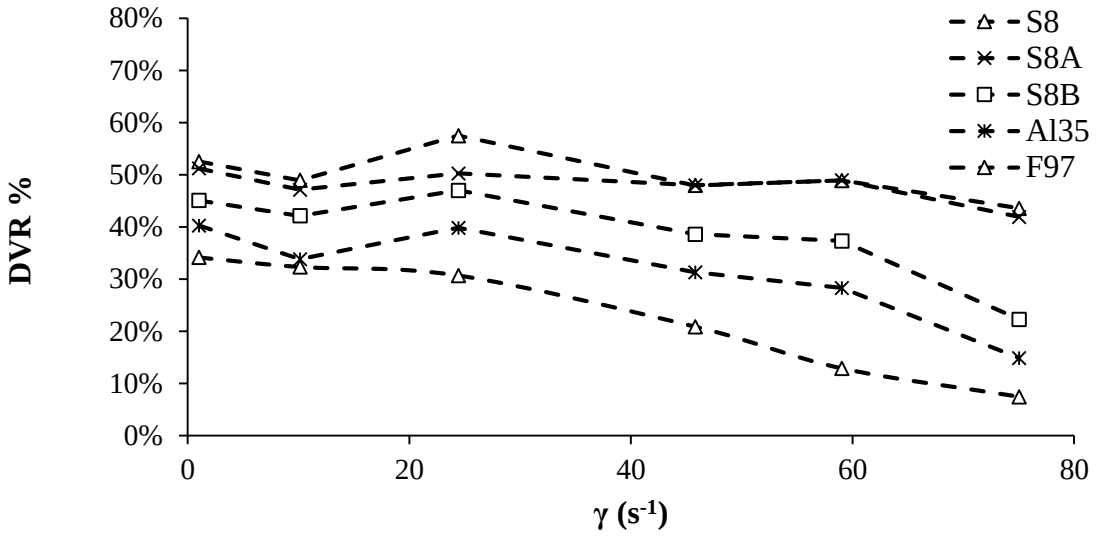

Figure 2.8 The degree of viscosity reduction of heavy oil in the presence of nanoparticles of different chemical nature at 1000 mg/L, 298 K and shear rate between 0 and 75 s^{-1}.

2.3.4 Temperature and high share rate effect.

The S8 nanoparticles at 1000mg/L exhibit the best performance. Therefore, we selected this nanoparticle to evaluate three different temperatures at high shear rates. The temperatures evaluated were 298, 318, and 333 K respectively, for shear rates between 0 and 500 s^{-1}. In Figure 2.9 shows the rheological responses for heavy oil matrix in the presence or absence of S8 nanoparticles at 298, 318 and 333 K, and at shear rates between 0 - 500 s^{-1}. The assessed concentration is 1000 mg/L, which is the value that has greater viscosity reduction previous evaluations concentration effect, as shown in Figure 1. The degree of viscosity reduction (DVR) for all temperatures tested is also presented.

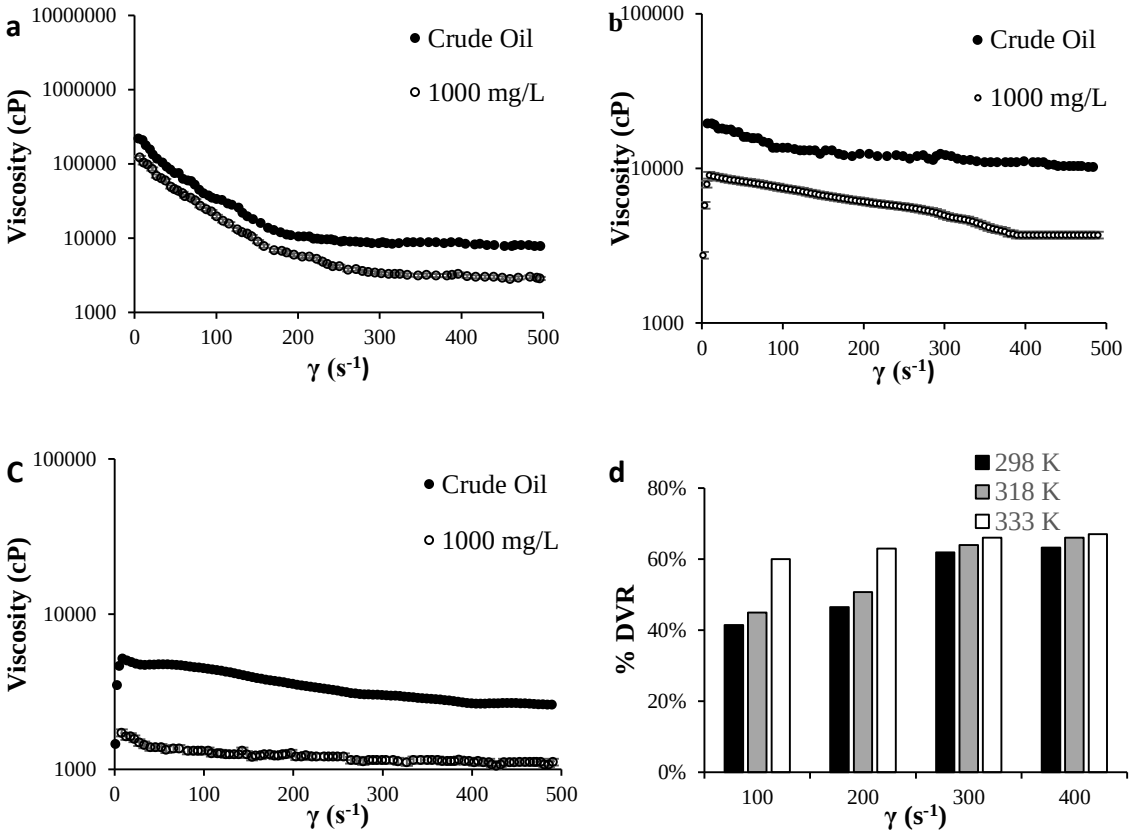

Figure 2.9 Rheological behavior of heavy oil in the presence of 1000 mg/L of S8 nanoparticles or their absence at a) 298 K, b) 318 K, and c) 333 K and the d) degree of viscosity reduction at shear rates between 0 and 500 s^{-1}.

At 298 K the fluid presents a pseudo-plastic type shear thinning behavior typical of these fluids [8, 35, 89]. This behavior wherein the viscosity decreases as shear rate increases are on notably due to the presence of asphaltenes and its tendency to self-aggregate [90, 91], for that reason as the stirring conditions increase, the internal structure is reorganized, producing that the viscosity decreases with increasing shear rate. With increasing temperature, the fluid exhibits a behavior close to a Newtonian fluid. These results are similar to those previously published by Shaw's research group [35, 36], namely that as the temperature increases the oil transitions from a non-Newtonian behavior to Newtonian one. This behavior can be noticed at high shear rates (> 300 s^{-1}) wherein the viscosity becomes constant.

In all scenarios evaluated, S8 nanoparticles produce heavy oil viscosity reduction. The best performance occurs when the temperature increases, with viscosity reduction of roughly 60%. By increasing the temperature and agitation, the oil viscosity decreases for that reason promoting the

dispersion of nanoparticles into the medium, since the liquid provides less resistance to movement of the solid particles. As the dispersion of the particles increases, the interactions between the heavy components of crude and nanoparticles is increased, favoring the viscosity reduction. This situation suggests that there is a synergistic effect between the inclusion of nanoparticles and temperature, which improves the viscosity reduction is controlled by adsorption of asphaltenes onto the nanoparticles and the diffusion of asphaltenes increased through the liquid medium [92].

If we consider that in the production process and transport, heavy oil is subjected to different conditions of temperature and agitation; one may consider adding nanoparticles as a promising technique to optimize the conditions for mobility of heavy oil by reducing its viscosity.

2.3.5 Heavy crude oil effect.

The S8 nanoparticles exhibit the best performance and therefore, we selected this nanoparticle to evaluate two different heavy crude oils. The first one is HO with 13°API, and the second is EHO with 6.4°API. Figure 2.10 depicts the rheological measurements for HO and EHO mixed with S8 nanoparticles at 1000 mg/L and 298 K. The rheograms reflect non-Newtonian behavior for these fluids. They may be characterized as pseudo-plastic fluids or shear thinning behavior. As expected, the EHO exhibits viscosity values much higher than the HO at all shear rates. This is due mainly to a high content of asphaltenes and a substantial decline in the API gravity. Equally, S8 nanoparticles are also effective to lower viscosity in this kind of fluids, suggesting that nanoparticles have similar behavior in both crude oils, interacting with asphaltene aggregates, altering their colloidal structure and generating a significant reduction in viscosity.

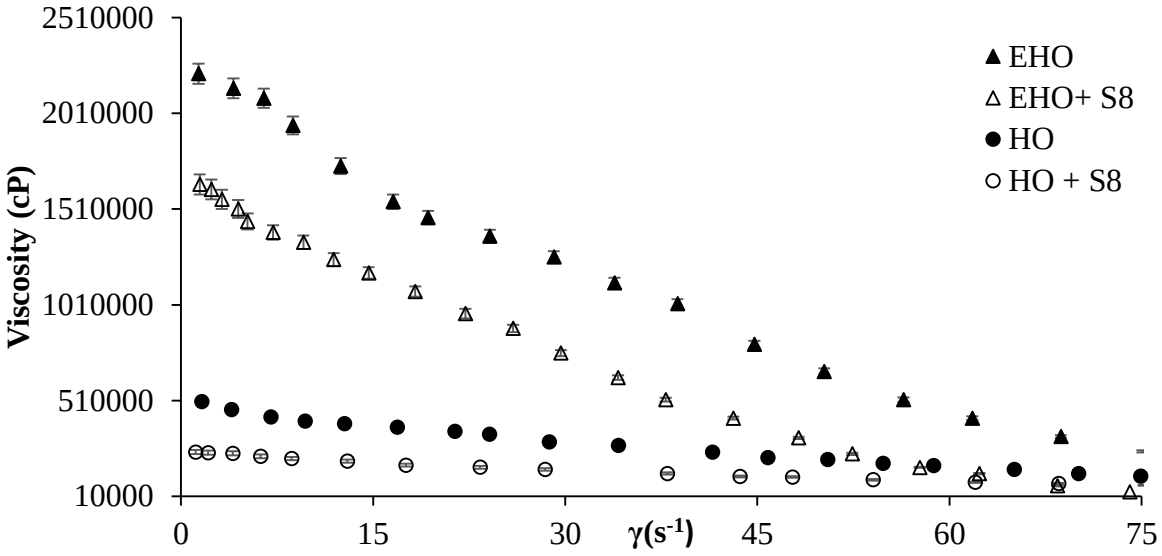

Figure 2.10 Viscosity of heavy oil and extra heavy oil in absence and presence of S8 nanoparticles at 1000 mg/L, 298 K and shear rate between 0 and 75 s^{-1}.

Figure 2.11 shows the DVR for HO and EHO in the presence of S8 nanoparticles at different shear rates (0-75 s^{-1}). The S8 nanoparticles produce viscosity reduction in both heavy and extra heavy crude oils and at all shear rates. The performance of the nanoparticles is greater at high shear rates, which is mainly due to a decrease in the viscosity of the oil without nanoparticles, typical of non-Newtonian fluids. The heavy oil intrinsic viscosity with and without NP's is reduced with the increase in shear rate. For this reason, the DVR decreases with increasing shear rate. The effectiveness of the S8 nanoparticles is higher in heavy oil than in extra heavy oil, caused by dispersion effects, as it is easier to disperse solid particles in a lower viscosity fluid. However, a reduction of more than 30% for extra-heavy crude oils with the addition of solid particles is significant and relevant for commercial applications. It is worth mentioning that a higher DVR can be obtained when a carrier fluid is added to the system, allowing a better diffusion of the nanoparticles trough the oil matrix. In our previous publication entitled "Effect of nanoparticles/nanofluids on the rheology of heavy crude oil and its mobility on porous media at reservoir conditions" [93]we have evaluated the use of nanoparticles of silica immersed in a flowing fluid. This publication explains how to prepare the fluid so that the particles are completely stable in the medium, and it was shown that the viscosity reduction is best obtained mainly by 2 factors: 1- The entraining fluid has effects as a diluent and can By itself reducing the viscosity of the crude oil and 2- because the particles can be evenly

distributed throughout the matrix of heavy crude and thus present a higher performance compared to when they are added solidly.

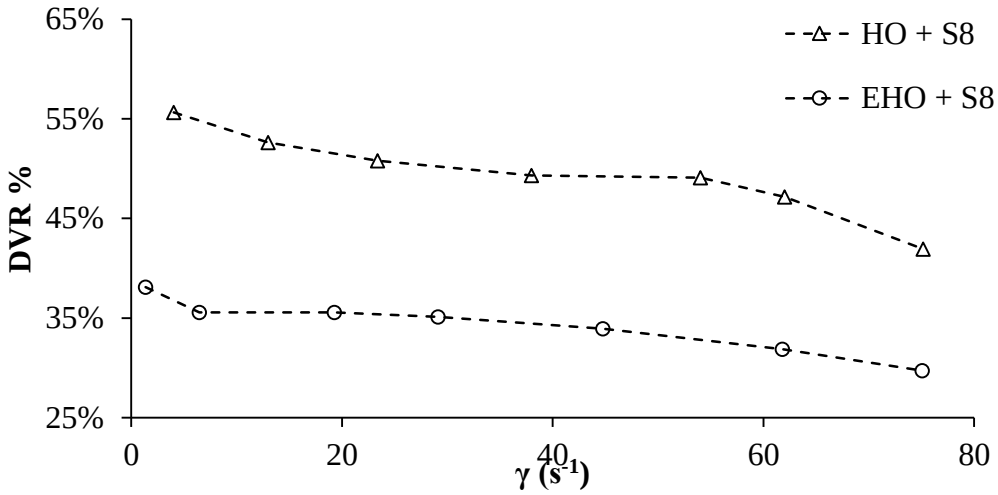

Figure 2.11 The degree of viscosity reduction of HO and EHO matrix on S8 nanoparticles, at 298 K and shear rate between 0-75 s^{-1}.

2.3.6 Relationship between asphaltene sorption capacity and viscosity reduction.

To determine the relationship between the adsorption capacity of the nanoparticles by the asphaltenes present in the crude oil and the performance as viscosity reducing agents, we proceeded to obtain an empirical correlation that can give an idea or an approximation of the degree of reduction of Viscosity that the particles may have.

It is difficult to compare the performance of a nanoparticle in a model solution of asphaltenes in toluene with the interaction of the nanoparticles in the heavy crude.

However, the phenomenon that produces the reduction of viscosity is the capture of asphaltenes, and this can be clarified by making model solutions of asphaltenes in toluene. Possibly, that nanoparticle that presents greater sportive capacity of asphaltenes in a solution model, also has the capacity to adsorb more amount of asphaltenes in the heavy crude matrix.

In order to establish the relationship between the asphaltene adsorption capacity and the viscosity reduction capacity, the adsorbed quantity points were taken at an equilibrium concentration of 1000 mg/L of asphaltenes on toluene, for multiple nanoparticles of different chemical nature and tested with their performance as viscosity reducing agents (degree of DVR viscosity reduction) at the same concentration of nanoparticles used in the heavy crude matrix 1000 mg/L.

Figure 2.12 shows the relationship between the adsorptive capacity of asphaltenes and the DVR for several nanoparticles at 25 ° C and a fixed cut-off rate of 5 s^{-1}. This value was selected because it exhibits the greatest change in viscosity.

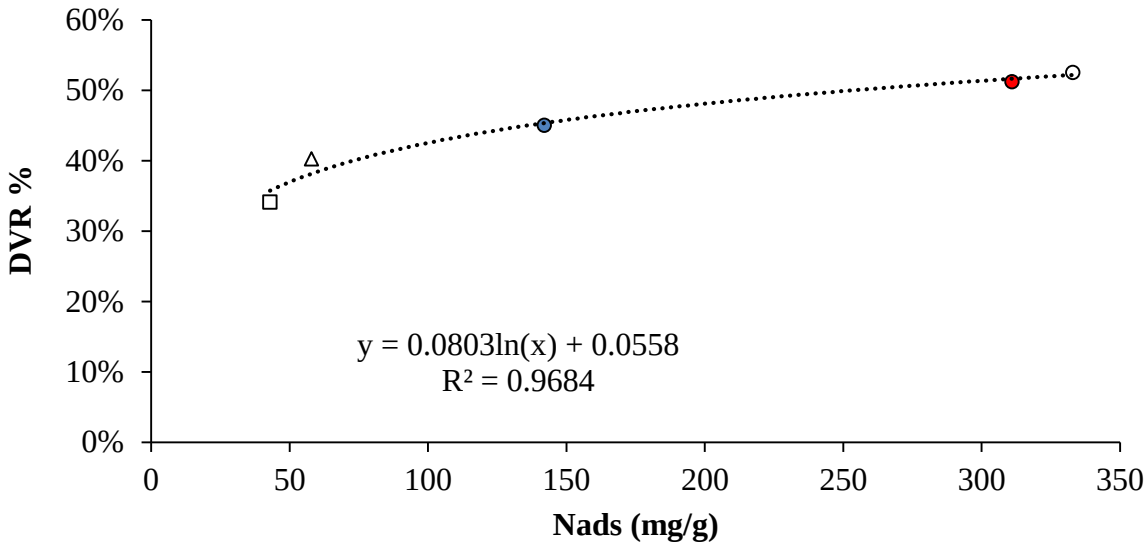

Figure 2.12 The relationship between the degree of viscosity reduction of HO nanoparticles, against the asphaltene uptake capacity, at 298 K.

Figure 2.12 shows a logarithmic trend between the values of adsorbed quantity and degree of reduction of viscosity. The nanoparticles with the highest degree of viscosity reduction are those with the highest adsorptive capacity in the model solutions of asphaltenes in toluene, the white circle refers to the nanoparticle S8, the red circle refers to the nanoparticle S8A, the blue circle to the S8B nanoparticle, the triangle and the square refer to the Al35 alumina and the F97 magnetite respectively.

In this way it is possible to establish a first approximation that allows to relate both parameters, and to facilitate the knowledge of the impact that the use of a nanoparticle would have on the rheological

conditions of heavy crude, simply realizing the construction of adsorption isotherms by any available method.

2.4 Partial conclusions

- The addition of nanoparticles of different chemical natures to heavy and extra heavy oil produces a viscosity reduction at low particle concentration contrary to expectations based on the behavior described through Einstein's theory on hydrodynamic viscosity.
- In this study, an experimental rheological evaluation of heavy and extra heavy oil was conducted. Al_2O_3, Fe_3O_4, and SiO_2 nanoparticles were evaluated, including particle sizes and degrees of surface acidity effects. SiO_2 nanoparticles with 8 nm in size at 1000 mg/L yield the best performance as viscosity-reducing agents.
- As the particle size increases, the effect on reduction of viscosity decreases, which could be mainly due to the increased packing factor, generating interaction and possible aggregation between particles, hampering interactions between them and the asphaltenes aggregates present in crude oil.
- Subsequently, the first mathematical approach to calculating the viscosity as a function of the concentration of nanoparticles is presented, expressed as a function of volume fraction based on a modification to the model Pal and Rhodes for suspensions viscosity. The model fits the experimental data well, for volume fractions between 0 and 3.7×10^{-4}. The solvation constant K and the form factor V follow a trend as a function of the shear rates evaluated and are consistent with the oil shear-thinning behavior.

2.5 References

1. Chew, K. J., The future of oil: unconventional fossil fuels. *Philosophical Transactions of the Royal Society of London A: Mathematical, Physical and Engineering Sciences* **2014,** 372, (2006), 20120324.
2. Meyer, R. F.; Attanasi, E. D., Heavy oil and natural bitumen-strategic petroleum resources. *World* **2003,** 434, 650-7.
3. Rana, M. S.; Samano, V.; Ancheyta, J.; Diaz, J., A review of recent advances on process technologies for upgrading of heavy oils and residua. *Fuel* **2007,** 86, (9), 1216-1231.
4. Shah, A.; Fishwick, R.; Wood, J.; Leeke, G.; Rigby, S.; Greaves, M., A review of novel techniques for heavy oil and bitumen extraction and upgrading. *Energy & Environmental Science* **2010,** 3, (6), 700-714.
5. Adams, J. J., Asphaltene adsorption, a literature review. *Energy & Fuels* **2014,** 28, (5), 2831-2856.

6. Ghanavati, M.; Shojaei, M.-J.; SA, A. R., Effects of asphaltene content and temperature on viscosity of Iranian heavy crude oil: experimental and modeling study. *Energy & Fuels* **2013,** 27, (12), 7217-7232.
7. Hinkle, A.; Shin, E.-J.; Liberatore, M. W.; Herring, A. M.; Batzle, M., Correlating the chemical and physical properties of a set of heavy oils from around the world. *Fuel* **2008,** 87, (13), 3065-3070.
8. Ghannam, M. T.; Hasan, S. W.; Abu-Jdayil, B.; Esmail, N., Rheological properties of heavy & light crude oil mixtures for improving flowability. *Journal of Petroleum Science and Engineering* **2012,** 81, 122-128.
9. Hasan, S. W.; Ghannam, M. T.; Esmail, N., Heavy crude oil viscosity reduction and rheology for pipeline transportation. *Fuel* **2010,** 89, (5), 1095-1100.
10. Acevedo, S.; Castillo, J.; Fernández, A.; Goncalves, S.; Ranaudo, M. A., A study of multilayer adsorption of asphaltenes on glass surfaces by photothermal surface deformation. Relation of this adsorption to aggregate formation in solution. *Energy & fuels* **1998,** 12, (2), 386-390.
11. Acevedo, S.; Castro, A.; Negrin, J. G.; Fernández, A.; Escobar, G.; Piscitelli, V.; Delolme, F.; Dessalces, G., Relations between asphaltene structures and their physical and chemical properties: The rosary-type structure. *Energy & fuels* **2007,** 21, (4), 2165-2175.
12. Al-Maamari, R. S.; Buckley, J. S., Asphaltene precipitation and alteration of wetting: the potential for wettability changes during oil production. *SPE Reservoir Evaluation & Engineering* **2003,** 6, (04), 210-214.
13. Franco, C. A.; Montoya, T.; Nassar, N. N.; Pereira-Almao, P.; Cortés, F. B., Adsorption and subsequent oxidation of colombian asphaltenes onto Nickel and/or Palladium oxide supported on fumed silica nanoparticles. *Energy & Fuels* **2013,** 27, (12), 7336-7347.
14. Mullins, O. C.; Betancourt, S. S.; Cribbs, M. E.; Dubost, F. X.; Creek, J. L.; Andrews, A. B.; Venkataramanan, L., The colloidal structure of crude oil and the structure of oil reservoirs. *Energy & Fuels* **2007,** 21, (5), 2785-2794.
15. Pacheco-Sánchez, J.; Zaragoza, I.; Martínez-Magadán, J., Asphaltene aggregation under vacuum at different temperatures by molecular dynamics. *Energy & fuels* **2003,** 17, (5), 1346-1355.
16. Rahimi, H.; Solaimany Nazar, A. R., Asphaltene aggregates fractal restructuring model, a population balance approach. *Energy & Fuels* **2009,** 24, (2), 1088-1093.
17. Victorov, A. I.; Smirnova, N. A., Thermodynamic model of petroleum fluids containing polydisperse asphaltene aggregates. *Industrial & engineering chemistry research* **1998,** 37, (8), 3242-3251.
18. Rastegari, K.; Svrcek, W. Y.; Yarranton, H. W., Kinetics of asphaltene flocculation. *Industrial & engineering chemistry research* **2004,** 43, (21), 6861-6870.
19. Mullins, O. C., Optical interrogation of aromatic moieties in crude oils and asphaltenes. In *Structures and dynamics of asphaltenes*, Springer: 1998; pp 21-77.
20. Mullins, O. C., The asphaltenes. *Annual Review of Analytical Chemistry* **2011,** 4, 393-418.
21. Leontaritis, K.; Amaefule, J.; Charles, R., A systematic approach for the prevention and treatment of formation damage caused by asphaltene deposition. *SPE Production & Facilities* **1994,** 9, (03), 157-164.
22. Yudin, I. K.; Anisimov, M. A., Dynamic light scattering monitoring of asphaltene aggregation in crude oils and hydrocarbon solutions. In *Asphaltenes, Heavy Oils, and Petroleomics*, Springer: 2007; pp 439-468.
23. Chuan, W.; Guang-Lun, L.; YAO, C.-j.; SUN, K.-j.; Gai, P.-y.; CAO, Y.-b., Mechanism for reducing the viscosity of extra-heavy oil by aquathermolysis with an amphiphilic catalyst. *Journal of Fuel Chemistry and Technology* **2010,** 38, (6), 684-690.
24. Hart, A., A review of technologies for transporting heavy crude oil and bitumen via pipelines. *Journal of Petroleum Exploration and Production Technology* **2014,** 4, (3), 327-336.

25. Saniere, A.; Hénaut, I.; Argillier, J., Pipeline transportation of heavy oils, a strategic, economic and technological challenge. *Oil & Gas Science and Technology* **2004,** 59, (5), 455-466.
26. Urquhart, R., Heavy oil transportation-present and future. *Journal of Canadian Petroleum Technology* **1986,** 25, (02).
27. Xia, T.; Greaves, M. In *3-D physical model studies of downhole catalytic upgrading of Wolf Lake heavy oil using THAI*, Canadian International Petroleum Conference, 2001; Petroleum Society of Canada: 2001.
28. Gateau, P.; Hénaut, I.; Barré, L.; Argillier, J., Heavy oil dilution. *Oil & gas science and technology* **2004,** 59, (5), 503-509.
29. Heim, W.; Wolf, F. J.; Savery, W. T., Heavy oil recovering. In Google Patents: 1984.
30. McMillen, J. M., Enhanced oil recovery; producing a solvent-crude mixture. In Google Patents: 1985.
31. Chen, D.-H.; Hong, L.; Nie, X.-W.; Wang, X.-L.; Tang, X.-Z., Study on rheological properties and relaxational behavior of poly (dianilinephosphazene)/low-density polyethylene blends. *European polymer journal* **2003,** 39, (5), 871-876.
32. Greaves, M.; Xia, T. In *CAPRI-Downhole Catalytic Process for Upgrading Heavy Oil: Produced Oil Properties and Composition*, Canadian International Petroleum Conference, 2001; Petroleum Society of Canada: 2001.
33. Hashemi, R.; Nassar, N. N.; Pereira Almao, P., Enhanced heavy oil recovery by in situ prepared ultradispersed multimetallic nanoparticles: A study of hot fluid flooding for Athabasca bitumen recovery. *Energy & Fuels* **2013,** 27, (4), 2194-2201.
34. Yi, Y.; Li, S.; Ding, F.; Yu, H., Change of asphaltene and resin properties after catalytic aquathermolysis. *Petroleum Science* **2009,** 6, (2), 194-200.
35. Mortazavi-Manesh, S.; Shaw, J. M., Effect of diluents on the rheological properties of Maya crude oil. *Energy & Fuels* **2016,** 30, (2), 766-772.
36. Mortazavi-Manesh, S.; Shaw, J. M., Thixotropic rheological behavior of Maya crude oil. *Energy & Fuels* **2014,** 28, (2), 972-979.
37. Amanullah, M.; Al-Tahini, A. M. In *Nano-technology-its significance in smart fluid development for oil and gas field application*, SPE Saudi Arabia Section Technical Symposium, 2009; Society of Petroleum Engineers: 2009.
38. Franco, C.; Cardona, L.; Lopera, S.; Mejía, J.; Cortés, F. In *Heavy Oil Upgrading and Enhanced Recovery in a Continuous Steam Injection Process Assisted by Nanoparticulated Catalysts*, SPE Improved Oil Recovery Conference, 2016; Society of Petroleum Engineers: 2016.
39. Franco, C. A.; Nassar, N. N.; Ruiz, M. A.; Pereira-Almao, P.; Cortés, F. B., Nanoparticles for inhibition of asphaltenes damage: adsorption study and displacement test on porous media. *Energy & Fuels* **2013,** 27, (6), 2899-2907.
40. Mohammadi, M.; Akbari, M.; Fakhroueian, Z.; Bahramian, A.; Azin, R.; Arya, S., Inhibition of asphaltene precipitation by TiO2, SiO2, and ZrO2 nanofluids. *Energy & Fuels* **2011,** 25, (7), 3150-3156.
41. Schmid, G., *Nanoparticles: from theory to application*. John Wiley & Sons: 2011.
42. Nassar, N. N., Asphaltene adsorption onto alumina nanoparticles: kinetics and thermodynamic studies. *Energy & Fuels* **2010,** 24, (8), 4116-4122.
43. Rouguerol, F.; Rouguerol, J.; Sing, K., Adsorption by Powders and Porous Solid; Principles, Methodology and Applications. In Academic Press, San Diego: 1999.
44. Tarboush, B. J. A.; Husein, M. M., Adsorption of asphaltenes from heavy oil onto in situ prepared NiO nanoparticles. *Journal of colloid and interface science* **2012,** 378, (1), 64-69.
45. Kazemzadeh, Y.; Eshraghi, S. E.; Kazemi, K.; Sourani, S.; Mehrabi, M.; Ahmadi, Y., Behavior of Asphaltene Adsorption onto the Metal Oxide Nanoparticle Surface and Its Effect on Heavy Oil Recovery. *Industrial & Engineering Chemistry Research* **2015,** 54, (1), 233-239.

46. Franco, C.; Patiño, E.; Benjumea, P.; Ruiz, M. A.; Cortés, F. B., Kinetic and thermodynamic equilibrium of asphaltenes sorption onto nanoparticles of nickel oxide supported on nanoparticulated alumina. *Fuel* **2013,** 105, 408-414.
47. Nassar, N. N.; Franco, C. A.; Montoya, T.; Cortés, F. B.; Hassan, A., Effect of oxide support on Ni–Pd bimetallic nanocatalysts for steam gasification of nC 7 asphaltenes. *Fuel* **2015,** 156, 110-120.
48. Pereira-Almao, P.; Larter, S. In *An Integrated Approach to On Sitelin Situ Upgrading*, 19th World Petroleum Congress, 2008; World Petroleum Congress: 2008.
49. Snow, R. H. In *In-Situ Thermal Upgrading of Bitumen and Shale Oil by RF Electrical Heating*, SPE Heavy Oil Conference and Exhibition, 2011; Society of Petroleum Engineers: 2011.
50. Wichert, G.; Okazawa, N.; Moore, R.; Belgrave, J. In *In-situ upgrading of heavy oils by low-temperature oxidation in the presence of caustic additives*, SPE International Heavy Oil Symposium, 1995; Society of Petroleum Engineers: 1995.
51. Betancur, S. Desarrollo de Nanopartículas basadas en Sílice para la Inhibición de la Precipitación/Depositación de Asfaltenos Universidad Nacional de Colombia, Medellín, Colombia, 2015.
52. Cortés, F. B.; Mejía, J. M.; Ruiz, M. A.; Benjumea, P.; Riffel, D. B., Sorption of asphaltenes onto nanoparticles of nickel oxide supported on nanoparticulated silica gel. *Energy & Fuels* **2012,** 26, (3), 1725-1730.
53. Franco, C. A.; Martínez, M.; Benjumea, P.; Patiño, E.; Cortés, F. B., Water remediation based on oil adsorption using nanosilicates functionalized with a petroleum vacuum residue. *Adsorption Science & Technology* **2014,** 32, (2-3), 197-207.
54. Guzmán, J. D.; Betancur, S.; Carrasco-Marín, F.; Franco, C. A.; Nassar, N. N.; Cortés, F. B., Importance of the Adsorption Method Used for Obtaining the Nanoparticle Dosage for Asphaltene-Related Treatments. *Energy & Fuels* **2016**.
55. Zabala. R, F. C. A., Cortes. F.B., Application of Nanofluids for Improving Oil Mobility in Heavy Oil and Extra-Heavy Oil: A Field Test. *Society of Petroleum Engineers Journal* **2016**, 14.
56. Einstein, A., Eine neue bestimmung der moleküldimensionen. *Annalen der Physik* **1906,** 324, (2), 289-306.
57. Guth, E.; Simha, R., Untersuchungen über die viskosität von suspensionen und lösungen. 3. über die viskosität von kugelsuspensionen. *Colloid & Polymer Science* **1936,** 74, (3), 266-275.
58. Kitano, T.; Kataoka, T.; Shirota, T., An empirical equation of the relative viscosity of polymer melts filled with various inorganic fillers. *Rheologica Acta* **1981,** 20, (2), 207-209.
59. Mooney, M., The viscosity of a concentrated suspension of spherical particles. *Journal of colloid science* **1951,** 6, (2), 162-170.
60. Thomas, D. G., Transport characteristics of suspension: VIII. A note on the viscosity of Newtonian suspensions of uniform spherical particles. *Journal of Colloid Science* **1965,** 20, (3), 267-277.
61. Ouerfelli, N.; Bouanz, M., A shear viscosity study of cerium (III) nitrate in concentrated aqueous solutions at different temperatures. *Journal of Physics: Condensed Matter* **1996,** 8, (16), 2763.
62. Eilers, v. H., Die viskosität von emulsionen hochviskoser stoffe als funktion der konzentration. *Kolloid-Zeitschrift* **1941,** 97, (3), 313-321.
63. Roscoe, R., The viscosity of suspensions of rigid spheres. *British Journal of Applied Physics* **1952,** 3, (8), 267.
64. Chong, J.; Christiansen, E.; Baer, A., Rheology of concentrated suspensions. *Journal of applied polymer science* **1971,** 15, (8), 2007-2021.
65. Maron, S. H.; Pierce, P. E., Application of Ree-Eyring generalized flow theory to suspensions of spherical particles. *Journal of colloid science* **1956,** 11, (1), 80-95.
66. Krieger, I. M.; Dougherty, T. J., A mechanism for non-Newtonian flow in suspensions of rigid spheres. *Transactions of The Society of Rheology (1957-1977)* **1959,** 3, (1), 137-152.

67. Pal, R.; Rhodes, E., A novel viscosity correlation for non-Newtonian concentrated emulsions. *Journal of colloid and interface science* **1985,** 107, (2), 301-307.
68. Pal, R.; Vargas, F., On the interpretation of viscosity data of suspensions of asphaltene nano-aggregates. *The Canadian Journal of Chemical Engineering* **2014,** 92, (3), 573-577.
69. Barré, L.; Simon, S.; Palermo, T., Solution properties of asphaltenes. *Langmuir* **2008,** 24, (8), 3709-3717.
70. Bouhadda, Y.; Bendedouch, D.; Sheu, E.; Krallafa, A., Some preliminary results on a physico-chemical characterization of a Hassi Messaoud petroleum asphaltene. *Energy & fuels* **2000,** 14, (4), 845-853.
71. Jezequel, P.; Flaud, P.; Quemada, D., RHEOLOGICAL PROPERTIES AND FLOW OF CONCENTRATED DISPERSE MEDIA. II-STEADY AND UNSTEADY FLOW ANALYSIS OF HEAVY CRUDE OIL EMULSIONS. *Chemical engineering communications* **1985,** 32, (1-5), 85-99.
72. Plegue, T.; Frank, S.; Fruman, D.; Zakin, J., Concentrated viscous crude oil-in-water emulsions for pipeline transport. *Chemical Engineering Communications* **1989,** 82, (1), 111-122.
73. Sheu, E. Y.; Storm, D. A.; Maureen, M., Asphaltenes in polar solvents. *Journal of non-crystalline solids* **1991,** 131, 341-347.
74. Van der Waarden, M., Viscosity and electroviscous effect of emulsions. *Journal of Colloid Science* **1954,** 9, (3), 215-222.
75. Luo, P.; Gu, Y., Effects of asphaltene content on the heavy oil viscosity at different temperatures. *Fuel* **2007,** 86, (7), 1069-1078.
76. Pal, R.; Rhodes, E., Viscosity/concentration relationships for emulsions. *Journal of Rheology (1978-present)* **1989,** 33, (7), 1021-1045.
77. Pierre, C.; Barré, L.; Pina, A.; Moan, M., Composition and heavy oil rheology. *Oil & Gas Science and Technology* **2004,** 59, (5), 489-501.
78. Nassar, N. N.; Betancur, S.; Acevedo, S.; Franco, C. A.; Cortés, F. B., Development of a Population Balance Model to Describe the Influence of Shear and Nanoparticles on the Aggregation and Fragmentation of Asphaltene Aggregates. *Industrial & Engineering Chemistry Research* **2015,** 54, (33), 8201-8211.
79. Sherman., P., In *Encyclopedia of Emulsion Technology*, 1983 ed.; Becher, P., Ed. Marcel Dekker, Inc.: New York, 1983; Vol. 1, pp 415-420.
80. Franco, C. A.; Lozano, M. M.; Acevedo, S.; Nassar, N. N.; Cortés, F. B., Effects of Resin I on Asphaltene Adsorption onto Nanoparticles: A Novel Method for Obtaining Asphaltenes/Resin Isotherms. *Energy & Fuels* **2015,** 30, (1), 264-272.
81. Montgomery, D. C., *Design and analysis of experiments*. John Wiley & Sons: 2008.
82. KEE, D. D.; ASFOUR, A.-F. A.; Ning, H., Flow properties of Lloydminster and cold lake crudes. *Chemical Engineering Communications* **1988,** 70, (1), 203-213.
83. Alvarez, G.; Poteau, S.; Argillier, J.-F.; Langevin, D.; Salager, J.-L., Heavy oil− water interfacial properties and emulsion stability: Influence of dilution. *Energy & Fuels* **2008,** 23, (1), 294-299.
84. Nik, W. W.; Ani, F.; Masjuki, H.; Giap, S. E., Rheology of bio-edible oils according to several rheological models and its potential as hydraulic fluid. *Industrial Crops and Products* **2005,** 22, (3), 249-255.
85. Delgado, J. G., Asfaltenos. Composición, agregación, precipitación. *Universidad de los Andes. Mérida-Venezuela. Recuperado el* **2006,** 10.
86. Gharfeh, S.; Yen, A.; Asomaning, S.; Blumer, D., Asphaltene flocculation onset determinations for heavy crude oil and its implications. *Petroleum science and technology* **2004,** 22, (7-8), 1055-1072.
87. Williams, B., Heavy hydrocarbons playing key role in peak-oil debate, future energy supply. *Oil & Gas Journal* **2003,** 101, (29), 20-27.

88. Betancur, S.; Carmona, J. C.; Nassar, N. N.; Franco, C. A.; Cortés, F. B., Role of Particle Size and Surface Acidity of Silica Gel Nanoparticles in Inhibition of Formation Damage by Asphaltene in Oil Reservoirs. *Industrial & Engineering Chemistry Research* **2016**.
89. Khan, M. R., Rheological properties of heavy oils and heavy oil emulsions. *Energy Sources* **1996,** 18, (4), 385-391.
90. Argillier, J.; Barre, L.; Brucy, F.; Dournaux, J.; Henaut, I.; Bouchard, R. In *Influence of asphaltenes content and dilution on heavy oil rheology*, SPE International Thermal Operations and Heavy Oil Symposium, 2001; Society of Petroleum Engineers: 2001.
91. Bazyleva, A. B.; Hasan, M. A.; Fulem, M.; Becerra, M.; Shaw, J. M., Bitumen and heavy oil rheological properties: Reconciliation with viscosity measurements. *Journal of Chemical & Engineering Data* **2009,** 55, (3), 1389-1397.
92. Long, J.; Shen, B.; Ling, H.; Zhao, J.; Lu, J., Novel solvent deasphalting process by vacuum residue blending with coal tar. *Industrial & Engineering Chemistry Research* **2011,** 50, (19), 11259-11269.
93. Taborda, E. A.; Franco, C. A.; Lopera, S. H.; Alvarado, V.; Cortés, F. B., Effect of nanoparticles/nanofluids on the rheology of heavy crude oil and its mobility on porous media at reservoir conditions. *Fuel* **2016,** 184, 222-232.

3. Changes in the internal structure of crude oil by the addition of nanoparticles: Dynamic Rheology.

Since heavy and extra-heavy oils are highly viscous, the study of their rheology is vital for understanding and optimizing their production and transport. Rheology is part of the physics of continuum media that studies the deformation and flow of matter,[1, 2] and as such, it is essential for understanding the behavior of fluids in motion. Steady-state and dynamic oscillometry serve as rheological tools to analyze the viscoelastic behavior of heavy crude oils, which directly relates to the fluid internal composition and structure. Thus, multiple researchers[3-10] have used both the steady-state and transient rheology to characterize heavy and extra-heavy crude oils subjected to a variety of conditions with the objective of optimizing their mobility and transportation. One of the most commonly used techniques for reducing HO and EHO viscosities and hence increase oil production rate has been the dilution with solvents, light hydrocarbons,[11-16] and some R=O bounds-based chemical compounds.[17] In this way, several authors have focused on studying diluted HO and EHO with different solvents[17-20] often evaluating the rheology behavior of the fluid mixture.[4, 5, 18] Recently, Mortazavi-Manesh and Shaw[21] studied the effect of different types of chemical compounds on the rheological properties of Maya crude oil at different temperatures. The compounds used in their study were toluene, n-heptane and a 50/50 vol% mixture of toluene and butanone. The rheological evaluation was performed using steady-state methods at share rates 0-200 s^{-1}; as expected, dilution and temperature increase reduced oil viscosity. These mixtures exhibit a characteristic non-Newtonian shear-thinning behavior, but with increasing temperature, the Newtonian behavior becomes dominant. Solvents in decreasing viscosity reduction effectiveness for the entire range evaluated are a mixture of toluene-butanone > toluene > n-heptane. Earlier, Mortazavi-Manesh and Shaw[22] characterized Maya crude oil to investigate its thixotropic

characteristics as a function of temperature to determine the influence of time on viscosity measurements. The authors demonstrated that the thixotropic behavior of this oil increases as temperature decreases. Authors performed thixotropy measurements based on three tools widely used: hysteresis loops, step-wise change in shear rate and start-up experiments. The results are useful to optimize pipeline transport conditions, mainly in processes where pressure is required to restart fluid flow. Pierre et al.[4] evaluated the effect of asphaltenes on the viscosity of a Venezuelan heavy crude oil. First, they determined the influence of asphaltenes and resins on oil viscosity by extraction with n-pentane and n-nonane and the subsequent dissolution in xylene. For all experiments, the authors demonstrated that with increments of the asphaltene content, the viscosity increases significantly. Additionally, the authors characterized the heavy oil using a dynamic oscillometric method and examined the influence of asphaltenes on the crude oil viscoelastic behavior. The results showed the presence of an internal network of colloids formed by asphaltenes. Behzadfar and Hatzikiriakos[23] studied the viscoelastic properties of bitumen from the Athabasca oil sands by oscillometry at different temperatures; also, they proposed a constitutive equation based on the K-BKZ model, widely used in the rheology of polymer melts. The results indicate that the constitutive equation predicts reasonably well the linear viscoelastic response of the bitumen, for the range of temperatures evaluated. To describe the rheological behavior one should obtain the parameters to feed the K-BKZ equation, and for this reason, the authors used the generalized Maxwell model that fits the linear response of the bitumen in the dynamic flow corresponding to the small amplitude shear oscillator. Abivin and Taylor[24] studied the viscoelastic behavior of 13 different heavy crude oils from Asia and America, in a temperature range between -50 and 50 °C. The article presents comparative results of the viscoelastic properties such as phase angle, viscoelastic moduli and relaxation times, among crude oils with similar rheological behavior (Newtonian and non-Newtonian). The authors concluded that for some crude oils, the viscoelastic nature related to the presence of waxy paraffinic crystals. However, for another group of crude oils, the viscoelastic behavior related to the high content of asphaltenes, present in a high percentage, which produces a macroscopic behavior similar to a weak gel, due to the auto-associative tendency of asphaltenes to create an elastic network in the oil.

Recently, nanotechnology has been shown to enable viscosity reduction of heavy oil in experiments where nanoparticles were incorporated into the oil. These particles interact with the heavier fractions of the fluid and thereby alter the viscoelastic components of heavy crude oil. Due to their exceptional characteristics, such as small particle size (1-100 nm), large available surface area, high dispersibility and tunable physicochemical characteristics, nanoparticles are prone to selectively adsorb asphaltenes and inhibit their self-association.[25-27] Our research group has pioneered this novel topic

of research[26, 28, 29] and has demonstrated the ability of nanoparticles to reduce viscosity and increase the mobility of heavy oil at reservoir conditions as tested at both laboratory[30] and field scales.[31] It has been observed that SiO_2 nanoparticles are able to reduce the viscosity of heavy oil to a greater degree than other nanomaterials, which has been mainly attributed to high adsorptive capacities of asphaltenes that lead to the reduction of its mean aggregate size and consequently to the perturbation of the viscoelastic network formed.[30] Also, results of coreflooding tests at reservoir conditions showed that SiO_2 nanoparticles are able to increase heavy-oil mobility and therefore oil recovery.[30] When evaluated in the field,[31] its was found that by forcing an average amount of 175 bbl of nanofluid within a radius of penetration of ~3 ft, the oil rate can be increased approximately 56 and 63% for an HO and an EHO with API gravities of 12° and 8°, respectively. However, the phenomenon of viscosity reduction due to the presence of nanoparticles is not fully understood at present. Therefore, it is necessary to deepen our understanding of the mechanism involved, so that we can phenomenologically better explain the behavior arising from the interaction of the nanoparticles and the molecules in the oil matrix, which impacts the rheology and show a deviation of Einstein´s model [32] for viscosity.

To the best of our knowledge, there are no published reports in the specialized literature on the dynamic rheological response that explains the behavior as it relates to the interaction of nanoparticles and heavy oils. For this reason, this work seeks to determine changes in the internal structure of heavy oil in the presence of nanoparticles through: i) viscometric measurements at steady state using different dosages of nanoparticles, temperature and shear rates; and ii) dynamic oscillometric measurements at different temperatures, strain, and angular frequencies. The results of this research provide a phenomenological explanation for the viscosity reduction of heavy oil by the addition of solid nanoparticles, towards industrial applications to optimize the conditions of mobility and transport and thus provide a path for new technologies that produce savings economic, energy and good technical performance.

3.1 Experimental

3.1.1 Materials

n-Heptane (99%, Sigma-Aldrich, St. Louis, MO) was used as received for n-C7 asphaltene isolation and for the preparation of de-asphalted oil (DAO) and reconstituted oil. Two Colombian oils were used as HO and light oil crudes (LO). HO was used for the rheological tests and as a source of

asphaltenes. n-C7 asphaltenes were extracted following a standard procedure as described in previous works [26, 33, 34]. The properties of the selected HO and LO are presented in Table 3.1. The commercial SiO_2 nanoparticles of 8 nm (S8) were obtained from Sigma-Aldrich (St. Louis, MO). The mean particle size of the nanoparticles (dp) was measured using the dynamic light scattering (DLS) technique, with a nanoplus-3 from Micromeritics (Norcross, ATL) set at 298 K and equipped with a 0.9 mL glass cell.[28] The BET surface areas (S_{BET}) of the nanoparticle compounds were measured through nitrogen physisorption at 77 K using an Autosorb-1 from Quantacrome after outgassing samples overnight at 413 K under high vacuum (10-6 mbar). The S_{BET} of SiO_2 is 389 m^2/g.

To obtain the de-asphalted oil (DAO), a mixture with n-heptane and HO with a mass ratio 40:1 ratio was prepared. The mixture was stirred at 300 rpm for 24 h at 373 K using airtight vials, and every 15 minutes the mixture was sonicated for 1 minute to disperse the particles of precipitated asphaltenes. At this point, asphaltene precipitation was achieved, and the asphaltenes were separated from DAO through filtration with an 8 μm Whatman filter paper. At the end of the process, the n-heptane used is separated from the DAO by heating the mixture at 340 K until the weight reaches the weight of crude oil minus the weight of the extracted asphaltenes. The reconstituted crude is obtained by adding the 10 wt% of n-C7 asphaltenes to DAO. The mixture is carried out by stirring at 300 rpm for 45 minutes.[35]

Table 3.1. API gravity, viscosity and SARA analysis of the selected crude oils.

Material	**API (°)**	**Viscosity at 298 K (cP)**	**Saturates (wt%)**	**Aromatics (wt%)**	**Resins (wt%)**	**Asphaltenes (wt%)**
Heavy Oil (HO)	11.2	1.95×10^5	12.79	30.39	40.09	16.73
Light Oil (LO)	42.0	2.1	63.71	16.51	19.01	0.77

More information about materials and characterization methods are described in chapter 1.

3.1.2 Methods

- **Rheologic measurements**

Steady-state and dynamic rheological measurements were performed using a Kinexus Pro+ rotational rheometer (Malvern Instruments, Worcestershire - UK), equipped with a Peltier plate for temperature control, with a 20-mm plate-plate geometry at a gap of 300 μm. To analyze the change in viscosity induced by the addition of nanoparticles, several conditions were evaluated, including the effects of concentration and temperature. For the HO matrix, the concentration values tested were 100, 1000, and 10000 mg/L. In the LO matrix, concentrations of 10, 100, 1000 and 5000 mg/L SiO_2 nanoparticles were also tested.[30] The rheological measurements were conducted at 288, 298, and 313 K in a shear rate range 1-100 s^{-1}. Each experimental condition set was repeated three times. Nanoparticles were mixed with the oil by stirring at 500 rpm during 30 min until homogenization [30]. Additionally, yield stress measurements of HO and HO with 1000 mg/L SiO_2 nanoparticles were performed leading to a shear stress between 0 and 50 Pa at 298 K.[7, 36, 37] The accuracy of the rheological measurements is approximately ± 1%.[21, 22, 30, 38]

- **Dynamic oscillometry: amplitude sweep and frequency sweep tests.**

First, the linear viscoelastic region was determined through a strain-sweep test. Viscoelastic moduli measurements of HO and HO with 1000 mg/L SiO_2 nanoparticles were performed using an oscillatory amplitude test varying the percentage of strain (γ) between 0.1 and 100% at a fixed frequency (ω) of 10 rad/s. Dynamic rheological tests were then conducted at strain value (2%) that yielded a significant dynamic torque within the linear viscoelastic region.[4, 23, 39-41] Oscillatory frequency tests were carried out in frequency range between 0.1 and 100 rad/s at 298 K

Rheological measurements were performed using a Kinexus Pro+ rotational rheometer (Malvern Instruments, Worcestershire - UK), equipped with a Peltier plate for temperature control, with a 20-mm serrated plate-plate geometry at a gap of 300 μm. To analyze the change in viscosity induced by the addition of nanoparticles, several conditions were evaluated, including the effect of concentration, particle size, and the nanoparticle chemical nature. The rheological measurements were conducted at 298 K at a shear rate range of 1-75 s^{-1}. Each experimental condition set was repeated three times. Nanoparticles were mixed with the oil by stirring at 500 rpm for 30 min at room temperature until homogenization with a mixer model HP130915Q from Thermo Scientific (Waltham, Massachusetts, USA).

3.2 Results

Our previous chapter, we have shown that SiO_2 nanoparticles with mean particle size of 8 nm have the ability to adsorb heavy oil components such as asphaltenes and resins on their surface.[42] These results showed how nanoparticles could reduce the asphaltenes aggregates and may positively affect rheological properties of the oil, reducing its viscosity. For this reason, these particles were selected to evaluate their performance as modifying agents of the internal structure producing oil viscosity reductions in HO. The results are divided into two parts: i) rheology studies at steady state in the presence and absence of nanoparticles at three temperature values and ii) dynamic oscillometry of HO in the presence and absence of nanoparticles at three temperature values.

A group of several nanoparticles was evaluated, and for this reason, the concentration effect of nanoparticles was first tested, then the best-performing one was selected to evaluate the effect of particle size. Posteriorly, the chemical nature of nanoparticle and heavy oil effect were evaluated by testing two types of crude oils.

3.2.1 Steady state measurements of heavy crude oil

- ***SiO_2 nanoparticles concentration effect.***

Figure 3.1 shows the rheological measurements at steady state for HO containing nanoparticles at concentrations of 0, 100, 1000 and 10000 mg/L and shear rates between 0 100 s^{-1} at 298 K. The shape of the curves reflect a non-Newtonian shear thinning behavior, i.e., oil viscosity decreases with increasing shear rate, typical of this class of fluids; similar results were found by Mortazavi-Manesh and Shaw,[21, 22] Bazyleva et al.,[39] Mozaffari et al.,[38] Tao and Xu,[43] and Taborda et al.[30] The addition of nanoparticles produces viscosity reduction at all shear rates evaluated in the following order 1000 > 100 > 10000 mg/L. The results are in line with those found in our previous publication,[30] where the interaction between nanoparticles of different chemical nature and asphaltenes present in HO is demonstrated. It is worth recalling that asphaltenes represent the most polar fraction of crude oil, and due to their ability to self-associate they lead to the formation of large aggregates and the structuring of a viscoelastic network in the presence of resins, which is believed to be responsible for the high viscosity of HO.[44-46]

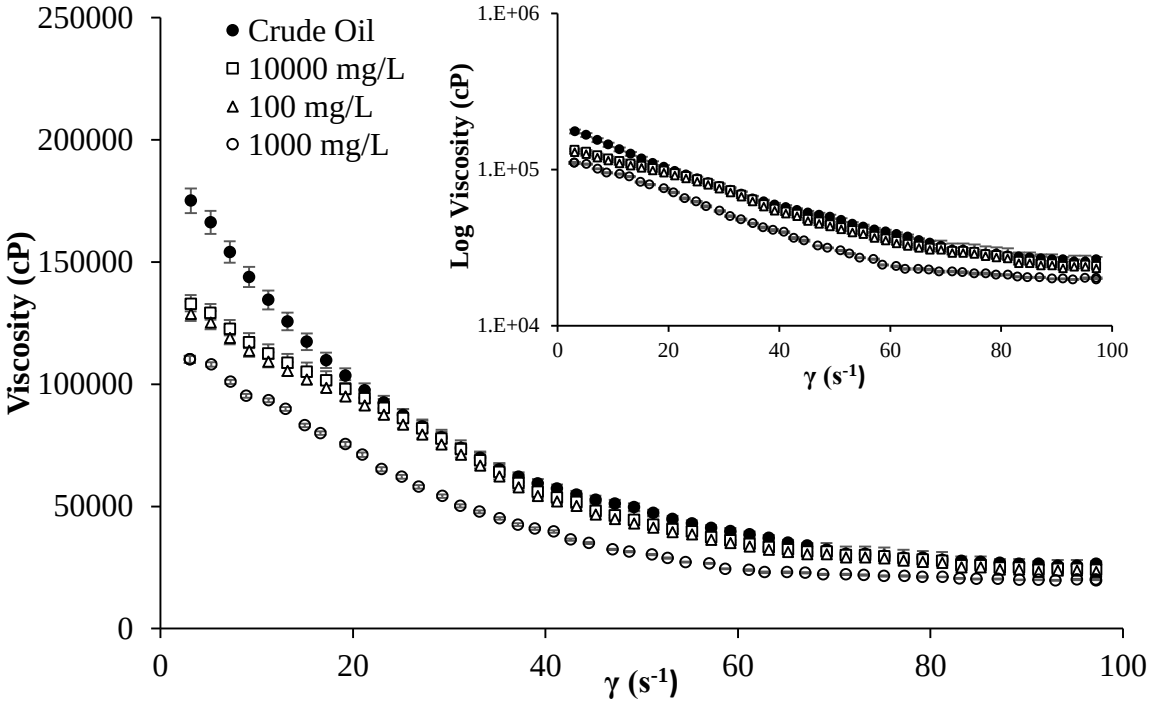

Figure 3.1 Heavy oil viscosity as a function of shear rate of in the presence or absence of SiO_2 nanoparticles for concentrations of 100, 1000 and 10000 mg/L at 298 K.

The largest drop in viscosity obtained for heavy oil corresponds to a nanoparticle concentration of 1000 mg/L. This concentration value was selected for all additional dynamic rheometric measurements.

- **Effect of temperature**

The temperature value at which any fluid is in the liquid state plays a key role in processes involving fluid motion.[20, 47, 48] In the case of heavy crude oils, it is necessary to study the impact of SiO_2 nanoparticles as reducing agents of HO viscosity at different conditions of temperature and high agitation, either through increased turbulence generated by pumping equipment for transportation in surface or pumping from the downhole, or due to the constant injection of nanofluids into the reservoir. In this order, the degree of viscosity reduction (DVR) after nanoparticles inclusion is calculated according to Eq. (6):[5]

$$DVR\% = \frac{\left(\mu_{HO} - \mu_{np}\right)}{\mu_{HO}} \times 100 \quad (1)$$

where, μ_{HO} and μ_{np} are the crude oil viscosity values before and the after nanoparticles were added, measured at shear rates between 0 and 100 s^{-1}, respectively.

Figures 3.2 a-d depict the effect of nanoparticles in reducing the viscosity of heavy oil at a) 288 K, b) 298 K and c) 313 K along with d) the degree of viscosity reduction. For the three temperatures tested, viscosity reduction is obtained after the addition of 1000 mg/L of SiO_2 nanoparticles. As expected, as the temperature increases, the viscosity decreases considerably, and results are in agreement with those found previously.[7, 8, 22, 24] In addition, for all samples, a shear thinning behavior is observed as viscosity decreases at higher values of shear rate. By adding nanoparticles to HO, a decrease in viscosity is observed, but this does not alter the non-Newtonian character of the fluid under the conditions evaluated, i.e., the fluid shows a continuous pseudo-plastic behavior.

Figure 2d shows the degree of viscosity reduction calculated for the three temperatures tested. The values of DVR show that the best performance of nanoparticles at which the greatest change in viscosity occurs is at 288 K with and DVR average of 45%. At the highest temperature tested (313 K), the average viscosity reduction is roughly 12%. This happens as a result of natural changes in the reference values (the viscosity of heavy crude without nanoparticles), as the DVR is calculated as a percentage, it is expected that at a lower temperature, the viscosity change is greater compared to generated at higher temperatures. The increasing shear rate slightly decreases the DVR benefit, which is mainly due to a change in the internal structure of the fluid[7, 22] that causes a decrease in viscosity. For this reason, the oil viscosity without nanoparticles is lower at high rather than at low shear rates, although the nanoparticles have an effect on any shear rate, its performance is slightly lower at higher shear rates.

It is worth noting the importance of using nanoparticles as viscosity reducing agents of heavy crude oil under operating processes involving temperature changes, as shown in the results.

If the nanoparticles decrease the viscosity of heavy oil, they may alter the yield stress, as such yield stress measurement was performed on HO with and without nanoparticles, and the results are presented next.

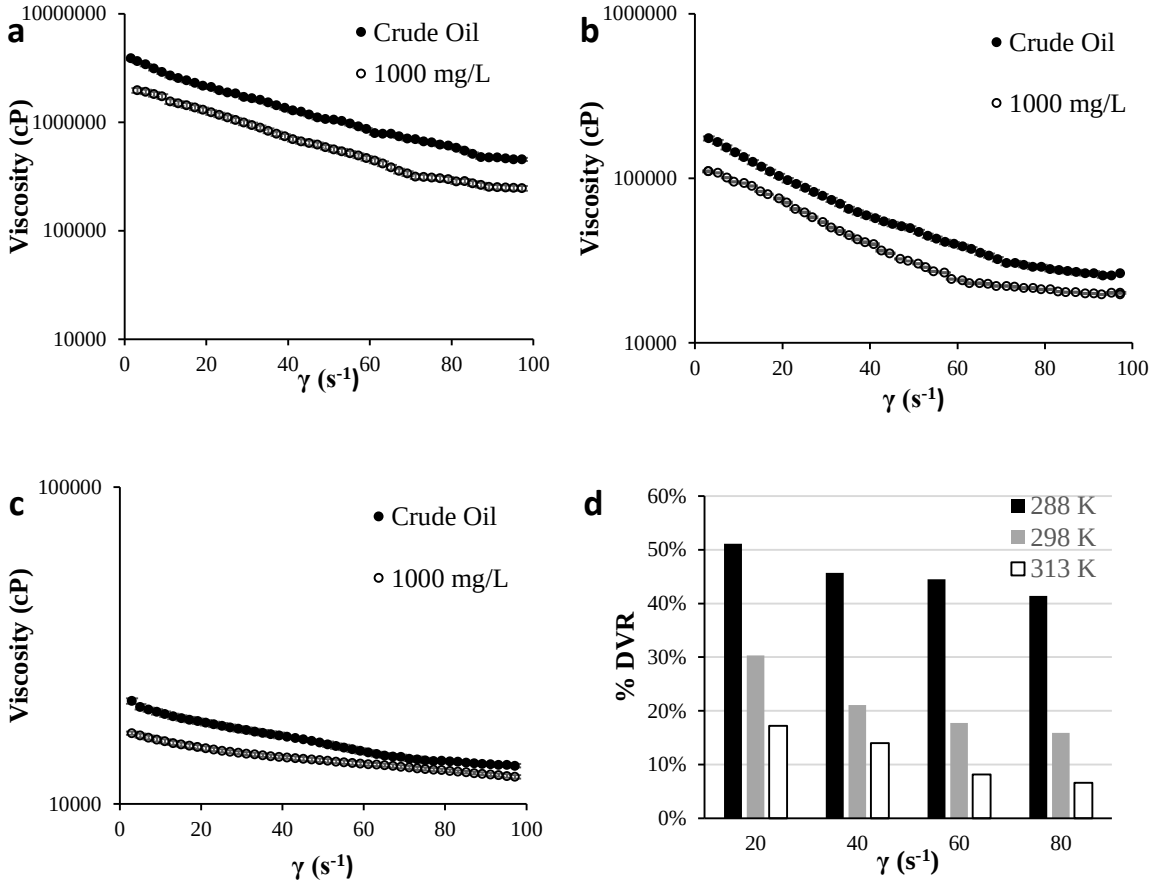

Figure 3.2 Rheological behavior of heavy oil in the presence of 1000 mg/L of SiO_2 nanoparticles or their absence at a) 288 K, b) 298 K, and c) 313 K and the d) degree of viscosity reduction at shear rates between 0 and 100 s^{-1}.

- **Yield stress measurement.**

Usually, pseudoplastic fluids exhibit a non-negligible yield stress, which in practical terms is the minimum stress value required for the fluid flow to occur.[36, 49] Figure 3.3 shows the yield stress of heavy oil in the presence or absence of 1000 mg/L of nanoparticles for shear stress between 0 and 50 Pa and at 298 K. At low shear stress, the fluid exhibits a very high viscosity, which is strictly connected to the aggregation state of asphaltenes and the formation of a three-dimensional network composed of clusters.[7, 49] The yield stress for the fluid without nanoparticles has a value of 0.8 Pa, where it reaches its maximum value of viscosity around of 1.1 x 10^{10} cP. Ghannam et al.[7] report similar results. Meanwhile, by adding 1000 mg/L SiO_2 nanoparticles, the yield stress decreased to a value of 0.35 Pa with a maximum viscosity of 7.7 x 10^{8} cP. These results clearly highlight a

connection between the internal viscoelastic network and the steady-state response observed for HO with or without particles. As shown, nanoparticles simultaneously reduced both viscosity and yield stress, in excess of 50% by addition of nanoparticles, which translates in practical terms into a required stress to start HO flow that is half the value needed for heavy crude oil without nanoparticles. Industrially, it is possible to decrease the pumping power requirements twofold, which would generate energy and cost savings of great importance, which can be achieved simply by adding 1000 mg/L of fumed silica nanoparticles. Yield stress results so far are insufficient to link changes in the internal structure of the oil with the addition of nanoparticles conclusively. More specifically, the notion that an alteration of the asphaltene viscoelastic network is dominantly responsible for an HO viscosity reduction cannot be definitely concluded.

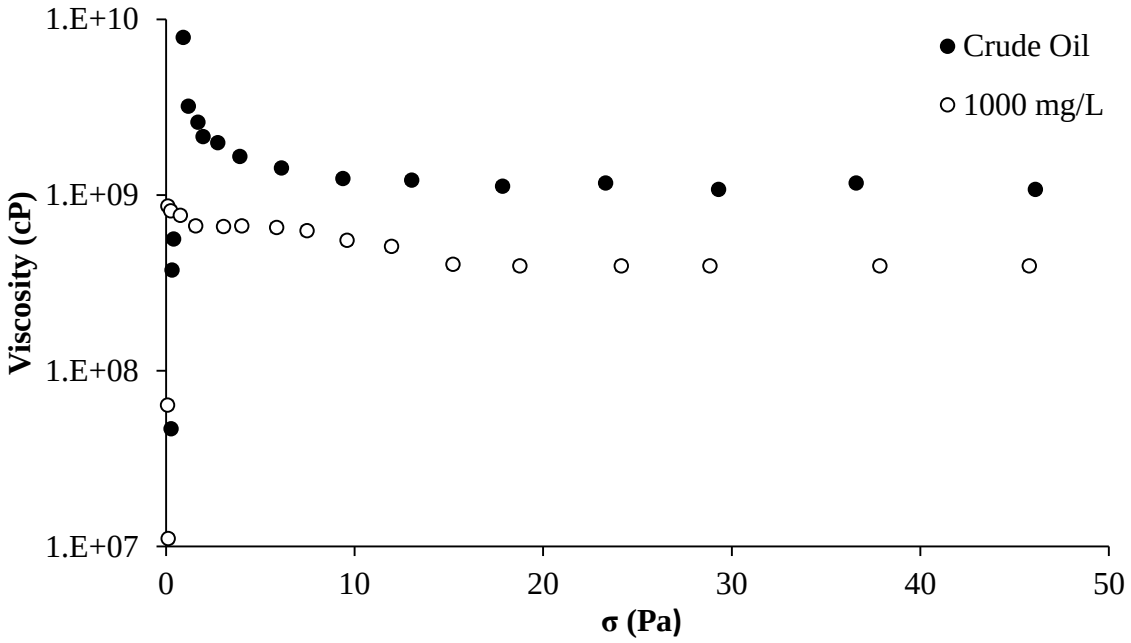

Figure 3.3 Viscosity as a function of shear stress for yield stress measurement for heavy oil in the presence of 1000 mg/L of SiO_2 nanoparticles or their absence of at 298 K.

In previous publications,[26, 28, 29] the high affinity of the nanoparticles of SiO_2 and asphaltenes was demonstrated, and in turn the nanoparticle ability to decrease the size of the aggregates. Therefore, we proceeded to evaluate the performance of the nanoparticles in a de-asphalted oil obtained from the oil matrix and the same HO crude asphaltenes rebuilt with the addition to DAO.

- **Rheometry of de-asphalted, reconstituted and light crude oils**

Figure 3.4 shows the rheological behavior of DAO and the reconstituted oil with 10 wt% asphaltenes, in the presence or absence of SiO_2 nanoparticles, for values of shear rate between 0 and 100 s^{-1} at 298 K. The DAO shows a Newtonian behavior, i.e. their shear stress versus shear rate ratio is constant, and as such, viscosity is not shear-rate dependent [50]. The results obtained are in agreement with those reported by several authors.[19, 51, 52] When 1000 mg/L of SiO_2 nanoparticles were added, the viscosity increases by roughly 20%. This result is consistent with expectations of the theory of hydrodynamic viscosity of Einstein,[32] which states that the viscosity of a solid suspension is directly proportional to the content of solid particles. The DAO is equivalent to an asphaltenes-free crude oil, and therefore viscosity increases upon adding solid particles. The latter is largely due to lack of interactions between asphaltenes and the solid particles that remain dispersed in the medium, contrary to what happens in a heavy oil with high asphaltene content.

The reconstituted oil is obtained by mixing 10% asphaltenes with the DAO, providing assurances that the resulting fluid contains stabilized asphaltenes in the oil matrix. The viscosity increases considerably, a result that confirms that stipulated by Mortazhavi and Shaw [21, 22] who claim that asphaltenes are responsible for the high viscosity of heavy crude oils. The behavior shown by this type crude oil is also non-Newtonian (pseudoplastic). By adding 1000 mg/L of SiO_2 nanoparticles, the viscosity of the reconstituted crude oil is reduced approximately 30%, for all shear rates evaluated. Thus, the hypothesis that reducing viscosity heavy oils is given by the interaction of the nanoparticles with the viscoelastic network formed by asphaltenes in the presence of resins seems clear now. The presence of the resins is very important for the ability of nanoparticles to reduce the viscosity of the heavy crude oil through interactions with the viscoelastic network formed by asphaltenes.[45, 46]

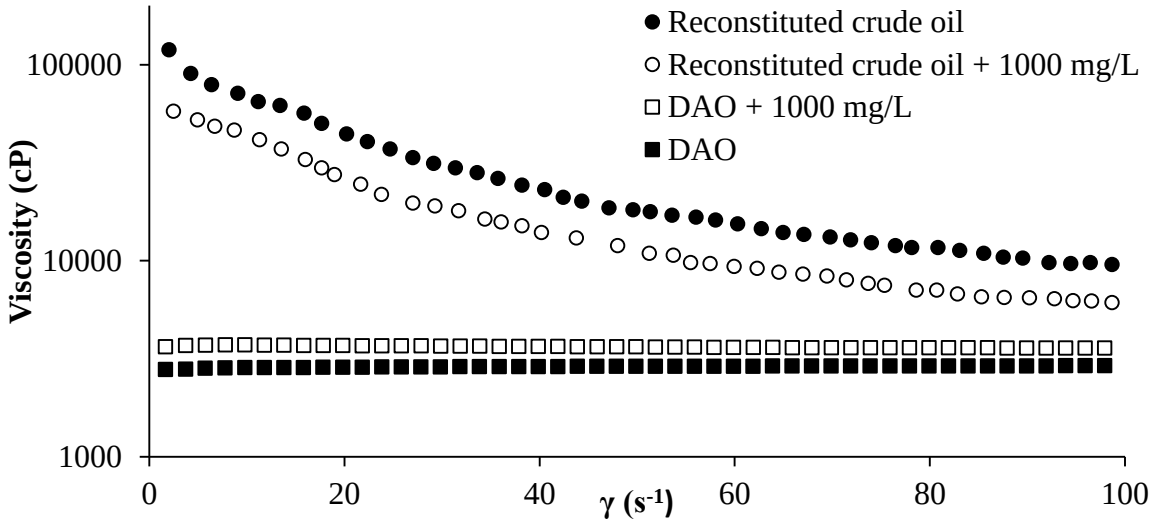

Figure 3.4 Viscosity as function of shear rate for de-asphalted and re-constituted oil in the presence of 1000 mg/L of SiO_2 nanoparticles or their absence, at 298 K

An additional test was performed to evaluate the performance of SiO_2 nanoparticles in a light crude with low asphaltene content with the objective of showing that nanoparticles require the interaction as well as resins and asphaltenes to reduce the oil viscosity. Viscosity results for LO at various concentrations of nanoparticles (including no particles) are shown in Figure 3.5. The LO in the absence of nanoparticles exhibits a Newtonian behavior with a value of viscosity of 2 cP. As nanoparticles concentration increases in the mixture, the viscosity increases. The largest change in viscosity occurs with the addition of 5000 mg/L with a viscosity of 2.56 cP for an increase of 22% with respect to oil without nanoparticles, for a concentration of 1000 mg/L value is 2.36 cP with an increase of 19%. These results are similar to the change observed by adding nanoparticles to DAO (Figure 3.4), and the explanation also lies in the viscosity increase by adding solid particles is largely due to lack of interactions with asphaltenes. Therefore, it can be stated that the nanoparticles are able to reduce oil viscosity when there is an asphaltene-to-resin ratio at which the viscoelastic network forms and can be further modified. In this way, the nanoparticles reduce the viscosity of the crude oil that exhibits a non-Newtonian rheological behavior while in the crude oils with Newtonian behavior, the viscosity increases by increasing the nanoparticles concentration. Nevertheless, the optimal performance conditions considering nanoparticle and asphaltene content necessary for the reduction of viscosity needs to be determined and will be the object of a subsequent study.

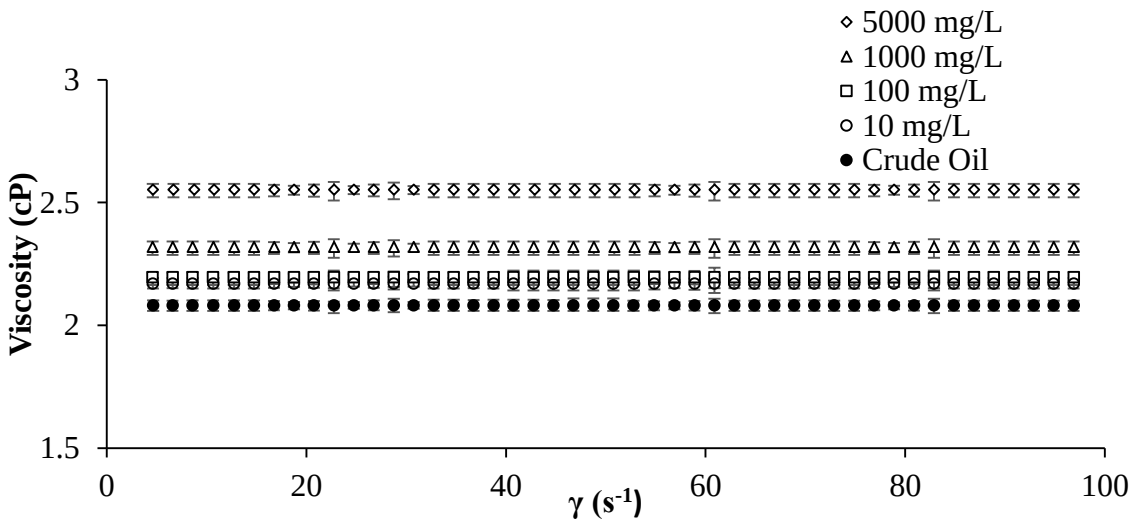

Figure 3.5. Viscosity as a function of shear rate for light crude oil in presence and absence of 10, 100, 1000 and 5000 mg/L SiO_2 nanoparticles, at 298 K.

To determine more precisely the role of nanoparticles in the rheological properties of HO, dynamic rheology measurements were performed. The results are shown in the next section.

3.2.2 Dynamic oscillometry of heavy crude oil.

- **Linear viscoelasticity region**

To determine changes in the internal structure of the heavy oil, it is necessary to evaluate how the viscoelastic moduli are altered by the addition of SiO_2 nanoparticles. There are different types of materials, depending on their structure, exhibiting viscoelastic behavior. For instance, heavy crude oils at low deformations exhibit a linear relationship between the applied stress and the strain induced. This linearity is known as the linear viscoelastic region (LVR), indicating that the internal bonds of the sample structure are still intact [7]. Generally, the LVR of a material can be obtained by dynamic rheological experiments by testing the sweep width at a desired frequency. For this particular case, the LVR was obtained by performing an amplitude test sweep range from strain between 0.1 to 100% at an angular frequency of 10 rad/s, at 298 K. Figure 3.6 shows the amplitude sweep test for heavy oil in the presence of 1000 mg/L SiO_2 nanoparticles or in their absence.

The storage modulus G' characterizes the ability of the material to store energy and represents the elastic behavior of solids; the loss modulus G" characterizes the material's ability to dissipate energy

as it flows and represents the viscous behavior typical of liquids. The phase angle δ measures the coupling between the oscillatory input stimulus to the sample and the response. When the phase angle is equal to 0°, the material behaves like a hookean solid material; when delta equals 90°, the material is considered a Newtonian fluid. When the phase angle is equal to 45°, the contribution of the elastic component of material is equal to the viscous component (G' = G"). In an amplitude sweep test, the common observation is that as the strain is increased, the response of the moduli is constant to a limit, after which the non-linear response region is met.[7, 53, 54]

In Figure 3.6, the storage and loss modulus, G' and G", and the phase angle, δ, are presented. As the strain increases, the moduli remain constant up to about 5%, the point where the linearity is lost. For this reason, we can state that the LVR is between 0.5 and 5% strain. This happens to heavy oil with and without nanoparticles. The loss modulus G" is always greater than the storage modulus G', which indicates that the sample is governed by a more viscous rather than an elastic nature. A lower value of G', the fluid has a lower internal resistance, and for that reason lower viscosity. This happens when 1000 mg/L of SiO_2 nanoparticles are added. The storage modulus (G') represents the elastic behavior of solid itself, and these values are lower than the loss modulus (G"), a reason why the process is governed by the viscous fluid behavior. The phase angle is always greater than 45° or liquid-like.[7, 53, 54]

The linear viscoelastic region is slightly altered by the presence of nanoparticles, which may suggest a change in the internal structure of the material,[49] in this case the heavy oil. To determine the effect of nanoparticles on the viscoelastic properties of the material, frequency analysis was performed in the LVR.

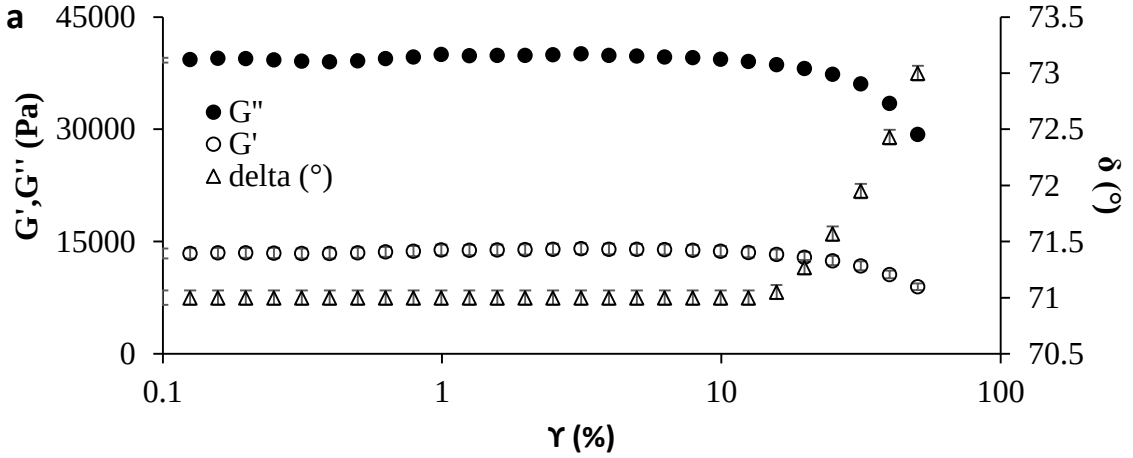

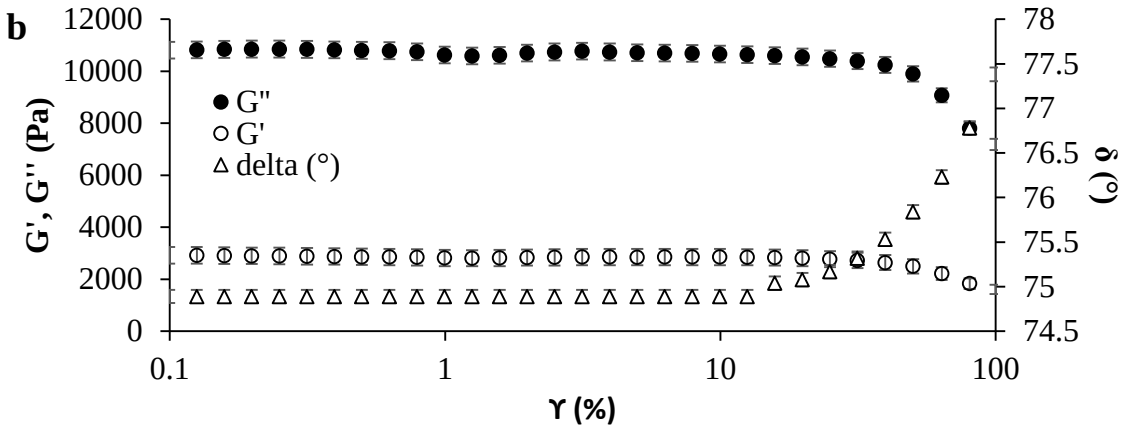

Figure 3.6 Amplitude sweep test for heavy oil in a) absence and b) presence of 1000 mg/L of SiO_2 nanoparticles at a fixed frequency of 10 rad/s and temperature of 298 K.

- **Frequency sweep test for heavy crude oil.**

To carry out the angular frequency analysis, the percentage of deformation was set at 2% (a large enough value within the LVR) and a sweep was performed from 0.1 to 100 rad/s, at 288, 298 and 313 K. The latter is conducted with the goal of identifying possible structural changes generated by the addition of nanoparticles. Figure 3.7 shows the viscoelastic moduli for crude oil with and without nanoparticles at 288 K. For HO without nanoparticles, the value of the loss modulus G" is always greater than that of the storage modulus G'. This indicates that the sample is governed by a more viscous behavior than elastic one throughout the frequency sweep evaluated. As the angular frequency increases, the values of the moduli increase. This behavior is so attributed to the arrangement of overlapped asphaltenes under shear rate behaving like a transient network of fractal aggregates.[23] In this concentrated regime, the particles interact with strong colloidal forces, which is in accordance with Mullins et al.;[55] Wong, Yen, and Fu;[56] and Yen and Chilingarian,[57] who have reported that heavy crude oils contain a suspension of asphaltene colloids stabilized by resins. The smallest colloid particles diameter is 2–4 nm and may form clusters with dimensions of 10–30 nm. Further asphaltene aggregation may lead to the formation of flocs and macrostructures. The presence of the viscoelastic behavior of the heavy crude oil indicates that interacting flocs and macrostructures form a certain network that will be affected by temperature, and the addition of light crude oil, solvents, and by the presence of nanoparticles as in the following figures.

Crude oil with nanoparticles exhibits a behavior similar to that of crude oil, i.e. the value of the loss modulus G" is always greater than the storage modulus G'. However, when comparing the moduli values for crude oil without nanoparticles, they decrease approximately 40 % in the presence of nanoparticles. For this reason, both viscous and elastic contributions decrease, and this is reflected in decreased dynamic viscosity shown in Figure 2a. The decrease in viscosity, explained from the change in the viscoelastic properties of the material by the addition of nanoparticles, has a positive impact on the optimization of operational conditions associated with the transport and mobility of heavy oil.

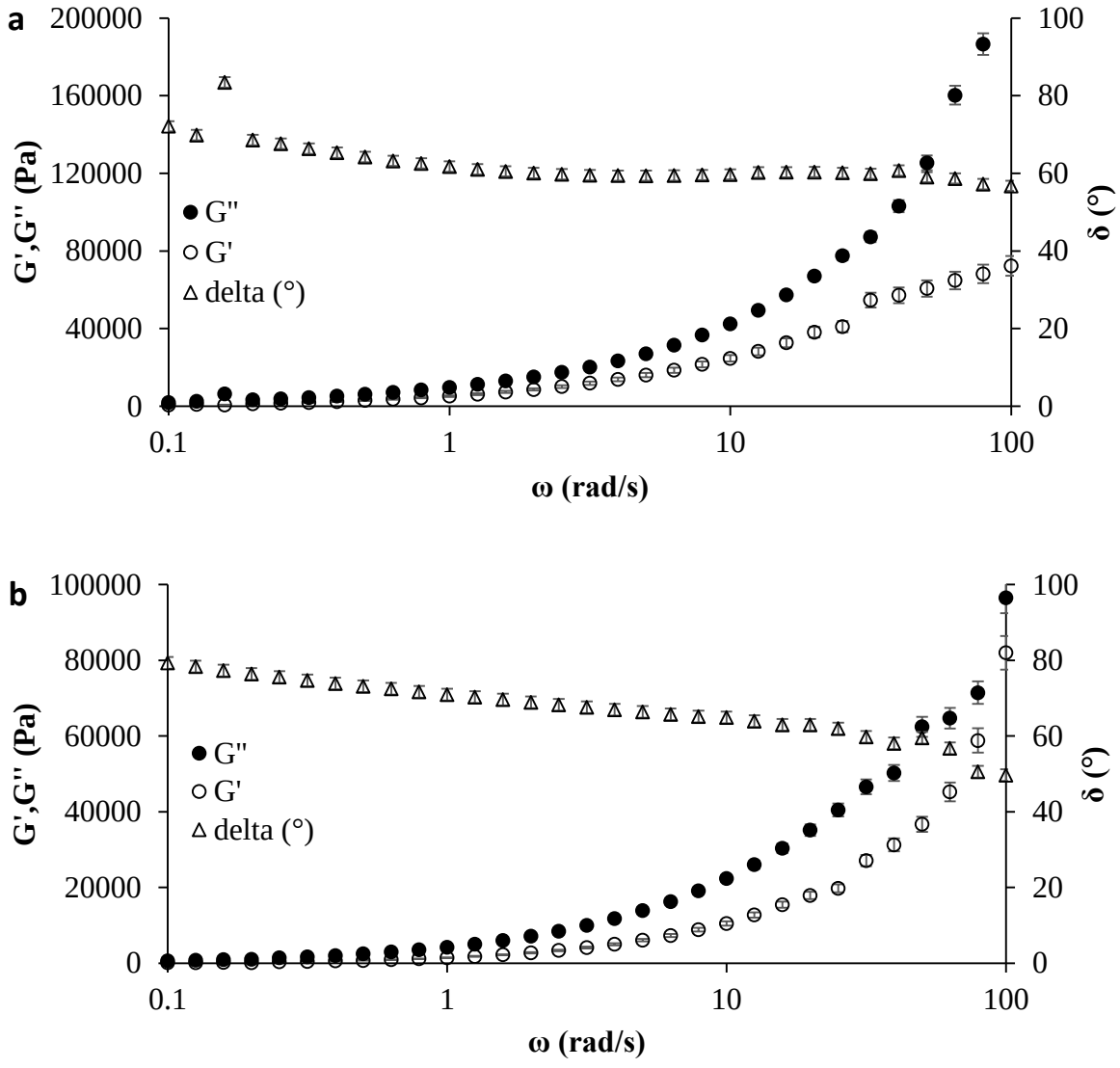

Figure 3.7 Master curve for heavy oil in a) absence and b) the presence of 1000 mg/L of SiO_2 nanoparticles at 288 K and for a fixed strain of 2%.

The behavior of viscoelastic moduli at 298 K presented in Figure 3.8 is similar to that shown in Figure 3.7. The value of the loss modulus G" is always greater than the storage modulus G', which indicates that the sample is governed by a behavior more viscous rather than elastic in the entire frequency range evaluated. An increase in temperature is expected to lead to a decrease in the values of the G' and G" moduli, similar to results found by Bazaleya et al.,[39] Behzadfar and Hatzikiriakos,[23] and Pierre et al.[4] The presence of nanoparticles in the matrix of heavy oil generates a change in the internal structure of the fluid that is reflected in the decline of the viscoelastic moduli, G' and G", and a slight increase in the phase angle δ. For instance, at a fixed frequency of 1 rad/s the loss modulus G" decreases down from 2191 Pa to 979 Pa, G" decreases down from 684 Pa to 229 Pa, and the phase angle δ increases from 72.6° to 76.8°. The decrease of G' and G" refers to a decrease in the elastic and viscous contributions; an increased value of δ suggests a more liquid-like than a solid-like response, which explains reduction viscosity of heavy crude. Therefore, the elastic and viscous contributions decrease at the same time as viscosity decreases. The phase angle has a slightly decreasing trend with increasing angular frequency, however, it is always above 45°, which confirms that the fluid behavior is dominated by the contribution of the viscous component. At 298 K a direct effect of nanoparticles on the internal structure of heavy oil is not clearly observed, and for this reason, oscillometric tests were performed at 313 K.

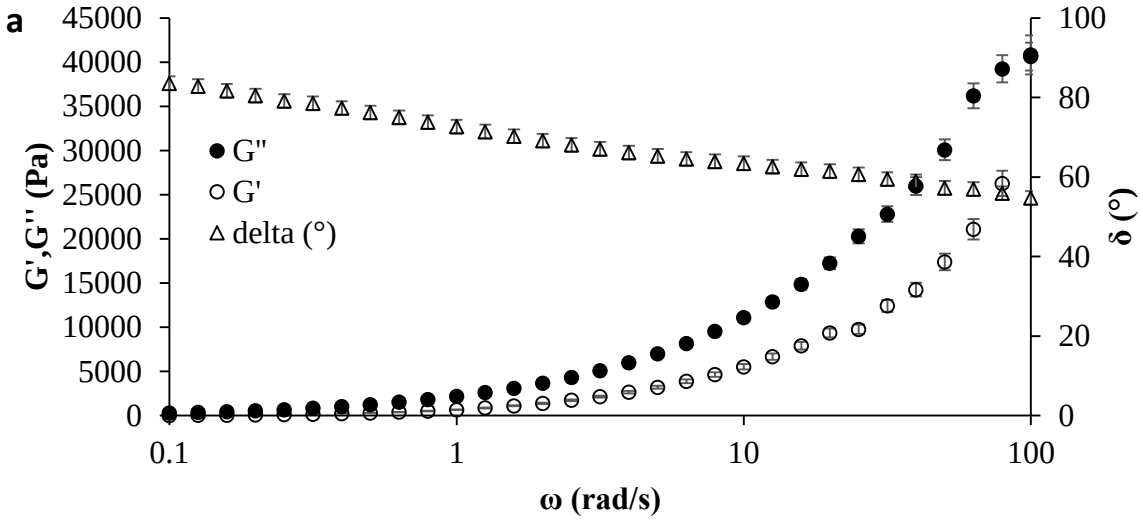

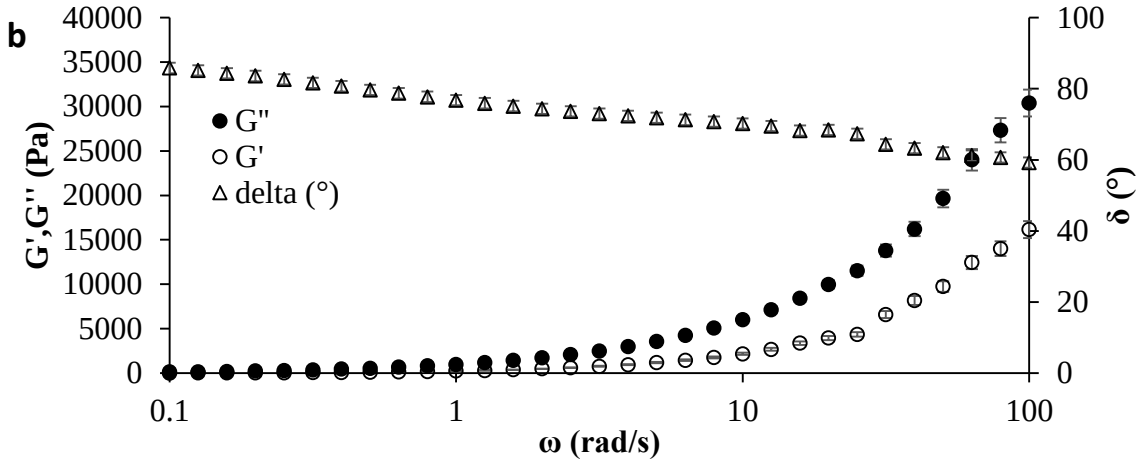

Figure 3.8 Master curve for heavy oil in a) absence and b) the presence of 1000 mg/L of SiO_2 nanoparticles at 298 K and for a strain of 2%.

Figure 3.9 shows the analysis of oscillometric frequency sweep between 0.1 and 100 rad/s for crude oil without and with nanoparticles at 313 K. In Figure 3.9, it is observed that the crude oil in the absence of nanoparticles exhibits a behavior that is more governed by the viscous component (G" greater than G') at a frequency near 30 rad/s. However, at higher frequencies, the value of the storage modulus considerably exceeds the value of the loss modulus, which decreases considerably, just as the phase angle suffers decreases in value to 38° approximately.

If we consider that lower values of 45° the own elastic component of the solid has more impact on the rheological behavior than the viscous component, we can say that under these conditions of temperature and frequency, the material behaves more like a solid than as a liquid.[7, 53, 54] However, by adding 1000 mg/L SiO_2 nanoparticles, it is clearly noted that for all the frequency sweep the viscous component (related to G") is always greater than the elastic component (related to G'). As the phase angle is always above 45°, it can be said that the material in the presence of nanoparticles behaves more like a liquid rather than as a solid.

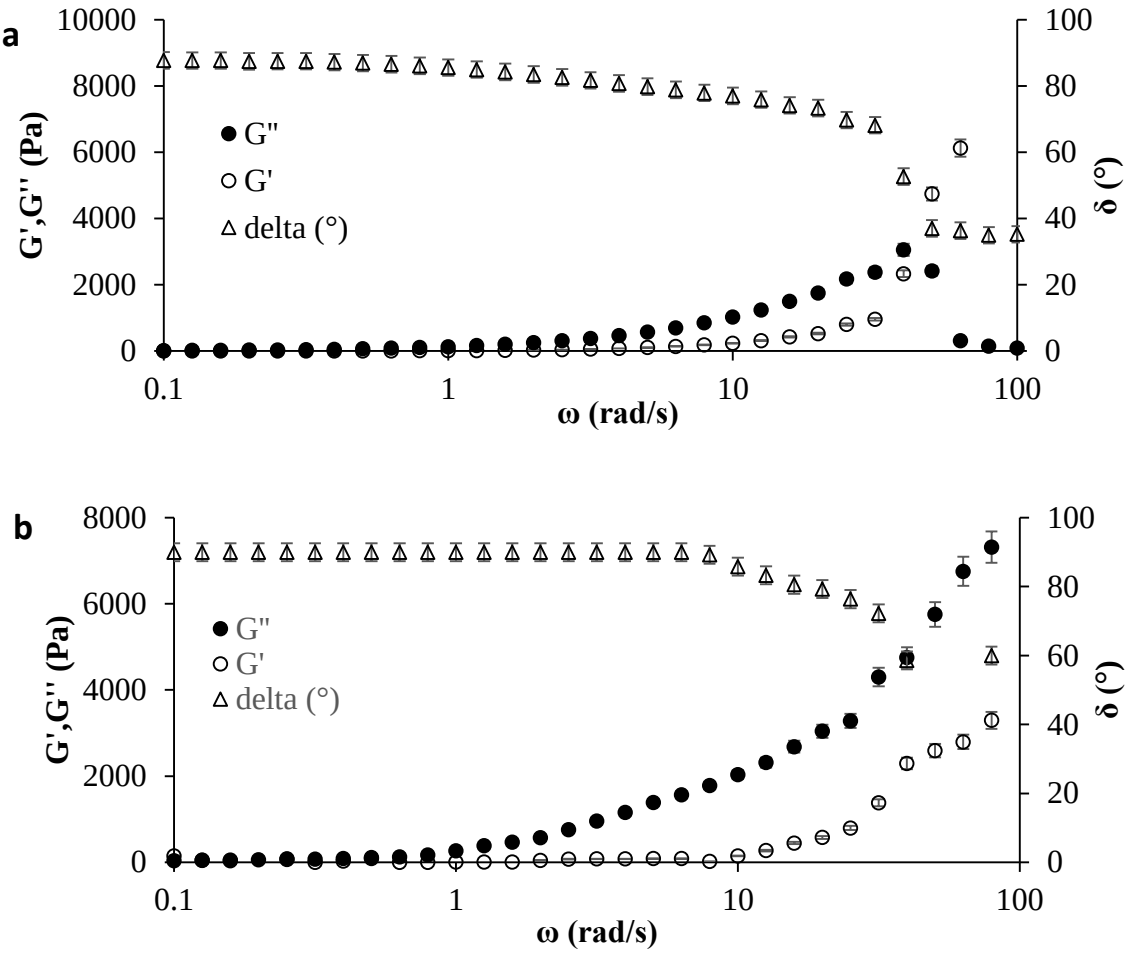

Figure 3.9 Master curve for heavy oil in a) absence and b) the presence of 1000 mg/L of SiO_2 nanoparticles at 313 K and for a strain of 2%.

Figure 3.10 shows the comparative loss modules and storage for heavy oil in absence and presence of 1000 mg/L of nanoparticles for each temperature tested. Clearly, the values related to G'and G" moduli decrease as the temperature increases. In this order, the viscosity decrease can be interpreted as a decrease in the contribution of the elastic and viscous components of the material and these results are consistent with those found in the literature by several authors [4, 23, 39].

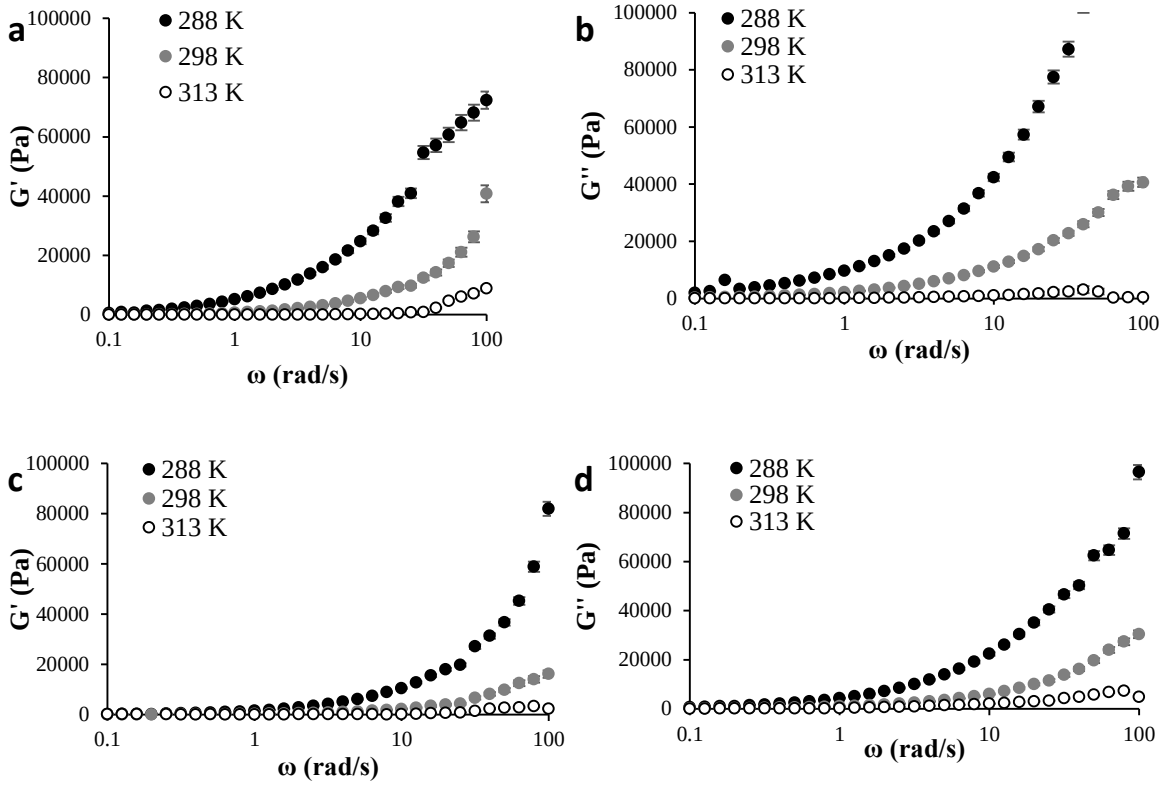

Figure 3.10 Heavy crude oil moduli for a strain of 2% and at 288, 298, and 313 K: a) G' for heavy oil, b) G" for heavy oil, c) G' for heavy oil in the presence of 1000 mg/L of SiO_2 nanoparticles and d) G" for heavy oil in presence of 1000 mg/L of SiO_2 nanoparticles.

In Table 3.2, the ratio of G' for heavy crude oil without nanoparticles and G' of heavy crude oil with 1000 mg/L of SiO_2 nanoparticles ($G'_{HO}/G'_{Np's}$) is given for a frequency sweep between 0.1 and 100 rad/s, at the three values of temperature evaluated 288, 298 and 313 K. The corresponding ratio for G" is also given.

At 288 and 298 K, the ratios ($G'_{HO}/G'_{Np's}$) and ($G''_{HO}/G''_{Np's}$) decrease as the frequency increases, which means that the effect of nanoparticles on the viscoelastic properties of the fluid is lower at higher frequencies, however, the value is greater than 1. Consequently, the addition of nanoparticles always yields a reduction in the magnitudes of G' and G", which in turn may explain the reduced viscosity by the addition of nanoparticles.[24, 53]

At 313 K, the action of nanoparticles impacts more the storage modulus G' than the loss modulus G" at high frequencies, therefore the ratio ($G'_{HO}/G'_{Np's}$) is bigger than 1, and the ratio ($G''_{HO}/G''_{Np's}$) is lower than 1. Consequently, nanoparticles increase the magnitude of the viscous component, but decreases in a greater way the elastic component of the sample, which is why, in the presence of

nanoparticles, the rheological behavior is considered governed by the viscous component (own of liquids) rather that the elastic component (own solid) thus reducing viscosity by adding silica nanoparticles explained.

Table 3.2. The ratios between moduli of heavy oil in absence and presence of SiO_2 nanoparticles at different frequencies. Data obtained at 288, 298, and 313 K.

ω	288 K		298 K		313 K	
(rad /s)	$G'_{HO}/G'_{Np's}$	$G''_{HO}/G''_{Np's}$	$G'_{HO}/G'_{Np's}$	$G''_{HO}/G''_{Np's}$	$G'_{HO}/G'_{Np's}$	$G''_{HO}/G''_{Np's}$
0.1	5.065	2.950	3.843	2.483	0.004	0.391
0.5	3.990	2.503	3.108	2.314	0.041	0.614
1	3.576	2.358	2.978	2.237	1.039	0.489
5	2.633	2.298	2.756	1.970	1.205	0.411
10	2.361	2.009	2.561	1.847	1.576	0.502
50	1.652	1.951	2.528	1.531	1.827	0.420
100	1.132	1.894	1.787	1.337	3.887	0.081

Strong combined evidence in this work indicates that changes in the viscoelastic properties of the sample are due to structural changes in the viscoelastic network originally formed by asphaltenes and their colloidal behavior in the presence of resins. Alteration of this viscoelastic network is reflected through the viscosity reduction of the heavy oil sample for the three temperatures tested in the presence of SiO_2 nanoparticles.

3.2.3 NMR T_2 Measurements.

Knowledge of oil viscosity is important when estimating hydrocarbon reserves and evaluating the potential for waterflooding or EOR processes. This information is especially important in heavy oil and bitumen, viscosity is usually the major impediment to recovery of these reserves. As oil viscosity increases, obtaining a laboratory measurement is difficult and prone to error, and viscosities measured in the lab may not be representative of field conditions. Nuclear magnetic resonance (NMR) is therefore an attractive alternative method for determining viscosity oil.[58]

In recent years, nuclear magnetic resonance techniques have been applied to study liquid systems, from liquids with a single molecule such as water, to complex liquids such as crude ones. Nuclear magnetic resonance can be considered the most important analytical technique for structural analysis of molecules in solution.[59, 60] This method probes molecular properties by interrogating atomic nuclei with magnetic fields and radio-frequency irradiation. More specifically the NMR denotes the resonant interaction of the magnetic moments in a time-invariant magnetic field with the magnetic component of an electromagnetic wave.

Several correlations already exist for determining viscosity oil using NMR. Some of these correlations compare the geometric mean T_2 relaxation time to oil viscosity. NMR measures the response of hydrogen protons inside an external magnetic field. The protons inside oil and water are polarized in the direction of the field, called the longitudinal direction. Another magnetic field is applied to a radio frequency press the direction of the protons on the transverse plane, where they rotate in phase with one another. As the protons give off energy to one another and to their surroundings, the Magnetic signal in the transverse plane decays. This is known as relaxation.[61]

For this reason, this section intends to evaluate the effect of nanotechnology on the T_2 relaxation times of crude oil and presents a mathematical relationship between T_2 and viscosity.

The results presented in this section were obtained at the University of Wyoming, where the international internship was carried out, for that reason a different heavy crude was used. The heavy crude selected to carry out the measurements came from Mexico, the heavy crude oil has a density of 0.98 gr/mL and a C_5 – asphaltene content of 23.7 wt%.

The results are divided into two parts, the rheological evaluation of heavy crude in the presence of nanoparticles at various concentrations, and the measurement of T_2 relaxation times using a Minispec LF 110 NMR.

- **Rheologic measurements with Np's**

Figure 3.11 shows the rheometry of heavy crude in the presence of SiO_2 nanoparticles of 8 nm diameter (S8), at concentrations of 200, 500, 800, 1000, 2000 and 10000 mg/L respectively, for 3 temperature values a) 303, b) 313 and c) 323 K. It also presents the highest degree of viscosity reduction for each temperature evaluated.

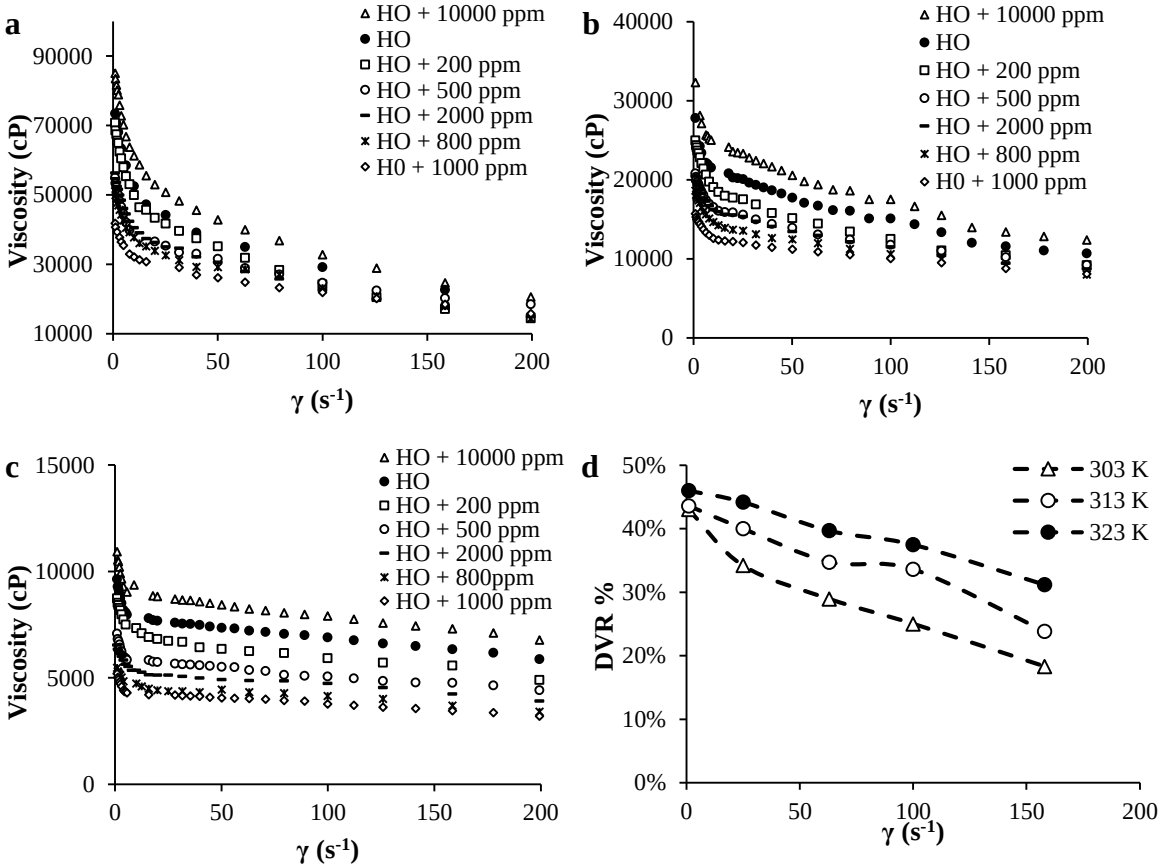

Figure 3.11. Rheologic curves for HO with nanoparticles for concentrations of 200, 500, 800, 1000, 2000 and 1000 mg/L at a) 303, b) 313, c) 323 K, and d) the DVR of HO+1000 mg/L.

The results presented in Figure 3.11 present trends similar to those obtained in the previous chapters, that is, viscosity reductions by increasing the content of nanoparticles, but to a limit. In this case the optimum point is again 1000 mg/L. At concentrations of 10000 mg/L the viscosity increases due to the increase in the packing factor, this is understood from the point of view that it is a lot of solid particles in so little liquid volume, therefore they tend to agglomerate and increase the viscosity of the solid.

Figure 3.11 presents the performance of the optimum concentration of nanoparticles (1000 mg/L) at each temperature, expressed as a percentage of DVR. It can be observed that the nanoparticles show better performance with increasing temperature, possibly because they are better dispersed at higher temperatures, due to the decrease of viscosity of the fluid at higher temperature, in this way the particles can travel more easily Internally in the crude and produce greater points of contact and greater interaction with the asphaltenes present in the heavy crude matrix.

- **NMR T_2 relaxation times measurements.**

Figure 3.12 shows the T_2 relaxation times measured for each sample prepared at the same temperature values as the measurements in the rheological tests.

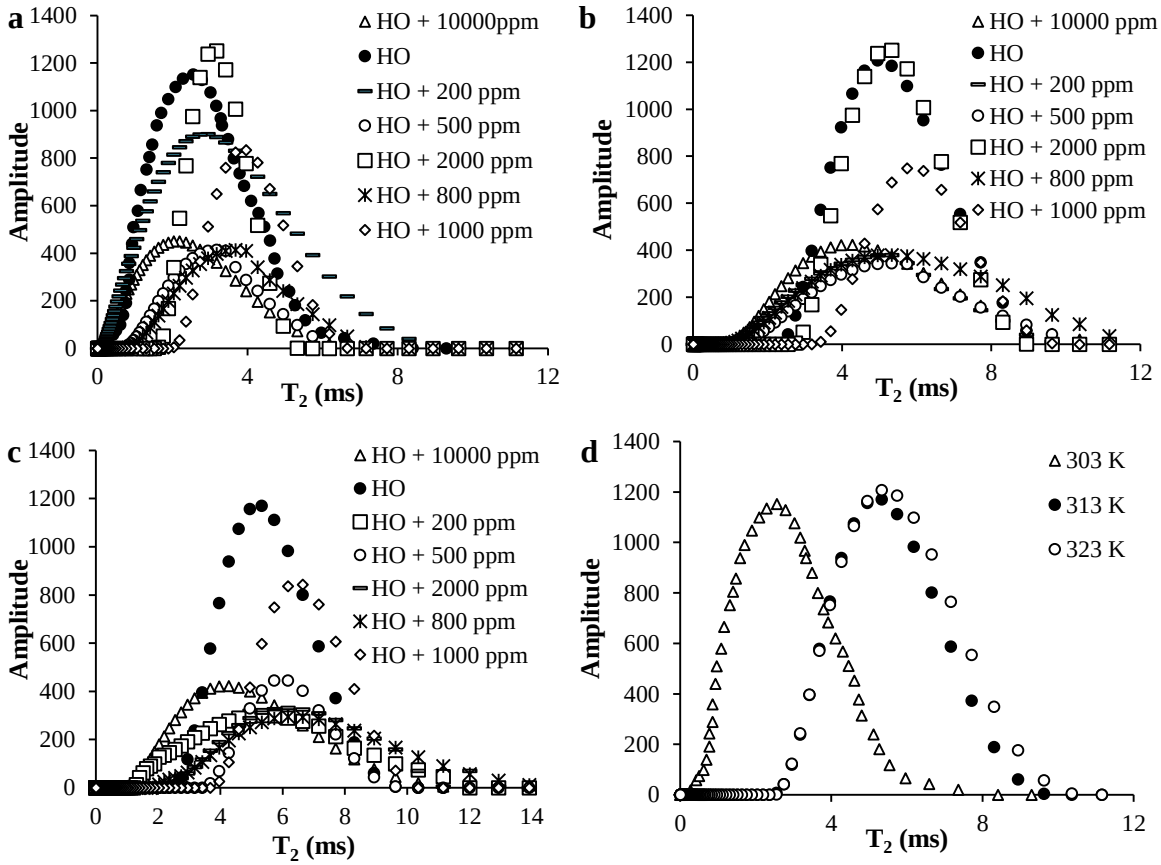

Figure 3.12. T_2 relaxation times curves for HO with nanoparticles for concentrations of 200, 500, 800, 1000, 2000 and 1000 mg/L at a) 303, b) 313, c) 323 K, and d) the HO without nanoparticles.

The results presented in Figure 3.12 indicate a clear trend in relaxation times when adding nanoparticles. For all evaluated temperatures, the tendency presented is similar to the trend obtained in the reduction of viscosity. The relaxation time T_2 is very small, this is according to the results obtained previously in literature.[58, 62, 63] The time increases from lowest to highest with the following trend 10000 < HO < 200 < 500 < 2000 < 800 < 1000 mg/L. The speed at which the hydrogen molecules vibrate is affected by two fundamental reasons, the first is by the presence of a solid surface of SiO_2, and the second by the viscosity reduction of the fluid produced by the nanoparticles. Figure 3.13 shows a relationship between the relaxation times and the nanoparticle concentration

and the viscosity of the fluid. These results are in line with those presented in literature[58, 62, 63] where as the viscosity decreases the relaxation time increases.

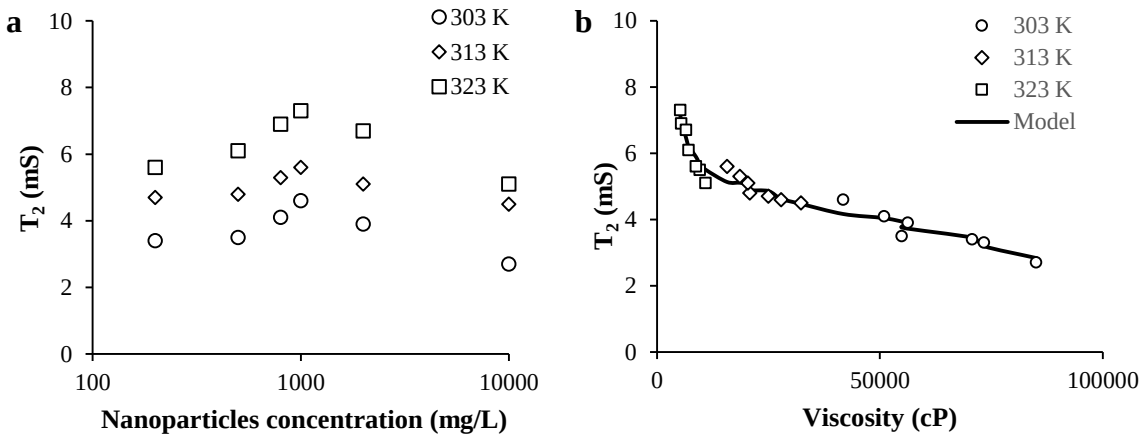

Figure 3.13. Relationship between T_2 relaxation times and a) nanoparticles concentrations and b) viscosity of the heavy oil, at 303, 313, and 323 K.

In Figure 3.13a. It is possible to identify a maximum point where the relaxation time is higher than any other value, this means that the hydrogen molecules take longer to achieve a state of equilibrium when they are subjected to a magnetic field and this is removed. The value agrees with that obtained in all rheological characterizations of the HO sample in the presence of nanoparticles. Figure 3.13b shows the trend of the T_2 relaxation times with the viscosities obtained for all mixtures measured at fixed shear rate of $1s^{-1}$. Clearly the process that dominates relaxation times is the viscosity of the medium. It proposes an empirical correlation that allows to estimate the viscosity of the fluid using NMR, is presented in equation (3.1).

$$T_2 = 5 - 3e^5\mu + \frac{5e^7}{\mu^2} \tag{3.1}$$

In this way it is possible to expand the range of possibilities to obtain viscosities of complex fluids such as heavy crude

3.3 Partial conclusions

- The effect of SiO_2 nanoparticles with mean particle size of 8 nm on the rheological properties of heavy oil was studied through viscometry test at steady state as well as dynamic

oscillometry. Heavy oil viscosity reduces as shear rate increases following a shear thinning non-Newtonian behavior. The addition of nanoparticles at a concentration of 1000 mg/L reduces the viscosity of heavy oil 12 to 45%, for shear rates between 0 - 100 s^{-1} and temperatures of 288, 298 and 313 K.

- Nanoparticles decrease the yield stress of heavy oil by more than 50%, and this helps to reduce the mechanical stress needed for the fluid to start flowing. The addition of nanoparticles increases the viscosity of the light crude oil and de-asphalted oil, the reason why we conclude that the nanoparticles interact directly with the asphaltenes and hence with the viscoelastic network.
- It was viscoelastic moduli values indicate that samples fluid flow is governed dominated by viscous dissipation at all strain and frequencies evaluated. This leads to the conclusion that asphaltenes overlap acts like a transient network of fractal aggregates. The shear thinning behavior is so-attributed to the arrangement of overlapped asphaltenes under shear. However, at 313 K and higher frequencies (> 30 rad/s), the value of the storage modulus exceeds the value of the loss modulus, which considerably decreases, just as the phase angle decreases to a value of approximately 38°. Therefore, we can say that under conditions of temperature and these frequency values, the heavy oil in the absence of nanoparticles behaves more like a solid than as a liquid.
- However, by adding 1000 mg/L SiO_2 nanoparticles, it is clearly noted that for all the frequency sweep the viscous component (related to G") is always greater than the elastic component (related to G'). Consequently, the material in the presence of nanoparticles behaves more like a liquid rather than as a solid.
- NMR T2 measurements reflect that the nanoparticles alter the viscosity of the heavy crude and as the times increase, the viscosity decreases. The trend obtained is identical to the rheological behavior of crude oil. A new mathematical model that correlates these two variables is presented
- The results obtained by combining techniques of rheometry at steady state and dynamic oscillometry confirm the hypothesis that nanoparticles affect the internal structure of the heavy oil, by modifying the viscoelastic network of asphaltenes at high concentrations (greater than 4 wt%) in the presence of resins [64, 65]. This modification is due to the interaction forces between silica nanoparticles and asphaltenes present in the matrix of heavy oil. This study further supports the proposed hypothesis on the effect of nanoparticles in the reduction of heavy oils viscosity and opens a better direction for application of this novel and cost-effective technology.

3.4 References

1. Chen, D. T.; Wen, Q.; Janmey, P. A.; Crocker, J. C.; Yodh, A. G., Rheology of soft materials. *Condensed Matter Physics* **2010,** 1.
2. Ranalli, G., *Rheology of the Earth*. Springer Science & Business Media: 1995.
3. Qi, Y.; Zakin, J. L., Chemical and rheological characterization of drag-reducing cationic surfactant systems. *Industrial & engineering chemistry research* **2002,** 41, (25), 6326-6336.
4. Pierre, C.; Barré, L.; Pina, A.; Moan, M., Composition and heavy oil rheology. *Oil & Gas Science and Technology* **2004,** 59, (5), 489-501.
5. Hasan, S. W.; Ghannam, M. T.; Esmail, N., Heavy crude oil viscosity reduction and rheology for pipeline transportation. *Fuel* **2010,** 89, (5), 1095-1100.
6. Jezequel, P.; Flaud, P.; Quemada, D., RHEOLOGICAL PROPERTIES AND FLOW OF CONCENTRATED DISPERSE MEDIA. II-STEADY AND UNSTEADY FLOW ANALYSIS OF HEAVY CRUDE OIL EMULSIONS. *Chemical engineering communications* **1985,** 32, (1-5), 85-99.
7. Ghannam, M. T.; Hasan, S. W.; Abu-Jdayil, B.; Esmail, N., Rheological properties of heavy & light crude oil mixtures for improving flowability. *Journal of Petroleum Science and Engineering* **2012,** 81, 122-128.
8. Khan, M. R., Rheological properties of heavy oils and heavy oil emulsions. *Energy Sources* **1996,** 18, (4), 385-391.
9. Sztukowski, D. M.; Yarranton, H. W., Rheology of asphaltene-Toluene/water interfaces. *Langmuir* **2005,** 21, (25), 11651-11658.
10. Chong, J.; Christiansen, E.; Baer, A., Rheology of concentrated suspensions. *Journal of applied polymer science* **1971,** 15, (8), 2007-2021.
11. Al-Maamari, R. S.; Buckley, J. S., Asphaltene precipitation and alteration of wetting: the potential for wettability changes during oil production. *SPE Reservoir Evaluation & Engineering* **2003,** 6, (04), 210-214.
12. Gharfeh, S.; Yen, A.; Asomaning, S.; Blumer, D., Asphaltene flocculation onset determinations for heavy crude oil and its implications. *Petroleum science and technology* **2004,** 22, (7-8), 1055-1072.
13. Oskui, G.; Reza, P.; Jumaa, M. A.; Folad, E. G.; Rashed, A.; Patil, S. In *Systematic Approach for Prevention and Remediation of Asphaltene Problems During CO2/Hydrocarbon Injection Project*, The Twenty-first International Offshore and Polar Engineering Conference, 2011; International Society of Offshore and Polar Engineers: 2011.
14. Heim, W.; Wolf, F. J.; Savery, W. T., Heavy oil recovering. In Google Patents: 1984.
15. McMillen, J. M., Enhanced oil recovery; producing a solvent-crude mixture. In Google Patents: 1985.
16. Hart, A., A review of technologies for transporting heavy crude oil and bitumen via pipelines. *Journal of Petroleum Exploration and Production Technology* **2014,** 4, (3), 327-336.
17. Gateau, P.; Hénaut, I.; Barré, L.; Argillier, J., Heavy oil dilution. *Oil & gas science and technology* **2004,** 59, (5), 503-509.
18. Alvarez, G.; Poteau, S.; Argillier, J.-F.; Langevin, D.; Salager, J.-L., Heavy oil− water interfacial properties and emulsion stability: Influence of dilution. *Energy & Fuels* **2008,** 23, (1), 294-299.
19. Argillier, J.; Barre, L.; Brucy, F.; Dournaux, J.; Henaut, I.; Bouchard, R. In *Influence of asphaltenes content and dilution on heavy oil rheology*, SPE International Thermal Operations and Heavy Oil Symposium, 2001; Society of Petroleum Engineers: 2001.
20. Martínez-Palou, R.; de Lourdes Mosqueira, M.; Zapata-Rendón, B.; Mar-Juárez, E.; Bernal-Huicochea, C.; de la Cruz Clavel-López, J.; Aburto, J., Transportation of heavy and extra-heavy

crude oil by pipeline: A review. *Journal of Petroleum Science and Engineering* **2011,** 75, (3), 274-282.
21. Mortazavi-Manesh, S.; Shaw, J. M., Effect of diluents on the rheological properties of Maya crude oil. *Energy & Fuels* **2016,** 30, (2), 766-772.
22. Mortazavi-Manesh, S.; Shaw, J. M., Thixotropic rheological behavior of Maya crude oil. *Energy & Fuels* **2014,** 28, (2), 972-979.
23. Behzadfar, E.; Hatzikiriakos, S. G., Viscoelastic properties and constitutive modelling of bitumen. *Fuel* **2013,** 108, 391-399.
24. Abivin, P.; Taylor, S. D.; Freed, D., Thermal behavior and viscoelasticity of heavy oils. *Energy & Fuels* **2012,** 26, (6), 3448-3461.
25. Amanullah, M.; Al-Tahini, A. M. In *Nano-technology-its significance in smart fluid development for oil and gas field application*, SPE Saudi Arabia Section Technical Symposium, 2009; Society of Petroleum Engineers: 2009.
26. Franco, C. A.; Nassar, N. N.; Ruiz, M. A.; Pereira-Almao, P.; Cortés, F. B., Nanoparticles for inhibition of asphaltenes damage: adsorption study and displacement test on porous media. *Energy & Fuels* **2013,** 27, (6), 2899-2907.
27. Schmid, G., *Nanoparticles: from theory to application*. John Wiley & Sons: 2011.
28. Nassar, N. N.; Betancur, S.; Acevedo, S.; Franco, C. A.; Cortés, F. B., Development of a Population Balance Model to Describe the Influence of Shear and Nanoparticles on the Aggregation and Fragmentation of Asphaltene Aggregates. *Industrial & Engineering Chemistry Research* **2015,** 54, (33), 8201-8211.
29. Zabala. R, F. C. A., Cortes. F.B., Application of Nanofluids for Improving Oil Mobility in Heavy Oil and Extra-Heavy Oil: A Field Test. *Society of Petroleum Engineers Journal* **2016**, 14.
30. Taborda, E. A.; Franco, C. A.; Lopera, S. H.; Alvarado, V.; Cortés, F. B., Effect of nanoparticles/nanofluids on the rheology of heavy crude oil and its mobility on porous media at reservoir conditions. *Fuel* **2016,** 184, 222-232.
31. Zabala, R.; Franco, C.; Cortés, F. In *Application of Nanofluids for Improving Oil Mobility in Heavy Oil and Extra-Heavy Oil: A Field Test*, SPE Improved Oil Recovery Conference, 2016; Society of Petroleum Engineers: 2016.
32. Einstein, A., Eine neue bestimmung der moleküldimensionen. *Annalen der Physik* **1906,** 324, (2), 289-306.
33. Franco, C.; Patiño, E.; Benjumea, P.; Ruiz, M. A.; Cortés, F. B., Kinetic and thermodynamic equilibrium of asphaltenes sorption onto nanoparticles of nickel oxide supported on nanoparticulated alumina. *Fuel* **2013,** 105, 408-414.
34. Franco, C. A.; Montoya, T.; Nassar, N. N.; Pereira-Almao, P.; Cortés, F. B., Adsorption and subsequent oxidation of colombian asphaltenes onto Nickel and/or Palladium oxide supported on fumed silica nanoparticles. *Energy & Fuels* **2013,** 27, (12), 7336-7347.
35. Lee, J. M.; Shin, S.; Ahn, S.; Chun, J. H.; Lee, K. B.; Mun, S.; Jeon, S. G.; Na, J. G.; Nho, N. S., Separation of solvent and deasphalted oil for solvent deasphalting process. *Fuel Processing Technology* **2014,** 119, 204-210.
36. Ovarlez, G.; Tocquer, L.; Bertrand, F.; Coussot, P., Rheopexy and tunable yield stress of carbon black suspensions. *Soft Matter* **2013,** 9, (23), 5540-5549.
37. Olmedo, H.; Rojas, N.; Torres, S.; Azócar, A.; Gómez, C.; Briceño, M. I., Flow behaviour of colloidal petroleum coke-in-water suspensions. *Journal of Non-Newtonian Fluid Mechanics* **2015,** 220, 108-115.
38. Mozaffari, S.; Tchoukov, P.; Atias, J.; Czarnecki, J.; Nazemifard, N., Effect of Asphaltene Aggregation on Rheological Properties of Diluted Athabasca Bitumen. *Energy & Fuels* **2015,** 29, (9), 5595-5599.
39. Bazyleva, A. B.; Hasan, M. A.; Fulem, M.; Becerra, M.; Shaw, J. M., Bitumen and heavy oil rheological properties: Reconciliation with viscosity measurements. *Journal of Chemical & Engineering Data* **2009,** 55, (3), 1389-1397.

40. Dimitriou, C. J.; McKinley, G. H., A comprehensive constitutive law for waxy crude oil: a thixotropic yield stress fluid. *Soft Matter* **2014,** 10, (35), 6619-6644.
41. Ershov, D.; Stuart, M. C.; van der Gucht, J., Mechanical properties of reconstituted actin networks at an oil–water interface determined by microrheology. *Soft Matter* **2012,** 8, (21), 5896-5903.
42. Franco, C. A.; Lozano, M. M.; Acevedo, S.; Nassar, N. N.; Cortés, F. B., Effects of Resin I on Asphaltene Adsorption onto Nanoparticles: A Novel Method for Obtaining Asphaltenes/Resin Isotherms. *Energy & Fuels* **2015,** 30, (1), 264-272.
43. Tao, R.; Xu, X., Reducing the viscosity of crude oil by pulsed electric or magnetic field. *Energy & fuels* **2006,** 20, (5), 2046-2051.
44. Andreatta, G.; Bostrom, N.; Mullins, O. C., High-Q ultrasonic determination of the critical nanoaggregate concentration of asphaltenes and the critical micelle concentration of standard surfactants. *Langmuir* **2005,** 21, (7), 2728-2736.
45. Andreatta, G.; Bostrom, N.; Mullins, O. C., Ultrasonic Spectroscopy of Asphaltene Aggregation. In *Asphaltenes, Heavy Oils, and Petroleomics*, Springer: 2007; pp 231-257.
46. Yang, X.; Czarnecki, J., Tracing sodium naphthenate in asphaltenes precipitated from Athabasca bitumen. *Energy & Fuels* **2005,** 19, (6), 2455-2459.
47. Batchelor, G. K., *An introduction to fluid dynamics*. Cambridge university press: 2000.
48. Egbogah, E. O.; Ng, J. T., An improved temperature-viscosity correlation for crude oil systems. *Journal of Petroleum Science and Engineering* **1990,** 4, (3), 197-200.
49. Visintin, R. F.; Lapasin, R.; Vignati, E.; D'Antona, P.; Lockhart, T. P., Rheological behavior and structural interpretation of waxy crude oil gels. *Langmuir* **2005,** 21, (14), 6240-6249.
50. Rao, M. A., *Rheology of fluid and semisolid foods: principles and applications: principles and applications*. Springer Science & Business Media: 2010.
51. Angle, C. W.; Lue, L.; Dabros, T.; Hamza, H. A., Viscosities of heavy oils in toluene and partially deasphalted heavy oils in heptol in a study of asphaltenes self-interactions. *Energy & fuels* **2005,** 19, (5), 2014-2020.
52. Hasan, M. A.; Shaw, J. M., Rheology of reconstituted crude oils: Artifacts and asphaltenes. *Energy & Fuels* **2010,** 24, (12), 6417-6427.
53. Behura, J.; Batzle, M.; Hofmann, R.; Dorgan, J., Heavy oils: Their shear story. *Geophysics* **2007,** 72, (5), E175-E183.
54. Lesueur, D., The colloidal structure of bitumen: Consequences on the rheology and on the mechanisms of bitumen modification. *Advances in colloid and interface science* **2009,** 145, (1), 42-82.
55. Mullins, O. C.; Sheu, E. Y.; Hammami, A.; Marshall, A. G., *Asphaltenes, heavy oils, and petroleomics*. Springer Science & Business Media: 2007.
56. Wong, G. K.; Yen, T. F., An electron spin resonance probe method for the understanding of petroleum asphaltene macrostructure. *Journal of Petroleum Science and Engineering* **2000,** 28, (1), 55-64.
57. Yen, T. F.; Chilingarian, G. V., *Asphaltenes and asphalts, 2*. Elsevier: 2000; Vol. 40.
58. Bryan, J.; Kantzas, A.; Mirotchnik, K., Viscosity determination of heavy oil and bitumen using NMR relaxometry. *Journal of Canadian Petroleum Technology* **2003,** 42, (07).
59. Bovey, F. A.; Mirau, P. A.; Gutowsky, H., *Nuclear magnetic resonance spectroscopy*. Elsevier: 1988.
60. Ernst, R. R.; Bodenhausen, G.; Wokaun, A., *Principles of nuclear magnetic resonance in one and two dimensions*. Clarendon Press Oxford: 1987; Vol. 14.
61. Coates, G. R.; Xiao, L.; Prammer, M. G., NMR logging. *Principles and Applications: Houston, Halliburton Energy Services* **1999**.
62. de Oliveira Ramos, P. F.; de Toledo, I. B.; Nogueira, C. M.; Novotny, E. H.; Vieira, A. J. M.; de Vasconcellos Azeredo, R. B., Low field 1 H NMR relaxometry and multivariate data analysis

in crude oil viscosity prediction. *Chemometrics and Intelligent Laboratory Systems* **2009,** 99, (2), 121-126.
63. Yang, Z.; Hirasaki, G. J., NMR measurement of bitumen at different temperatures. *Journal of Magnetic Resonance* **2008,** 192, (2), 280-293.
64. Mullins, O. C.; Betancourt, S. S.; Cribbs, M. E.; Dubost, F. X.; Creek, J. L.; Andrews, A. B.; Venkataramanan, L., The colloidal structure of crude oil and the structure of oil reservoirs. *Energy & Fuels* **2007,** 21, (5), 2785-2794.
65. Yudin, I. K.; Anisimov, M. A., Dynamic light scattering monitoring of asphaltene aggregation in crude oils and hydrocarbon solutions. In *Asphaltenes, Heavy Oils, and Petroleomics*, Springer: 2007; pp 439-468.

4. Optimization of transport conditions of heavy crude oil through the use of nanofluids: Reduction of naphtha consume.

Techniques commonly used to improve their transport through oleoducts includes the addition of solvents (light crude oil, naphtha, diesel, among others) or gasses (mainly, CO2), as they contribute to reducing oil viscosity.[1-4] However, these techniques can prompt issues such as the precipitation and/or deposition of asphaltenes in the production systems, and pipelines.[1, 2] Naphtha is one of the most commonly used diluents, and its application is based on the requirements for transport through pipelines, amounting to roughly 400 cSt at 311 K, 18ºAPI and 0.5% of sediments and water (%BSW).[5-7]

The transport of crude oils in Colombia has increased considerably since 2005, going from 150,000 to 450,000 barrels per day (bpd) transported in 2016.[8] This considerable growth in resource market availability brings along significant economic impacts of the order of 20% of total production costs, even in some cases higher costs.[8] To better understand the magnitude of this impact it is worth recalling that the total production costs amounted to more than US$ 8.00 billion dollars recently, in which case 20% translates into roughly US$ 1.60 billion in transportation costs.[9] The latter represents a significant economic impact on the national company, Ecopetrol S.A (ECP). Ecopetrol S.A, Colombia's largest operating company, holds ownership of 77% of the pipeline transportation capacity in Colombia. As of December 31, 2012, the network of pipelines spanned approximately 8,760 kilometers in length.[10] At present, ECP has 8 projects to improve transportation capacity through the construction and improvement of pipelines, storage and pumping stations. These investments total more than 6,00 billion US$.[9] Considering that Colombia has more than 13,000 Mbpd[11] in proven reserves of heavy crude oil, investments become a must to exploit these resources. The increase in oil volumes causes strain on the system in various ways, including the need to revamp pipeline capacity as well as the volume of diluent (naphtha) required to address the growing

demand.[8, 12] These changes, in turn, create national pressures due to economic impacts associated with limitations in naphtha supply, which must be heavily supplemented with imports. ECP had to increase naphtha imports, representing a 44% increase in annual purchases.[10] The consumption of naphtha reported by Ecopetrol S.A is approximately 70,000 bpd,[13] representing costs more than USD$ 5.5 million per day. Alternatives to the traditional use of naphtha become critical for Colombia, which is also necessary to address power requirements to pump the heavy, viscous hydrocarbons long distances that must be mitigated through viscosity reduction.

The methods used for transporting heavy oil and bitumen through pipelines are generally grouped into two categories:[14] i) viscosity reduction, e.g. injection of solvents or light hydrocarbons, emulsification through formation of O/W emulsions, and preheating of crude oil, and ii) drag/friction reduction, such as the use of drag reducing additives and core annular flow.

Viscosity reduction as a way to improve the mobility of heavy crude oil has been extensively studied.[6, 15-25] For instance, Castro et al.[26] and the company Geo-Estratos S.A report the use of different viscosity reducing agents. They investigate the rheological behavior of solutions with terpolymers at different shear rates and temperatures. They synthesized terpolymers with different contents of styrene (S), n-butyl acrylate (BA), and vinyl acetate (VA) by semi-continuous emulsion polymerization. The results confirm that the viscosity of the crude is reduced when the terpolymers have a high percentage in S and lesser amounts of BA or VA. The molecular weight of the terpolymers plays an important role in their performance as viscosity reducers. Geo-Estratos S.A[26] offers viscosity bioreducers based on vegetable oils, reaching reductions in viscosity of up to 60% by injecting only 3 %v/v, applied to a reservoir at a temperature of 323 K and a depth of 1280 m, in emulsions with a water content of 2%. Mortazavi - Manesh & Shaw[7] studied the effect of different types of chemical compounds on the rheological properties of Maya crude oil at different temperatures. The compounds used in their study were toluene, n-heptane and a mixture 50 %v/v of toluene and butanone. Results show that the mixture toluene + butanone is promising based on the resulting viscosity reduction. Another common diluent used is naphtha, a product derived from petroleum. Naphtha has a high API gravity and shows good compatibility with asphaltenes and with other compounds of crude oil due to its chemical nature. Gateau et al.[18] proposed that a blend of naphtha and organic solvent would reduce the quantity of diluents needed to lower the viscosity of heavy oil-to-pipeline transportation specifications. However, the high consumption of these solvents increases transportation costs and generates different environmental risks due to the production of polluting gasses, making it an unattractive technique.[27]

An alternative technique for enhancing heavy crude oil flowability through pipelines is the formation of an oil-in-water emulsion. In this technology, the heavy crude oil is emulsified in water and

stabilized with the aid of surfactants. The emulsion is formed by the dispersion of the crude in the form of drops in the continuous aqueous phase, leading to viscosity reduction.[15, 24] The list of methods used to generate the oil droplets to create the emulsions includes the use of devices such as dispersing machines, mixing with rotor–stator, colloid mills, high-pressure homogenizers applying high shearing stresses, emulsification by a membrane and ultrasonic waves.[6, 28, 29] At the industrial level, the application of emulsions to transport heavy crude oils through the use of Orimulsión®, developed by the State Oil Company of Venezuela, PDVSA, in the eighties, consists of a crude oil-in-water emulsion with a dominant/high fraction of oleic phase. The technology was developed with the aim of facilitating the transportation of heavy crude because the dilution with conventional diesel oil was no longer economically attractive,[30-33] though the resulting emulsion can be used as an effective fuel in fuel-fired power plants. Another method commonly used to reduce the high viscosity of heavy crude oil and bitumen, and thereby improve their flowability, is the application of heat. Heating the pipeline causes a rapid reduction in viscosity that lowers the resistance of the oil to flow.[34, 35] However, heating involves a considerable amount of energy and cost as well. Another issue relates to greater internal corrosion problems, due to the increase in temperature. However, heating the pipeline may induce changes in the rheological properties of the crude oil that may result in flow instability in the. Numerous heating stations are required, consequently adding to the overall operating cost, in addition to heat losses occurring along the pipeline as a result of the modest oil flow.

The second method used to transport heavy oil is drag/friction reduction through either the use of drag reducing additives or core annular flow. The use of drag reducing agents seeks to reduce friction near the pipe walls to prevent the growth of turbulence by absorbing the energy released in the lamellar layer.[32] The main reducing agents can be divided into surfactants, fibers, and polymers. An important requirement is the solubility of the drag reducing agents in the heavy crude, in addition to having good resistance to thermal and chemical degradation. Common difficulties encountered in the use of entrainment additives include the tendency of the additive to separate when stored, the dissolution of the additives in the heavy crude oil and the problem of shear degradation when dissolved in heavy crude oil. The first report of the core-annular flow technique was published by Isaacs & Speed,[19] who proposed the possibility of channeling of viscous fluids through water lubrication of the pipe walls. This technique consists of surrounding the core of the heavy crude oil with water or a solvent film layer adjacent to the pipeline wall, which acts as a lubricant for oil flow. In this sense, water or the solvent behaves like a ring, while the heavy crude is the core in the flow through the pipe. The required water or solvent fraction is in the 10-30 wt% range,[24, 36] This implies that the pressure drop along the pipe depends weakly on the viscosity of the heavy oil, but strongly

on that of water. Also, Bensakhria et al.[16] found that with heavy oil as the center of the pipe and water near the surface of the pipe wall, the reduction in pressure drop was in excess of 90% compared to crude oil flow without lubrication. However, some of the limitations include the formation of waves that are created at the interface of the lubrication layer and the oil that hinders the flow.[16, 19] Additionally, when the density difference between oil and water is large, the resulting buoyancy force produces a radial movement of the oil core.[16, 19] Also, the stability of the flow system is still under investigation.[17, 19] A few publications propose nanofluids as viscosity reducers for heavy and extra-heavy crude oils. In our previous study,[37] we synthesized nanofluids composed of SiO_2 nanoparticles and generated viscosity reduction of heavy crude oil, focused on the improvement of in situ mobility of crude oil. Recently, the same authors[38] showed that the addition of nanoparticles alters the heavy crude internal structure, which is responsible for the observed viscosity reduction. If we consider that the effect of reducing viscosity in heavy crude oil by the addition of nanoparticles can considerably reduce energy and solvent consumption, the outcome will represent an innovative, viable alternative for improvement of heavy and extra-heavy crude mobility as well as the mitigation of the aforementioned issues in production and transportation stages. Therefore, the main objective of this chapter is to evaluate the effect of the SiO_2-based nanofluids in the reduction of naphtha consumptions for heavy and extra-heavy crude oils. In this way, four nanofluids were prepared using different solvents (toluene, biodiesel, and biodiesel with two surfactants, one ionic and another non-ionic) and nanoparticles of fumed silica for evaluating the reduction of naphtha use in the transport process. The analysis of this work was based mainly on the steady state rheological study and dynamic flow tests in a pipeline for the two crude oils evaluated. Also, an economic approach and environmental impact were carried out for evaluating the potentiality of this nanofluids type in the transport applications of heavy and extra-heavy crude oils.

4.1 Experimental

4.1.1 Materials

Two Colombian oils, one heavy oil (HO) and one extra heavy oil (EHO), were used in experiments. Properties of the selected HO and EHO are presented in Table 1. Four nanofluids were prepared with different diluents. Toluene (99.5%, Merck KGaA, Germany), biodiesel, and naphtha were used as diluents; these last two were provided by Ecopetrol S.A (Colombia). Cetyltrimethylammonium Bromide CTAB (98%, PanReac, Spain) and non-ionic surfactant Tween 80 (Sigma-Aldrich, St.

Louis, MO) were employed for nanofluids preparation. The nanofluid is prepared using four different carrier fluids: toluene, biodiesel, biodiesel + Tween 80, and biodiesel + CTAB. When surfactants were added to biodiesel, 1 wt% of the respective surfactant is mixed with the biodiesel at 300 rpm and 298 K, on a stirring plate. An amount of nanoparticles selected for the preparation of nanofluid is 1000 mg/L with respect to the volume of crude oil. This nanoparticle concentration was selected using criteria from our previous work.[37] Nanoparticles were added to the carrier fluid using a magnetic stirrer at 300 rpm for 1 h at 298 K and subsequently sonicated for 30 min to guarantee the correct dispersion of the nanoparticles in the liquid medium.[39-43] The properties of the prepared nanofluids are summarized in Chapter 1

4.1.2 Methods

- **Rheologic measurements**

Steady-state rheological measurements were performed using a Kinexus Pro+ rotational rheometer (Malvern Instruments, Worcestershire - UK), equipped with a Peltier plate for temperature control, with a cone-plate geometry at a gap of 1.35 mm. Several conditions were evaluated to analyze the change in viscosity induced by the addition of nanofluids. For the HO and EHO, the nanofluids were evaluated at concentrations of 5 and 10% v/v. The rheological measurements were conducted at 311 K at a shear rate range of 1-100 s^{-1}. Experiments were performed for dry nanoparticles and the prepared nanofluids. Each experimental condition set was repeated three times. The accuracy of the rheological measurements is approximately ± 1%.[7, 37, 44, 45]

- **Dynamic flow test**

Dynamic flow tests are performed to determine the best nanofluid formulation that leads to the largest viscosity reduction according to rheological measurements. The selected nanofluid was added to a heavy or extra-heavy crude oil, and a positive displacement pump drove the mixture through a stainless steel pipeline 82 ft. in length and 1/4 inch in inner diameter designed exclusively for these tests. To this end, 1.0 L of the mixture was used, while the pressure differential was continuously measured during the test. Figure 4.1 shows schematics of the setup employed for the dynamic tests. The experiments were carried out in triplicate ensuring fully developed flow by constantly measuring the pressure differential. The test was performed in a laminar regime, defined by a Reynolds number much lower than 2100. The results obtained during the test can be used as a starting point to develop

larger assemblies and to perform flow tests with higher flows and greater distance. The tests were performed at a constant flow rate of 5 mL/min at two different temperatures of 298 K and 313 K.

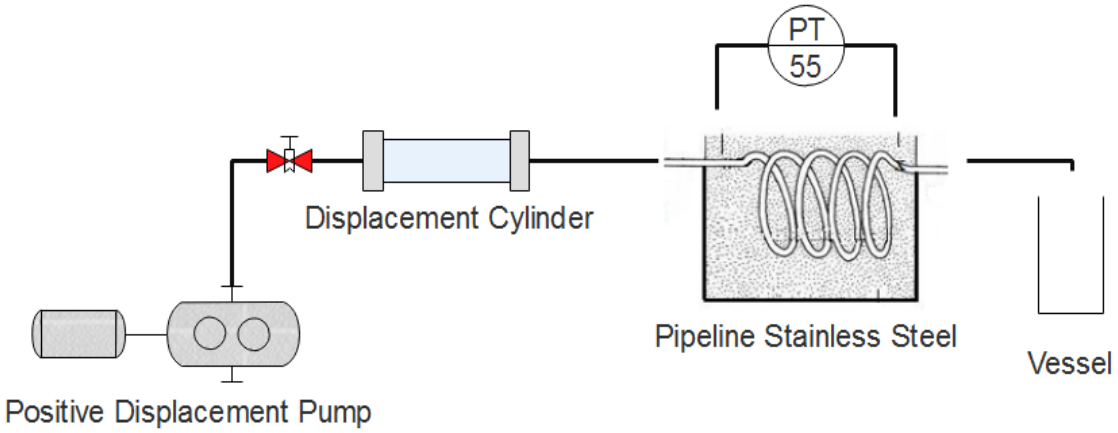

Figure 4.1 Schematic representation of experimental setup for the dynamic flow test.

4.2 Modeling

4.2.1 Rheological model

The Herschel-Bulkley (H-B) model was used for describing the rheological behavior of heavy and extra heavy oil mixtures in the presence or absence of the nanofluids as a function of the shear rate γ (s^{-1}).[46-48] The flow behavior index n_H was investigated for different mixtures and was used as a proxy for the rheological behavior of the fluid. Values of $n_H \leq 1.0$ indicate that the fluid follows a pseudoplastic behavior.[46] Consistency index K_H ($Pa \cdot s^n$) refers to the fluid viscosity. The limiting viscosity parameters $\mu_{0,\gamma}$ (cP) and $\mu_{\infty,\gamma}$ (cP) indicate the behavior of the fluid when subjected to conditions of zero and infinite stresses, respectively. The H-B model is described as follows:

$$\mu = K_H(\gamma^{(n_H-1)}) + \mu_{\infty,\gamma} \quad (4.1)$$

where, μ is the viscosity of the fluid at a predetermined shear rate. The accuracy of the H-B model for describing the rheological behavior of the fluids was evaluated by examining the root-mean-square error (*RMSE%*) and the correlation coefficient R^2.[49]

4.3 Results

In the previous chapters, have shown that S8 nanoparticles with a mean particle size of 8 nm have the ability to effectively adsorb heavy oil components such as asphaltenes and resins on their surfaces [50], resulting in a considerable reduction in fluid viscosity. Based on our previous work,[37, 38, 51] results in this chapter are divided into five main sections: (1) rheological characterization of the heavy oil in the presence of naphtha at 311 K, (2) performance of different nanofluids for the reduction of crude oil viscosity as well consumption of naphtha, (3) evaluation of the best nanofluid on an extra heavy oil, (4) dynamic tests in pipelines with a nanofluid selected according to the results obtained by the rheological measurements at steady state and (5) economic analysis and environmental impact.

4.3.1 Steady state measurements of heavy crude oil with naphtha

Experiments at different concentrations of naphtha added to an HO sample upon attaining a viscosity value close to that required for transportation in the pipeline (400 cSt at 311K) were conducted. For this reason, here the flow viscosity index (F_i) is defined with the objective of determining a numerical value that allows identifying whether a blend meets the minimum viscosity requirements to be transported, defined as follows:

$$F_i = \frac{\mu_{transp}}{\mu_{mixture}} \tag{4.2}$$

where, μ_{transp} is the viscosity required for heavy oil transportation, and $\mu_{mixture}$ is the viscosity of the mixture after addition of viscosity modifier. Values of $F_i \geq 1.0$ indicate that the dosage of treatment attains the requirements for fluid transportation. The viscosity was measured at shear rate of 90 s^{-1} since at values higher the fluid behaves in a completely Newtonian fashion, and its viscosity will not be altered with a further increase in the shear rate.

Figure 4.2 shows the rheological measurements at steady state for HO containing naphtha at dosages of 10, 20, 24, and 27 %, and shear rates 0 - 100 s^{-1} at 311 K. Naphtha was added to reach viscosity values lower than 400 cP (F_i close to 1.9) according to transportation requirements. The shape of the curve for HO exhibits a non-Newtonian, shear-thinning behavior, i.e. oil viscosity decreases with

increasing shear rate. Similar results were found by Mortazavi-Manesh & Shaw,[7, 44] Bazyleva et al.,[52] Mozaffari et al.,[45] Tao & Xu,[53] and Taborda et al.[37] The high viscosity of the heavy crude oil is due to the formation of a viscoelastic network made up of asphaltenes and resins that occur mainly when the content of asphaltenes in the heavy crude is greater than 5 wt%.[38]

The addition of naphtha produces viscosity reduction for all shear rate values evaluated and increases as the naphtha dosage rises. The rheology of HO after naphtha addition also shows a non-Newtonian behavior, although not as pronounced in comparison to the additive-free heavy crude oil. It can be observed from Figure 4.2 that by increasing the amount of naphtha in the system, a behavior closer to Newtonian fluids is obtained. The largest drop in viscosity obtained for heavy oil corresponds to a naphtha concentration of 27 % with an F_i = 0.99. In this case, where the asphaltene content of the evaluated HO is 12%, naphtha is expected to interact with the viscoelastic network of asphaltenes, disrupting the asphaltene aggregate system in crude oil, and thus generating the expected viscosity drop.

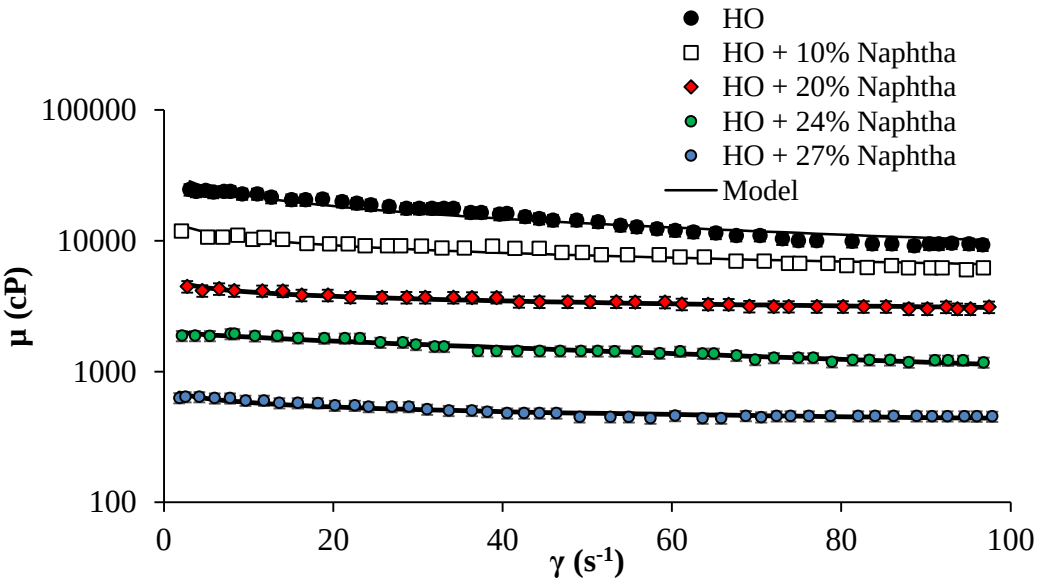

Figure 4.2 Heavy oil viscosity as a function of shear rate in the presence or absence of naphtha at concentrations of 10, 20, 24 and 27% at 311 K.

Table 4.1 presents the parameters of the Herschell-Bulkley rheological model and the values of the flow viscosity index for heavy oil samples with naphtha, nanoparticles, and nanofluids evaluated. As observed, the viscosity measured at an infinite shear rate and the consistency index K_H decreased by increasing the naphtha dosage. The flow behavior index n_H becomes closer to one as the amount

of diluent is increased, since the behavior tends to be more Newtonian. Similar results are reported by.[44]

Table 4.1 Herschell-Bulkley model parameters and flow viscosity index for mixtures between HO and different treatments at 311 K.

Treatment	Dosage	H-B model parameters					F_i
		K_H (Pa·S^n)	n_H	$\mu_{\infty,\gamma}$ (cP)	R^2	RSME%	
None	-	430221	0.987	8800	0.92	9.7	0.05
Naphtha	10%	152071	0.988	5567	0.91	9.9	0.07
	20%	31534	0.989	2850	0.93	8.2	0.14
	24%	15889	0.993	1077	0.94	7.1	0.38
	27%	5702	0.998	399	0.91	9.6	0.99
SiO_2	1000 mg/L	140988	0.988	5825	0.92	9.4	0.06
SiO_2 + Naphtha	1000 mg/L + 10%	13053	0.989	2545	0.92	8.7	0.16
	1000 mg/L + 14%	9338	0.990	1085	0.92	8.3	0.37
	1000 mg/L + 18%	1228	0.993	385	0.90	9.8	1.08
Toluene	5%	85483	0.989	5725	0.93	9.1	0.06
	10%	53094	0.990	4819	0.90	9.5	0.09
TNF	5%	60973	0.989	5577	0.91	9.1	0.07
	10%	12007	0.991	3925	0.90	9.7	0.11
Biodiesel	5%	95841	0.989	5025	0.91	9.6	0.06
	10%	15824	0.989	3128	0.90	9.8	0.12
Biodiesel + Tween 80	10%	31964	0.988	3354	0.93	8.1	0.11
Biodiesel + CTAB	10%	19046	0.989	3075	0.93	7.7	0.12
BNF	5%	81125	0.989	4875	0.93	8.1	0.08
	10%	11465	0.991	2225	0.90	9.5	0.19
BTWNF	10%	15814	0.989	2928	0.90	9.8	0.13
BCNF	10%	13339	0.990	2821	0.94	6.5	0.14
BNF + Naphtha	10% + 13%	5463	0.994	335	0.92	7.1	1.17

4.3.2 Steady state measurements of heavy crude oil with nanofluids

- **Reduction of heavy oil viscosity with toluene-based nanofluid.**

The first nanofluid was added to the heavy crude mixture at 5 and 10% by volume. Figure 4.3 presents the rheological behavior of heavy crude oil, crude oil with nanoparticles, crude oil in the presence of only the solvent, and finally crude oil in the presence of nanofluid. The curve corresponding to the heavy crude exhibits a non-Newtonian shear-thinning behavior. This behavior is governed by the presence of heavy hydrocarbons in the crude oil structure.[2, 45, 54-56] By adding the solvent, the heavy molecules dissolve, reducing the viscosity of the fluid considerably. As expected, as the solvent concentration in the mixture increases, the viscosity reduction increases. If we compare the viscosity values at a fixed shear rate (90 s^{-1}), we can determine the degree of viscosity reduction, expressed as the percentage reduction. In this sense, we note that for upon addition of 1000 mg/L SiO_2 nanoparticles the percentage of reduction is roughly 19%; for 5% toluene, the reduction is 26%, and for 5% of TNF, the reduction is 34%. For 10% toluene, the reduction is 45%, and for 10% of TNF, the reduction is 55%. When the SiO_2 nanoparticles are added, a viscosity reduction is obtained due to the redistribution of the viscoelastic network formed by the asphaltenes present in the crude [38]. However, when the nanofluid (TNF) is added, the highest viscosity reduction is obtained. The viscosity reduction obtained by the addition of a nanofluid is produced by two main factors: 1) the effect of the solvent on the oil components dissolving the large molecules and 2) the effect of the nanoparticles by altering the viscoelastic network formed by the asphaltenes in the presence of resins, as shown previously in several publications,[37, 38, 50, 57] nanoparticles have the ability to adsorb asphaltenes on their surface, inhibiting the self-aggregation of asphaltenes. In this way, a structural change is a surface, which produces the reduction of viscosity. Synergistic effects result from immersing the nanoparticles in a liquid medium, due to a more uniform distribution of the nanoparticles in the matrix of heavy crude oil, allowing greater points of contact between the heavy hydrocarbons and the nanoparticles.

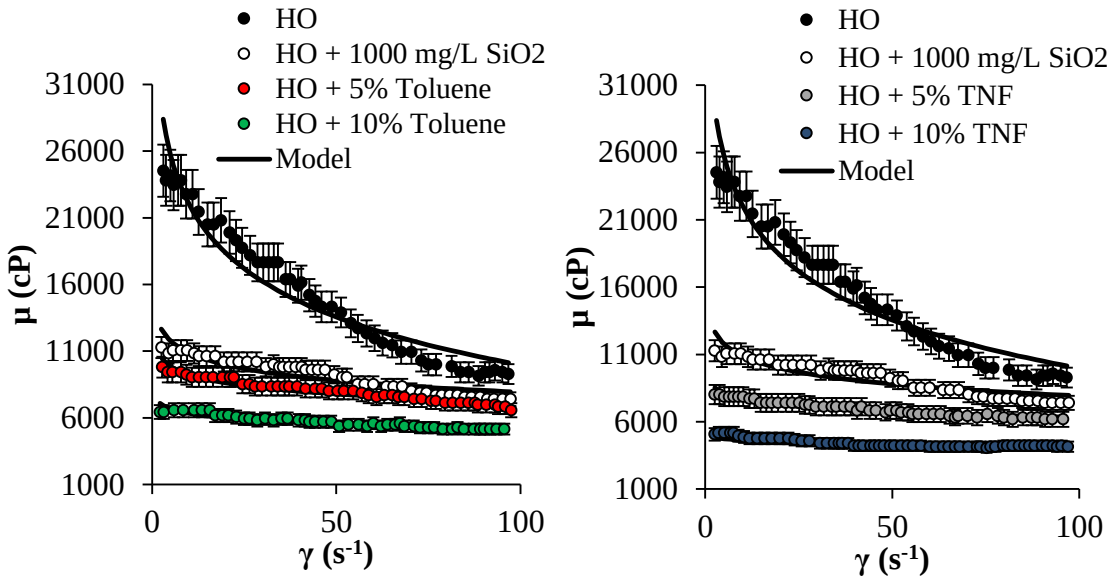

Figure 4.3 Heavy oil viscosity as a function of shear rate in the presence or absence of SiO_2 nanoparticles, toluene, and TNF at different concentrations at 311 K**.**

- **Reduction of heavy oil viscosity with biodiesel-based nanofluids.**

The solvent used for the preparation of the nanofluids in this subsection was biodiesel. Biodiesel is by definition a biofuel or liquid biofuel produced from vegetable oils and animal fats,[58] with soy being the rapeseed, and sunflower, the most commonly used raw materials worldwide for this purpose. The difference among nanofluids lies in the presence of surfactants of different chemical natures. Figure 4.4 shows the rheograms for HO, the suspension of SiO_2 nanoparticles in the crude matrix at 1000 mg/L concentration, the mixture between heavy crude and the diluent used in 5 and 10% nanofluid in volume, and BNF.

Like TNF, as the diluent fraction increases, the viscosity decreases considerably. The shapes of all curves are Newtonian, so the viscosity does not depend on the shear rate, except for heavy crude, and similarly to TNF, the best performance is obtained at a concentration of 10%. The BNF presents the best performance of all the evaluated mixtures. Biodiesel is characterized by having a more polar behavior than toluene because it contains more oxygen in its chemical structure. According to Mortazavi-Manesh and Shaw,[44] aromatic and polar diluents reduce viscosity more effectively, than non-polar alkanes.

Table 4.1 shows the parameters of the Herschell-Bulkley rheological model for heavy oil samples with nanoparticles, biodiesel, and BNF. The flow behavior index n_H becomes closer to one as the amount of biodiesel and BNF is increased, since the behavior tends to be more Newtonian.

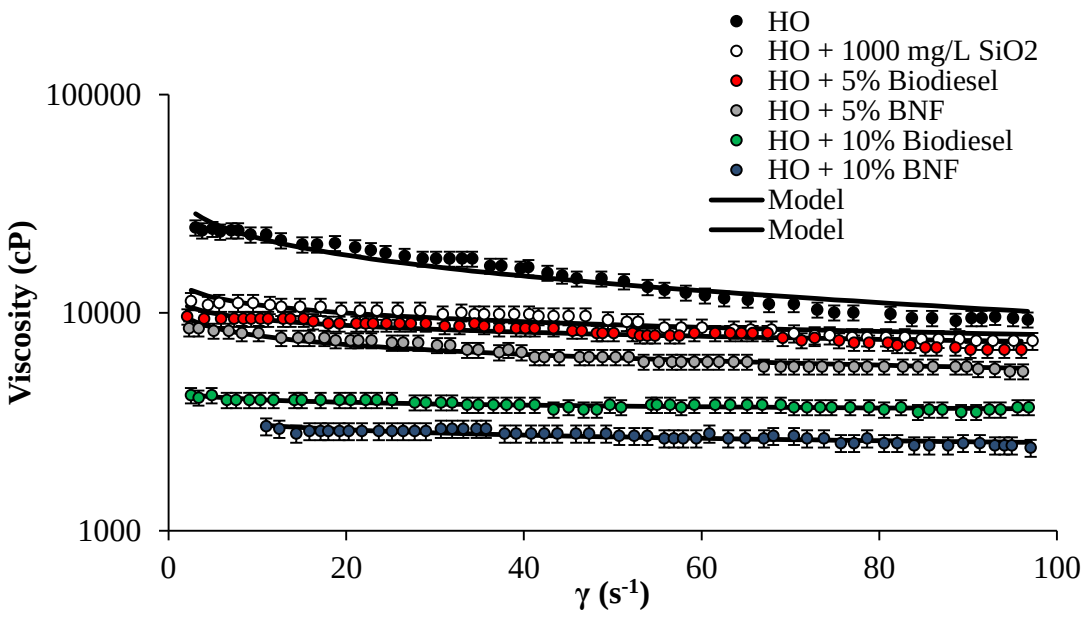

Figure 4.4 Heavy oil viscosity as a function of shear rate in the presence or absence of SiO_2 nanoparticles, biodiesel and BNF at different concentrations at 311 K.

Figure 5.5 depicts the performance of BNF, BTWNF, and BCNF compared to one another. The three nanofluids evaluated have high performance in terms of heavy crude oil viscosity reduction. However, the nanofluid without surfactant produces the greatest reduction in viscosity, which is probably caused by the relatively high concentration of surfactant used in the preparation of the nanofluid. We speculate that surfactant micelles inhibit the dispersion of the nanoparticles inside the liquid medium, and consequently, the performance of the nanofluid with a surfactant concentration is lower in comparison. The other nanofluids that contain surfactants in their formulation are less effective at viscosity reduction, which is why the internal movement of the fluid is difficult, and therefore the viscosity reduction tends to be lower in comparison to the nanofluid without a surfactant.

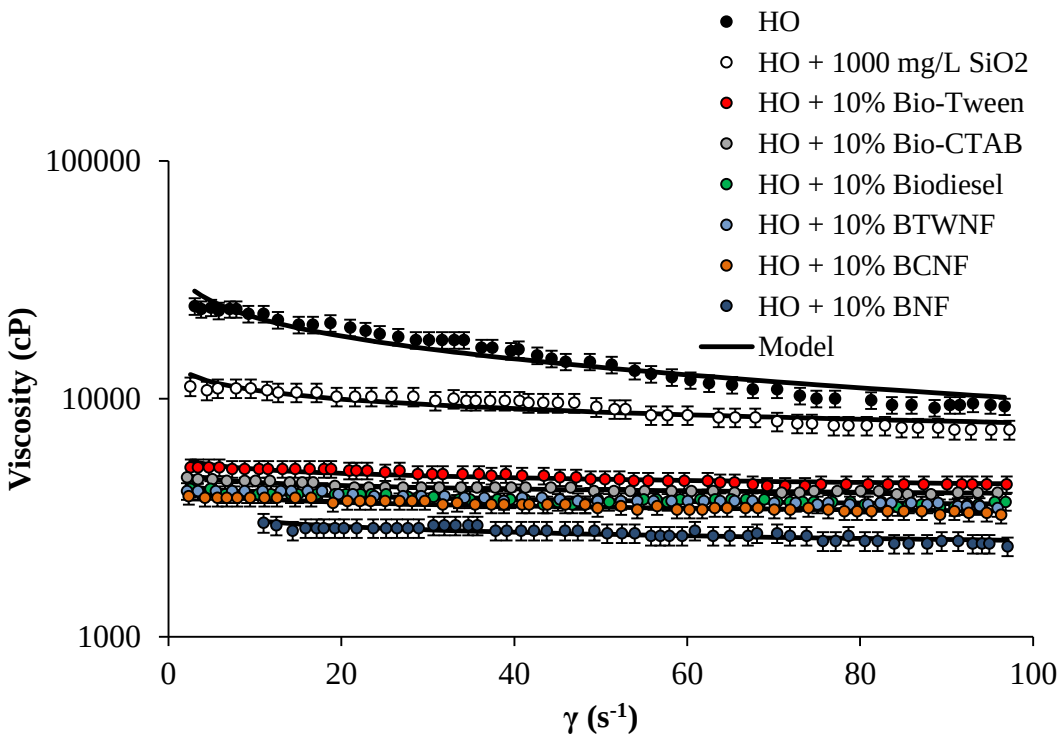

Figure 4.5 Heavy oil viscosity as a function of shear rate of in the presence of BNF, BTWNF, BCNF at 10% and 313K**.**

4.3.3 Steady-state measurements of heavy oil with nanofluids and naphtha.

The objective of formulating a nanofluid capable of reducing heavy crude oil viscosity and applying it to transport processes is to find mixtures leading to savings in naphtha consumption. According to previous assessments, BNF (biodiesel + nanoparticles) as the best performing viscosity reducing agent for heavy crude oil. In this vein, mixtures of heavy crude oil and extra-heavy oil were prepared with BNF and naphtha, to meet the aforementioned standards of transportation and mobility of crude oil.

By the same token, the mixture of solid nanoparticles with naphtha was evaluated with the objective of evaluating the performance of SiO_2 nanoparticles on the rheology of heavy crude. Figures 4.6 and 4.7 show the mixtures of crude, SiO_2 and naphtha nanoparticles.

- **Mixtures of crude oil, SiO_2 nanoparticles, and naphtha.**

The curves presented in Figure 4.6 illustrate the Newtonian behavior as naphtha is added to heavy and extra heavy crude mixed with 1000 mg/L of SiO_2 nanoparticles. As expected, the viscosity reduction improves as the amount of naphtha in the blend increases. The lowest viscosity point is obtained for the heavy oil matrix when 18% of naphtha is added, which meets the viscosity required for transport. If we compare the latter result with Figure 4.2, we find that naphtha consumption required for the viscosity requirements diminishes from 27 to 18%, i.e., a reduction of 33.3%.

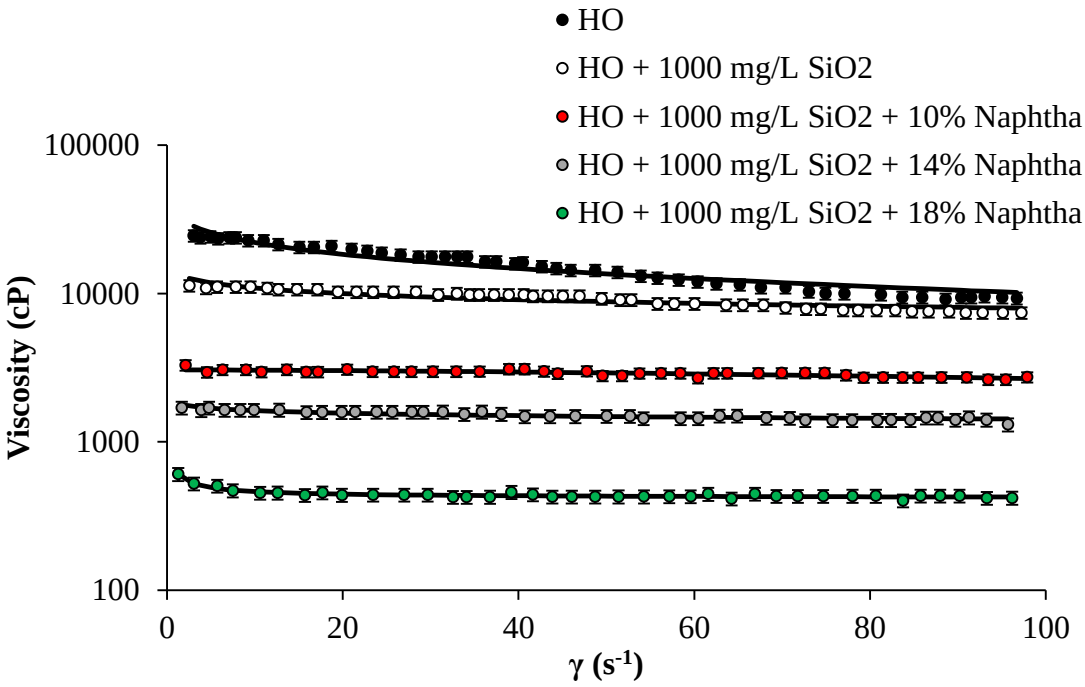

Figure 4.6 Viscosity as a function of shear rate of mixes of a) Heavy oil + 1000 ppm of SiO_2 nanoparticles and naphtha, evaluated at 311 K.

- **Mixtures of crude oil, BNF, and naphtha.**

According to the previous rheological evaluation, the nanofluid composed of biodiesel and SiO_2 nanoparticles was selected as the best performing fluid. For this reason, the evaluation of mixtures of heavy crude oil, BNF and naphtha are presented in Figure 4.7 to determine the amount of diluent necessary to bring the mixture to the standard conditions of mobility (400- 500 cP to 311K).

The use of 10 %v/v of the BNF allows viscosity reduction, thus generating savings in the consumption of naphtha to dilute the crude and to fulfill the standard viscosity of transport. To

determine the required amount of naphtha to bring the viscosity of the HO + 10% BNF mixture to optimum transport conditions, the mass base method proposed by Refutas[59] was used, which is described below.

A method proposed by Refutas[59] were used to calculate an estimated amount of naphtha to bring the viscosity of the blend to about 450 cP. The method consist in the calculation of the Viscosity Blending Number (VBN) of each component, and the used to calculate the VBN of the liquid mixture, with the next equation:

$$VBN_i = 14.534x\ln(\ln(v_i + 0.8)) + 10.975 \tag{4.3}$$

The VBN of the liquid mixture is then calculated as:

$$VBN_{mixture} = \sum_{i=0}^{N} x_i VBN_i \tag{4.4}$$

After that, we need to determinate the kinematic viscosity of the mixture, using the equation below.

$$v_{mixture} = \exp\left[\exp\left(\frac{VBN_{mixture} - 10.975}{14.534}\right)\right] - 0.8 \tag{4.5}$$

By factoring out the X value in equation (4.4), an estimated amount of naphtha of 13 %v/v is obtained. For this reason, a mixture of HO + 10% of BNF and 13 %v/v of naphtha was prepared, and its viscosity was measured at steady state at 311K and shear rate 0-100 s^{-1}. The results, presented in Figure 4.7, demonstrate the effectiveness of the nanofluid composed of biodiesel and nanoparticles of SiO_2 as a viscosity reducing agent for heavy crude oil. The curves reflect Newtonian behavior typical of this class of mixtures (heavy crude oil and diluent). The performance of the evaluated nanofluid can be measured in terms of savings in the consumption of naphtha that brings the mixture to standard conditions of mobility on the surface. In heavy crude oil, the reduction of naphtha consumption is 52%, since using 10% of BNF, it is necessary only to add 13 %v/v of Naphtha to reach the point of lower viscosity.

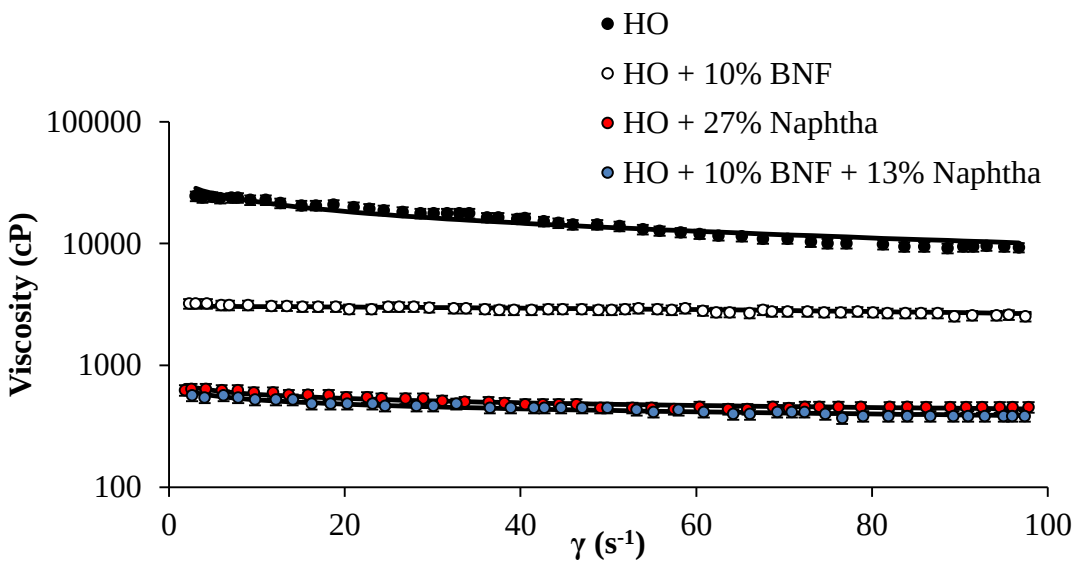

Figure 4.7 Viscosity as a function of shear rate of mixes of heavy oil + 10% of BNF and naphtha, at 311 K.

Table 4.1 shows the parameters of the Herschell-Bulkley rheological model for heavy oil samples with nanoparticles and naphtha. Also, present are the flow viscosity index for each mixture evaluated. The flow behavior index n_H becomes closer to one as the amount of naphtha is increases, since the behavior tends to be more Newtonian.

Because nanoparticles perform effectively through the interaction with the asphaltenes present in the crude oil, it is reasonable to assume that application of this technology to extra-heavy crude should perform equally or better. Therefore, we repeated some similar evaluations, but an extra-heavy crude was used instead.

4.3.4 Effect of crude oil type.

In this section, biodiesel-based nanofluid (BNF) results for another type of crude are analyzed. The intent is to determine if the proposed viscosity-reducing technology performs well with other oils. In this case, an extra-heavy crude oil was selected to examine the efficiency of this nanofluid. Like the tests performed on heavy crude oil, a rheological characterization was first carried out in the presence of naphtha, to serve as a baseline on the fraction of naphtha required to attain the necessary viscosity standard for transport processes. To further comparative results and thereby derive the incremental benefit of BNF for extra-heavy oil, the performance of the solid nanoparticles and the

BNF in the presence of naphtha were evaluated. Finally, the dynamic test of pipe flow was carried out as before.

- **Steady-state measurements of extra heavy oil with naphtha.**

Figure 4.8 shows steady-state rheological measurements for EHO containing naphtha at concentrations of 0, 20, 30, 40, 50, 58 and 63%, in the shear rate range 0 - 100 s^{-1} and at 311 K. Similarly to the HO case, the shape of the EHO rheograms exhibits a non-Newtonian behavior corresponding to a shear thinning fluid. In contrast with the HO characteristics, the EHO viscosity is higher by approximately one order of magnitude and is mainly controlled by the high content of asphaltenes.[56, 60] The rheology of EHO with different dosages of naphtha also shows a non-Newtonian behavior, and for a fixed value of the shear rate of 50 s^{-1}, the relative viscosity reduction is higher. A 63 %v/v of naphtha is necessary to reach the desired viscosity value.

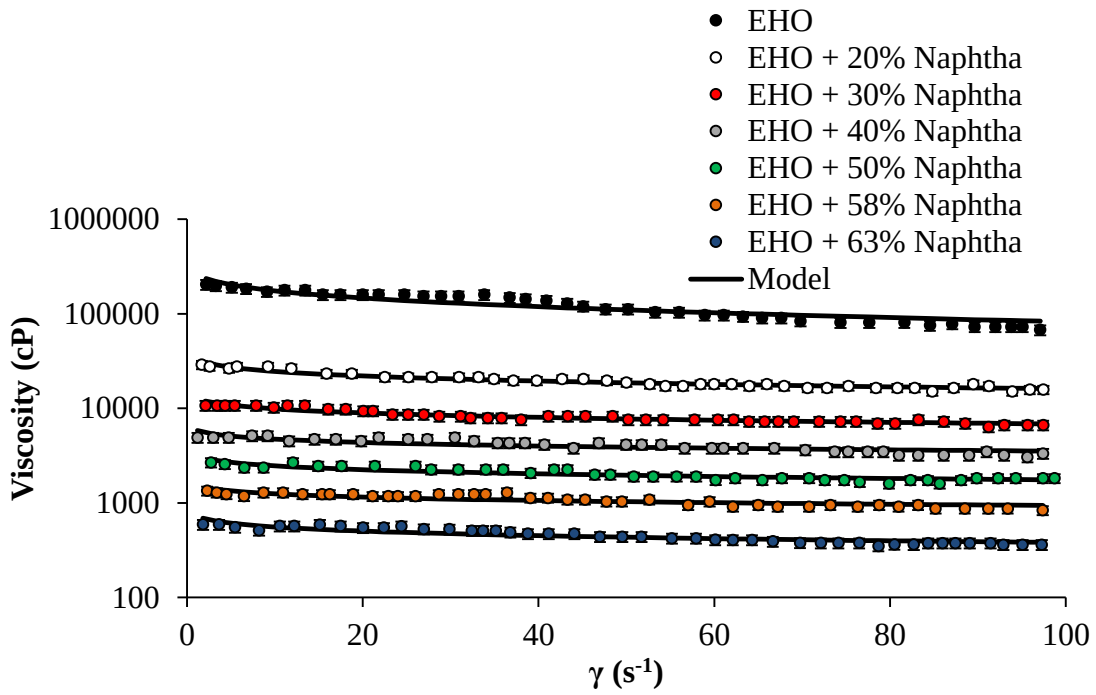

Figure 4.8 Extra-Heavy Oil viscosity as a function of shear rate in the presence or absence of naphtha at different concentrations of 0, 20, 30, 40, 50, 58 and 63% at 311 K.

Table 4.2 shows the parameters of the Herschell-Bulkley rheological model for the extra heavy oil samples, in cases where nanoparticles, BNF, and naphtha were added. Also presented are the flow viscosity index for each mixture evaluated. According to the model parameters, there is a tendency

to decrease the viscosity extrapolated at an infinite shear rate and the consistency index K_H by increasing the diluent content in the sample, as expected. The flow behavior index n_H approaches one as some diluents are increased, leading to a more Newtonian behavior. The mixture is having a flow viscosity index greater than one corresponds to that containing 63% of naphtha. Consequently, this is used as our reference or baseline result to examine possible savings in consumption of naphtha after introducing the BNF. The mixture having a flow viscosity index greater than one contains 1000 mg/L of SiO_2 nanoparticles plus 43 %v/v of naphtha. This latter result shows that mixing solid nanoparticles reduces the naphtha consumption, in contrast to other cases. These preliminary results for BNF are encouraging and given that optimization is possible, the expected benefits could certainly greater, in turn potentially generating greater savings in the consumption of diluent. The results are similar to the obtained in above section for the heavy crude oil and its mixtures with nanoparticles/nanofluids.

Table 4.2 Herschell-Bulkley model parameters and flow viscosity index for mixtures between EHO and naphtha.

Treatment	**Dosage**	**H-B model parameters**					F_i
		K_H **(Pa·S^n)**	n_H	$\mu_{\infty,\gamma}$ **(cP)**	R^2	***RSME* %**	
None	-	4499608	0.950	620000	0.92	9.1	0.01
Naphtha	20%	380135	0.964	13500	0.92	9.1	0.03
	30%	139510	0.989	6328	0.93	8.2	0.07
	40%	128574	0.991	2995	0.91	7.8	0.14
	50%	34405	0.993	1412	0.90	9.2	0.25
	58%	28713	0.995	635	0.90	9.6	0.54
	63%	11663	0.997	345	0.91	9.7	1.25
SiO_2	1000 mg/L	167304	0.971	235000	0.93	8.0	0.02
SiO_2 + Naphtha	1000 mg/L + 20%	109689	0.989	9300	0.91	9.2	0.04
	1000 mg/L + 30%	34263	0.989	3430	0.90	9.8	0.12
	1000 mg/L + 43%	6391	0.993	525	0.91	9.4	0.97
BNF	10%	1893	0987	445	0.99	2.1	0.94
BNF + Naphtha	10% + 26%	1663	0.997	345	0.91	9.3	1.25

- **Steady-state measurements of extra-heavy oil with nanofluids and naphtha.**

Figure 4.9 shows the viscosity of the extra-heavy crude blend with 1000 mg/L of SiO_2 nanoparticles and naphtha. Similar to the heavy crude blend, viscosity reduction occurs as the amount of diluent is increased. For this case, the lowest viscosity point is obtained when 43% of naphtha is added. Compared to the case in the absence of nanoparticles, a reduction in naphtha consumption of 32% is obtained (from 63 to 43%).

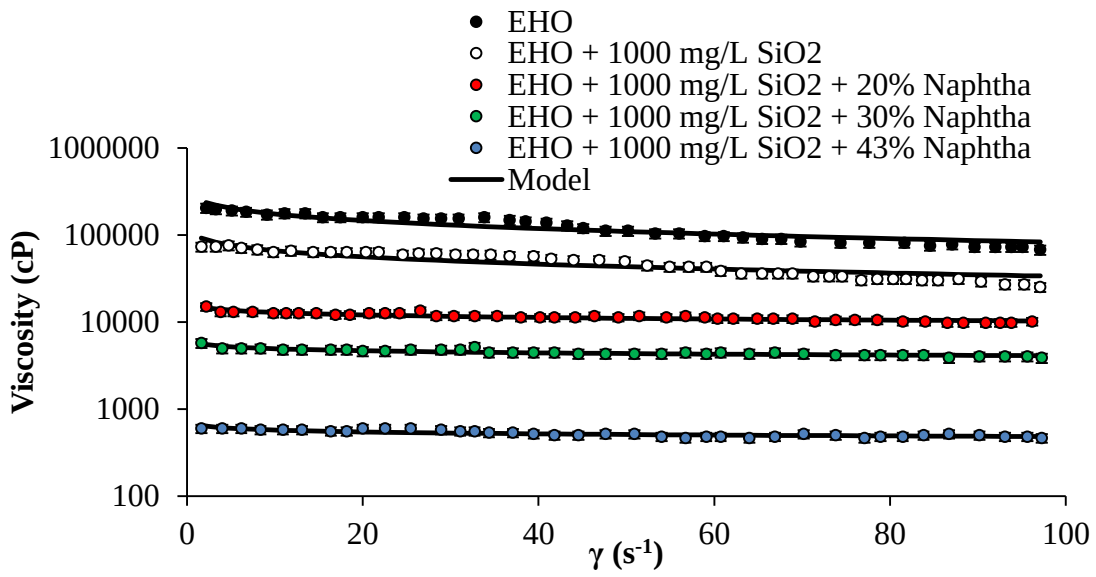

Figure 4.9 Extra - heavy oil viscosity as a function of shear rate of in the presence or absence of SiO_2 nanoparticles, and naphtha at different concentrations at 311 K.

Once again, the Refutas[59] method to estimate the viscosity of the mixture was used to try to find an estimated amount of naphtha that when blended with extra heavy oil plus 10% BNF, could reduce the viscosity to attain a flow viscosity index equal or greater than 1. According to this method, it is possible to calculate an estimated amount of naphtha. The estimated amount of naphtha of 26% is and rheological measurements at 311K corroborate the validity of the estimate. Results are shown in Figure 10. Similarly, in the extra-heavy crude blend, the nanofluid performs well, resulting in a decrease in viscosity of the crude oil to the standard, using 10% of BNF with 26 %v/v of naphtha. Thus, by comparing the mixture without nanofluid, a reduction in the consumption of naphtha of 58% is obtained.

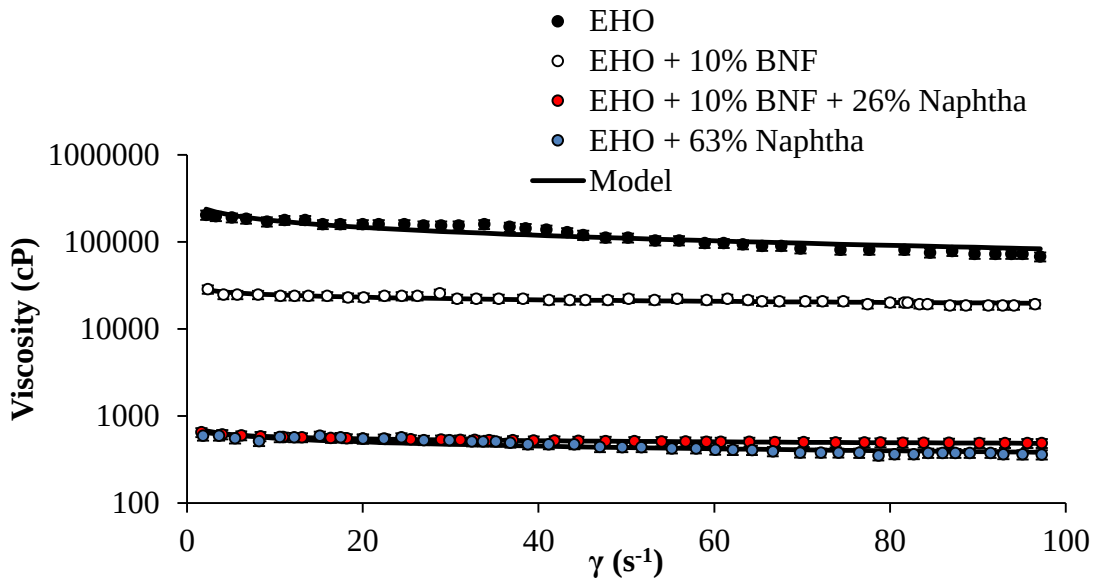

Figure 4.10 Extra - heavy oil viscosity as a function of shear rate of in the presence or absence of SiO_2 nanoparticles, BNF, and naphtha at different concentrations at 311 K.

Table 4 shows the parameters of the Herschell-Bulkley rheological model for extra heavy oil samples, BNF, and naphtha. Also, presented is the flow viscosity index for each mixture evaluated. Similar to the results obtained from the heavy crude oil, the combination of nanofluid produced with biodiesel and 1000 mg/L of SiO_2 nanoparticles with 26% of naphtha in an extra heavy crude matrix generates viscosity reductions reaching values close to 1 in the flow viscosity index, which guarantees a good performance of the technology to improve the transport conditions of heavy crude. In this way, it was then decided to evaluate the nanofluid in dynamic tests of flow through pipes.

4.3.5 Dynamic flow test.

To evaluate the BNF, two mixtures were prepared for each crude oil: For the HO matrix, the mixtures prepared were: 1) HO with 27% naphtha and 2) HO with 10% of BNF and 13% naphtha. For the EHO matrix, the mixtures prepared were: 1) EHO with 63% naphtha and 2) EHO with 10% of BNF and 27% naphtha, the tests were performed by flowing the mixture at a constant flow rate of 5 ml/min, at two temperatures, 298 and 313 K. The fluid volume was approximately 1000 ml. This volume quantity guarantees a fully developed flow where the pressure differential is stabilized. This pressure differential is constantly measured throughout the test.

Figure 4.11 shows the pressure differential for the flow of the two mixtures prepared with HO. Curve a) presents the value of the pressure differential and, the ratio between the flow rate and pressure differential at 298 K for HO matrix. Curve b) shows the same that curve a), but at 313 K. Figure 4.11 shows the results of the dynamic flow test through the pipeline for the two mixtures composed of naphtha, heavy crude oil, and BNF. At the beginning of the test the pressure differential varies up to 50 ml of injected fluid, this is completely normal because the system has not yet been filled, so it is necessary to do the analysis after a 50 ml volume injected in this part of the test, and the flow is fully developed and the pressure differential reaches a constant value during the rest of the test. Both fluids have a similar pressure differential of about 17 psi.

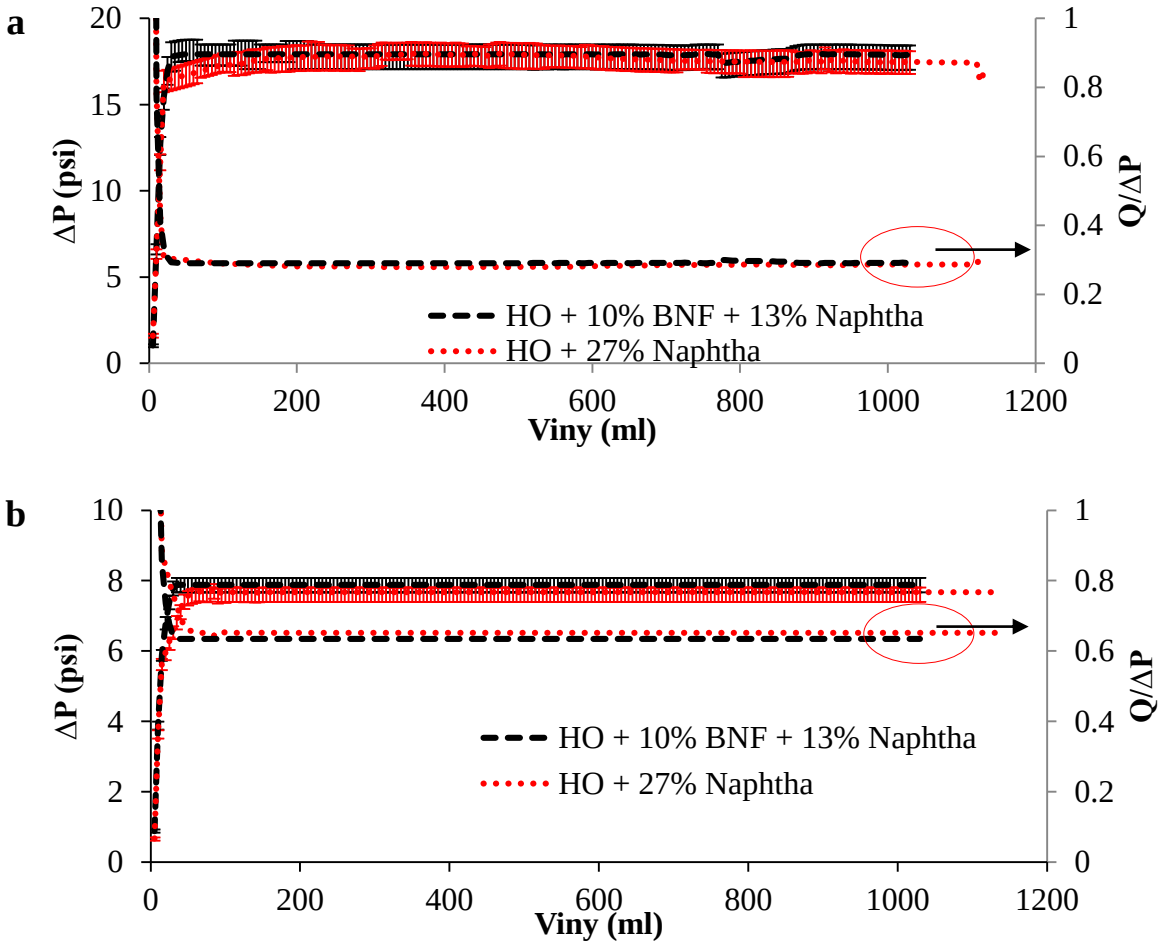

Figure 4.11 Dynamic flow test: Pressure differential against injected volumes of mixtures with HO, and the ratio between flow rate and pressure differential, evaluated at a) 298 K, and b) 313 K.

At 313K, the pressure differential is very similar for both fluids, at approximately 8 psi. As expected, the pressure differential at higher temperature decreases considerably due to the change in viscosity of the fluid, hence, it offers less resistance to flow. The results are again conclusive and confirm that nanotechnology can be used as an alternative technique to improve surface transport conditions of heavy and extra-heavy crude oil. Reduced consumption of solvent and energy consumption to transport the heavy/extra heavy crude through the pipeline. Similar to the tests developed for heavy crude oil, the two mixtures flow viscosity index was equal to or greater than 1 were prepared, which is why they meet the necessary requirements for pipeline transport.

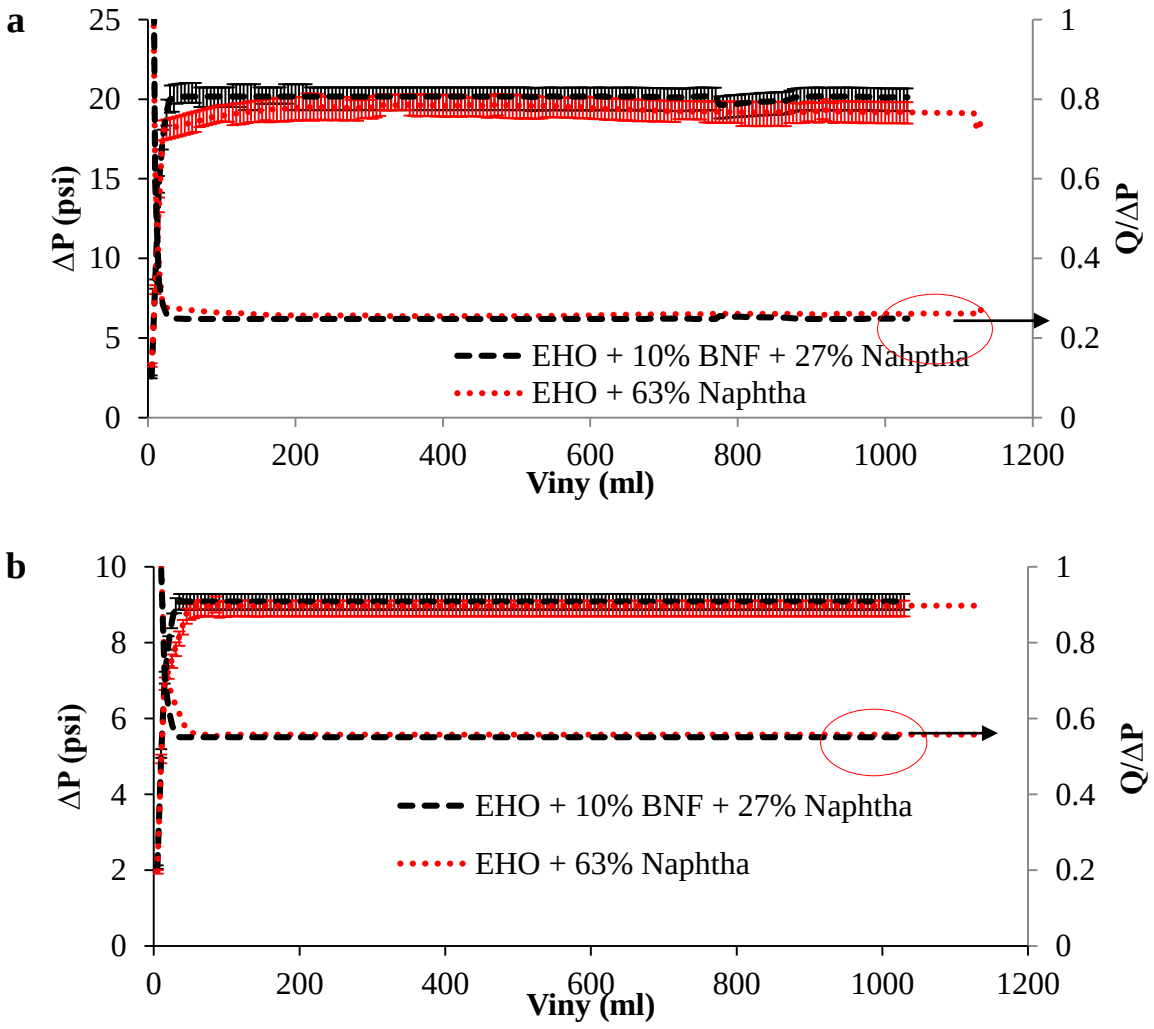

Figure 4.12 Dynamic flow test: Pressure differential against injected volumes of mixtures with EHO, and the ratio between flow rate and pressure differential, evaluated at a) 298 K, and b) 313 K.

The mixtures were EHO + 63% naphtha and EHO + 10% BNF + 27% naphtha. Figure 4.12 shows the pressure differential for each mixture evaluated at 298 and 313 K respectively. The pressure differential is very similar for both fluids, which at 298K is close to 18 psi, and close to 9 psi at 313K. As expected, the pressure differential at higher temperature decreases considerably due to the change in viscosity of the fluid. Thus it offers less resistance to flow. The results are again conclusive and confirm that nanotechnology can be used as an alternative technique to improve surface transport conditions of heavy and extra-heavy crude.

4.3.6 Preliminary economic and environmental impact analyses.

- **Environmental advantages.**

A scenario where the consumption of naphtha is reduced and replaced by biodiesel should in principle be more environmentally friendly. It is worth recalling that biodiesel offers advantages, such as conservation of the planet's natural non-renewable resources,[58, 61] ideal for low emissions in marine areas, national parks, and forests and especially in large cities, comes from a renewable resource and is biodegradable, free of sulfur,[58, 62] benzene and potentially carcinogenic flavorings, has products derived from the residue of its process as glycerin and organic fertilizers, reduces soil pollution and toxicity risks. In the case of accidental spillage, the advantages associated with being a biodegradable and non-toxic product enhance its profile as a substitute for petroleum-derived diluent.[58] On the technical side, the use of the nanoparticles in the proposed mixture does not generate an additional difficulty because nanoparticles do not have to be removed in a post-transport process, as the proposed amount is very small, and therefore it meets the minimum requirements of dispersed solids. In refining processes, it has been shown that the nanoparticles have high catalytic activity, which would favor a subsequent cracking process.[63, 64] The biodiesel has an excellent lubricity and greater flash point, which results in greater safety. All these characteristics make it a product much friendlier than naphtha. In addition, Colombia stands out as one of the countries with the greatest potential to produce biodiesel in Latin America,[65, 66] with a production that exceeds 500,000 tons per year in the last 5 years, placing the country as one of the production leaders in South America located third after Argentina and Brazil.[66] Another impact on the economy since biofuels implementation was the reduction of gasoline imports from 16 thousand barrels per day to just one

thousand bpd.[66] In this way, the use of biodiesel meets all expectations to position itself in the market of the Oil & Gas industry.

The proposed technology suggests the use of lower naphtha content, which would yield risks from the point of view of risks. In addition, the possibility of segregation/separation of fluids or precipitation of heavy molecules would be eliminated by the presence of lower amounts of naphtha in the mixture[67] consequently mitigating the risk of having a multiphase system that hinders the conditions of transport at critical points . A decrease in the naphtha content reduces the system's vapor pressure, reducing the risk of explosion by reducing the fraction of volatile components. In the case of explosion due to external causes (heating pipe, turbulence, terrorist attacks, among others) the pollution produced would be much smaller compared to the mixture with higher naphtha content. In the following calculation, an estimate of the vapor pressure and boiling booms of the considered mixtures is presented. For the calculation of the saturation pressure of the two mixtures the commercial software, CMG WINPRO Version 2016.10.6024 (Copyright © Computer Modelling Group Ltd 2016) was used, based on the Peng Robinson equation of state (PR_EOS).[68] The input data to the software was the composition of the fluids, which was obtained by a simulated distillation test based on the ASTM D7169. The mixture composed of EHO and Naphtha (63 %v/v) has a saturation pressure of 401 psi computed by CMG WINPRO Version 2016.10.6024 (Copyright © Computer Modelling Group Ltd 2016). Meanwhile, for the mixture composed of nanofluid (10 %v/v) and naphtha (27 %v/v), the saturation pressure turned out to be roughly 389 psi. The decrease in the saturation pressure of the mixture consequently increases its boiling temperature. This indicates that, as expected, moving in the direction of lowering the naphtha fraction through the addition of nanoparticles will produce environmental and operational risk-reducing benefits.

- **Dilution costs.**

In this section, we present a preliminary, simplistic financial analysis, some of which include the use of nanoparticles, mostly for comparison. The simplified economic analysis was conducted on a yearly basis using average economic indicators in Colombia in 2016. Light naphtha of good quality was preferentially used; its average price is 80 USD$/bbl.[69, 70] The price for silica nanoparticles was calculated by the price of Petroraza SAS (Medellín, Colombia), corresponding to 70 USD$/kg. The analysis was performed considering the use of nanofluid composed of biodiesel and SiO_2 nanoparticles, and the use of nanoparticles of silica mixed directly with naphtha. Both mixtures allow the reduction in the consumption of naphtha in extra-heavy crude oil. The cost of dilution of the extra-heavy oil used corresponds to the cost related to the consumption of naphtha, in this case, 63

%v/v. When using nanoparticles mixed with naphtha, that amount is reduced to 43%. If 10% of the BNF is used, the amount of naphtha is reduced to 27 %v/v. To carry out the exercise, the production field of the extra-heavy oil used for the development of the experiments was taken as reference a crude oil production of 10,000 bpd. The costs associated with the process are presented in Table 4.3.

Table 4.3 Economic impact of dilution with the use of nanotechnology in heavy and extra-heavy oil

Oil Rate = 10000 bpd						
Sample	**Naphtha (% v/v)**	**Naphtha Price (USD$)**	**Np's Price (USD$)**	**Biodiesel Price (USD$)**	**Total Price (USD$)**	**Balance**
HO	27	296.000	-	-	296.000	
HO + SiO_2 Np's	18	175.600	111.300	-	286.900	3%
HO + 10% BNF	13	135.000	111.300	152.380	398.680	-35%
EHO	63	1,360.000	-	-	1,360.000	-
EHO + SiO_2 Np's	43	600.000	111.300	-	711.300	48%
EHO + 10% BNF	27	343.000	111.300	152.380	606.680	55%

According to these results, if heavy crude oil is used, savings are only available when SiO_2 nanoparticles are used, roughly 3% of economic savings. Economic break-even point when nanofluid is used is that where the difference in naphtha consumption represents a higher value than the use of nanoparticles and biodiesel, in mixtures of heavy crude consuming more than 30% of naphtha, can be surpassed that point of equilibrium. In the case of extra-heavy crude oil, considerable energy savings are obtained with more than 50% is presented for each mixture evaluated. If we consider the consumption volumes of naphtha per year in Colombia, 70,000 bpd, this represents savings of more than 2.5 USD$ million per day. As a result, the potential high impacts of the proposed technology to improve the transport conditions of heavy crude, the performance meeting technical, economic and environmental benefits are clearly illustrated.

- **Energy savings in pumping fluids.**

If we consider the crude oil production of a field at 10,000 bpd, the final mixture containing 63% of naphtha produces a total volume of a mixture of 27,000 bpd of the mixture. The mixture containing nanoparticles contains 43 %v/v of naphtha, so for that reason, the volume of the mixture will be 17,500 bpd of the mixture. The mixture containing 10% of BNF contains 27% of naphtha, therefore

the volume of the mixture would be 15,800 bpd. In this way, it is possible to transport a higher net amount of crude per unit time using nanoparticles / nanofluids, or if the same amount of crude per unit of time is transported, the efficiency of the pump would be higher, and the energy consumption much lower. Equation (4.6) allows calculating the work performed by the pump, if it is calculated per unit time considering that the pressure differential is similar for the two fluids, the variation is presented in the flow rate.

$$\frac{W}{\dot{m}} = \int_1^2 v.dp \tag{4.6}$$

If we consider that the pressure changes are modest, the compressibility of the fluid can be neglected, and thereby the pumping power can be calculated as:

$$P = Q(\Delta P) \tag{4.7}$$

To perform the economic evaluation exercise, the production of the same field of heavy crude oil used as an example to perform calculations of diluent dilution was considered. This corresponds to a daily production of 10,000 bpd of extra heavy oil. The average price of electric power in Colombia in 2016 was 330 $/kWh,[71] which by the way is the fourth most expensive in Latin America. For comparison purposes, Colombia has higher costs with respect to the United States (78% more expensive), Peru (59%), Mexico (30%) and Ecuador (25%) [71], so if we use a fluid that reduces energy needs in terms of pumping power, it will also generate interesting economic savings.

Table 4.4 presents the economic saving generated by the decrease in the electric energy required to pump the crude oil.

Table 4.4 Economic analysis of the cost of pumping by pipelines using nanofluids

Oil rate = 10,000 bpd								
Sample	**Naphtha (% v/v)**	**Total Mixture Flow Rate (bpd)**	**Total Mixture Flow rate (m^3/s)**	**ΔP (psi)***	**ΔP (N/m^2)**	**Power (Kw)****	**Energy Cost (USD$/d)**	**Balance**
HO	27	13.700	0.026	12	82.736	2.531	6.681	-
HO + 10% BNF	13	12.900	0.023	12.1	83.426	2.257	5.960	11%
EHO	63	27.000	0.05	14	96.500	5.676	14.986	-
EHO + 10% BNF	27	15.800	0.03	14.6	100.600	3.551	9.374	37%

* Value taken from Figure 2.12, averaging the values at two temperatures

From this analysis, it can be determined that an additional saving potential at the simple cost of naphtha, the reduction in energy consumption per mixture pumping is 11% for heavy oil, and 37% for extra-heavy oil. This value represents a reduction in costs of more than 5,500 USD$/d, which per-year basis generates savings of over USD$ 2 million. In addition, we believe that the start of the pumps can be benefited when using a mixture containing nanofluids. In previous work,[38] we show that the presence of nanoparticles in the heavy crude generates an alteration of the internal structure of the oil and produces a considerable decrease in the yield stress, which impacts directly pumping and on the starting point.

Likewise, the transport capacity of the pipeline decreases by 40%, which means that if we use nanofluids to optimize transportation, we can increase production management at the surface by 40%, without the need to build new transportation systems, as the same infrastructure would support an increase in production and transportation volumes. This would not happen if nanofluid were not used, because of the high volumes of naphtha. In this way, it is possible to generate a reduction in capital expenditure (CAPEX) in the pipeline requirements, because, as mentioned earlier, higher volume of oil can be transported with the same infrastructure as more net oil mass can be pumped. Another aspect in favor of this technology is the ease in the storage of the diluent (Naphtha), because the consumption is reduced considerably, and consequently, it is necessary an infrastructure for the storage of smaller cost and smaller size.

4.4 Partial conclusions

- The effect of fumed silica nanofluids synthesized on the rheological properties of heavy and extra heavy crude was evaluated through rheological tests at steady-state conditions and in dynamic flow tests through a small-scale pipeline, mixing crude oil, nanofluid, and naphtha.
- Four nanofluids were synthesized with different solvents, namely Toluene, Biodiesel, and Biodiesel with surfactants, one ionic and another non-ionic. The criterion for determining the effectiveness of nanofluid was the reduction in the consumption of naphtha required to bring heavy and extra-heavy crude oils to the standards defined for surface mobility, 400-500 cP at 311K.
- Mixtures of heavy crude and extra-heavy crude oils were made with naphtha until the point of the viscosity of mobility was determined. To reach the minimum viscosity point, it was

necessary to add 27% of Naphtha to the blend with heavy crude and 63% of the blend with extra-heavy crude. The addition of 10% of nanofluid prepared with biodiesel and 1000 mg/L of SiO_2 nanoparticles is the one with the best performance in reducing the viscosity of the heavy/extra-heavy crude oils, resulting in savings in consumption of naphtha close to 50%, reaching the viscosity needed to move the crude.

- Using dynamic tests of flow in a pipeline, the pressure differential during the flow of 1000 ml of the mixture was measured. It was found that the blend of extra-heavy crude with 10% nanofluid and 27% naphtha needs the same pressure differential as the blend composed of extra-heavy crude and 63% of naphtha, and for the blend of heavy crude with 10% nanofluid and 13% naphtha needs the same pressure differential as the blend composed of heavy crude and 27% of naphtha
- By means of a simplified economic analysis based on a conventional mass balance, savings of roughly 50% can be obtained in comparison with the habitual consumptions, equivalent to more than USD $2.5 million per day. Also, there is a potential for energy savings in the pumping of heavy and extra-heavy crude oils, the required power and capacity of use of the pipeline is lower when using nanofluids, which generates savings close to 37%, generating savings of more than USD $2 million per year, and the possibility of increasing the volumes of production using the same infrastructure.
- Additionally, a discussion is presented from the environmental point of view, and the advantages of reducing naphtha consumption showed potential environmental benefits through risk mitigation. In this way, the performance of nanofluid is verified as an optimizing agent for the transport conditions of heavy and extra-heavy crude oils, and it opens a promising technique to generate savings in the energy and fuel consumptions of the oil and gas industry.

4.5 References

1. Al-Maamari, R. S.; Buckley, J. S., Asphaltene precipitation and alteration of wetting: the potential for wettability changes during oil production. *SPE Reservoir Evaluation & Engineering* **2003,** 6, (04), 210-214.
2. Gharfeh, S.; Yen, A.; Asomaning, S.; Blumer, D., Asphaltene flocculation onset determinations for heavy crude oil and its implications. *Petroleum science and technology* **2004,** 22, (7-8), 1055-1072.
3. Oskui, G.; Reza, P.; Jumaa, M. A.; Folad, E. G.; Rashed, A.; Patil, S. In *Systematic Approach for Prevention and Remediation of Asphaltene Problems During CO2/Hydrocarbon Injection*

Project, The Twenty-first International Offshore and Polar Engineering Conference, 2011; International Society of Offshore and Polar Engineers: 2011.
4. Kojima, T.; Tahara, K., Refinement and transportation of petroleum with hydrogen from renewable energy. *Energy conversion and management* **2001,** 42, (15), 1839-1851.
5. Alvarez, G.; Poteau, S.; Argillier, J.-F.; Langevin, D.; Salager, J.-L., Heavy oil− water interfacial properties and emulsion stability: Influence of dilution. *Energy & Fuels* **2008,** 23, (1), 294-299.
6. Hasan, S. W.; Ghannam, M. T.; Esmail, N., Heavy crude oil viscosity reduction and rheology for pipeline transportation. *Fuel* **2010,** 89, (5), 1095-1100.
7. Mortazavi-Manesh, S.; Shaw, J. M., Thixotropic rheological behavior of Maya crude oil. *Energy & Fuels* **2014,** 28, (2), 972-979.
8. López, E.; Montes, E.; Garavito, A.; Collazos, M. M., La economía petrolera en Colombia (Parte II). Relaciones intersectoriales e importancia en la economía nacional. *Borradores de economía* **2013,** 748.
9. Gutierrez, J. G., Plan de Inversiones ECOPETROL. In 8 de Marzo de 2011 ed.; www.infraestructura.org.co, 2011; p 34.
10. Ecopetrol, S., Reporte Integrado de Gestión Sostenible 2015. *Sourced from: www. ecopetrol. com. co/documentos/Ecopetrol_IA_2015_29marzo. pdf. Accessed on September 20th* **2016**.
11. Leyva, S.; Herrera, B.; Cadena, Á., Actualización de escenarios de oferta y demanda de hidrocarburos en Colombia. *Revista de Ingeniería* **2014**, (40), 69-80.
12. Franco, C.; Flórez, A.; Ochoa, M., Análisis de la cadena de suministros de biocombustibles en Colombia. *Revista de Dinámica de Sistemas* **2008,** 4, (2), 109-133.
13. UPME, M., Cadena del petróleo 2013. *Bogotá, Colombia* **2013**.
14. Hart, A., A review of technologies for transporting heavy crude oil and bitumen via pipelines. *Journal of Petroleum Exploration and Production Technology* **2014,** 4, (3), 327-336.
15. Al-Roomi, Y.; George, R.; Elgibaly, A.; Elkamel, A., Use of a novel surfactant for improving the transportability/transportation of heavy/viscous crude oils. *Journal of Petroleum Science and Engineering* **2004,** 42, (2), 235-243.
16. Bensakhria, A.; Peysson, Y.; Antonini, G., Experimental study of the pipeline lubrication for heavy oil transport. *Oil & Gas Science and Technology* **2004,** 59, (5), 523-533.
17. Chang, C.; Nguyen, Q. D.; Rønningsen, H. P., Isothermal start-up of pipeline transporting waxy crude oil. *Journal of non-newtonian fluid mechanics* **1999,** 87, (2), 127-154.
18. Gateau, P.; Hénaut, I.; Barré, L.; Argillier, J., Heavy oil dilution. *Oil & gas science and technology* **2004,** 59, (5), 503-509.
19. Isaac, J. D.; Speed, J. B. Method of piping fluids. 1904.
20. Joseph, D. D.; Bai, R.; Mata, C.; Sury, K.; Grant, C., Self-lubricated transport of bitumen froth. *Journal of fluid mechanics* **1999,** 386, 127-148.
21. Kessick, M. A.; Denis, C. E. S., Pipeline transportation of heavy crude oil. In Google Patents: 1982.
22. Khan, M. R., Rheological properties of heavy oils and heavy oil emulsions. *Energy Sources* **1996,** 18, (4), 385-391.
23. McKibben, M. J.; Gillies, R. G.; Shook, C. A., A laboratory investigation of horizontal well heavy oil—water flows. *The Canadian Journal of Chemical Engineering* **2000,** 78, (4), 743-751.
24. Saniere, A.; Hénaut, I.; Argillier, J., Pipeline transportation of heavy oils, a strategic, economic and technological challenge. *Oil & Gas Science and Technology* **2004,** 59, (5), 455-466.
25. Selim, M. Y., Reducing the viscosity of Jojoba Methyl Ester diesel fuel and effects on diesel engine performance and roughness. *Energy Conversion and Management* **2009,** 50, (7), 1781-1788.
26. Castro, L. V.; Flores, E. A.; Vazquez, F., Terpolymers as Flow Improvers for Mexican Crude Oils†. *Energy & Fuels* **2011,** 25, (2), 539-544.
27. Urquhart, R., Heavy oil transportation-present and future. *Journal of Canadian Petroleum Technology* **1986,** 25, (02).

28. Ashrafizadeh, S.; Kamran, M., Emulsification of heavy crude oil in water for pipeline transportation. *Journal of Petroleum Science and Engineering* **2010,** 71, (3), 205-211.
29. Lin, C.-Y.; Chen, L.-W., Emulsification characteristics of three-and two-phase emulsions prepared by the ultrasonic emulsification method. *Fuel Processing Technology* **2006,** 87, (4), 309-317.
30. Hashemi, R.; Nassar, N. N.; Pereira Almao, P., Enhanced heavy oil recovery by in situ prepared ultradispersed multimetallic nanoparticles: A study of hot fluid flooding for Athabasca bitumen recovery. *Energy & Fuels* **2013,** 27, (4), 2194-2201.
31. Langevin, D.; Argillier, J.-F., Interfacial behavior of asphaltenes. *Advances in colloid and interface science* **2015**.
32. Martínez-Palou, R.; de Lourdes Mosqueira, M.; Zapata-Rendón, B.; Mar-Juárez, E.; Bernal-Huicochea, C.; de la Cruz Clavel-López, J.; Aburto, J., Transportation of heavy and extra-heavy crude oil by pipeline: A review. *Journal of Petroleum Science and Engineering* **2011,** 75, (3), 274-282.
33. Salager, J.-L.; Briceño, M. I.; Bracho, C. L., Heavy hydrocarbon emulsions. Making use of the state of the art in formulation engineering. *Encyclopedic Handbook of Emulsion Technology* **2001,** 20, 455-495.
34. Probert, S.; Chu, C., Laminar flows of heavy-fuel oils through internally insulated pipelines. *Applied energy* **1983,** 15, (2), 81-98.
35. Probert, S.; Chu, C., Optimal pipeline geometries and oil temperatures for least rates of energy expenditure during crude-oil transmission. *Applied Energy* **1983,** 14, (1), 1-31.
36. Wylde, J.; Leinweber, D.; Low, D.; Botthof, G.; Oliveira, A.; Royle, C.; Kayser, C. In *Heavy oil transportation: advances in water-continuous emulsion methods*, Proceedings of the world heavy oil congress, Aberdeen, 2012; 2012.
37. Taborda, E. A.; Franco, C. A.; Lopera, S. H.; Alvarado, V.; Cortés, F. B., Effect of nanoparticles/nanofluids on the rheology of heavy crude oil and its mobility on porous media at reservoir conditions. *Fuel* **2016,** 184, 222-232.
38. Taborda, E. A.; Alvarado, V.; Franco, C. A.; Cortés, F. B., Rheological demonstration of alteration in the heavy crude oil fluid structure upon addition of nanoparticles. *Fuel* **2017,** 189, 322-333.
39. Aladag, B.; Halelfadl, S.; Doner, N.; Maré, T.; Duret, S.; Estellé, P., Experimental investigations of the viscosity of nanofluids at low temperatures. *Applied energy* **2012,** 97, 876-880.
40. Islam, M. R.; Shabani, B.; Rosengarten, G., Nanofluids to improve the performance of PEM fuel cell cooling systems: A theoretical approach. *Applied Energy* **2016,** 178, 660-671.
41. Farzaneh, H.; Behzadmehr, A.; Yaghoubi, M.; Samimi, A.; Sarvari, S., Stability of nanofluids: Molecular dynamic approach and experimental study. *Energy Conversion and Management* **2016,** 111, 1-14.
42. Kibria, M.; Anisur, M.; Mahfuz, M.; Saidur, R.; Metselaar, I., A review on thermophysical properties of nanoparticle dispersed phase change materials. *Energy Conversion and Management* **2015,** 95, 69-89.
43. Ilyas, S. U.; Pendyala, R.; Narahari, M.; Susin, L., Stability, rheology and thermal analysis of functionalized alumina-thermal oil-based nanofluids for advanced cooling systems. *Energy Conversion and Management* **2017,** 142, 215-229.
44. Mortazavi-Manesh, S.; Shaw, J. M., Effect of diluents on the rheological properties of Maya crude oil. *Energy & Fuels* **2016,** 30, (2), 766-772.
45. Mozaffari, S.; Tchoukov, P.; Atias, J.; Czarnecki, J.; Nazemifard, N., Effect of Asphaltene Aggregation on Rheological Properties of Diluted Athabasca Bitumen. *Energy & Fuels* **2015,** 29, (9), 5595-5599.
46. Nik, W. W.; Ani, F.; Masjuki, H.; Giap, S. E., Rheology of bio-edible oils according to several rheological models and its potential as hydraulic fluid. *Industrial Crops and Products* **2005,** 22, (3), 249-255.

47. Sarpkaya, T., Flow of non-Newtonian fluids in a magnetic field. *AIChE Journal* **1961,** 7, (2), 324-328.
48. Shao, S.; Lo, E. Y., Incompressible SPH method for simulating Newtonian and non-Newtonian flows with a free surface. *Advances in water resources* **2003,** 26, (7), 787-800.
49. Montoya, T.; Coral, D.; Franco, C. A.; Nassar, N. N.; Cortés, F. B., A Novel Solid–Liquid Equilibrium Model for Describing the Adsorption of Associating Asphaltene Molecules onto Solid Surfaces Based on the "Chemical Theory". *Energy & Fuels* **2014,** 28, (8), 4963-4975.
50. Franco, C. A.; Lozano, M. M.; Acevedo, S.; Nassar, N. N.; Cortés, F. B., Effects of Resin I on Asphaltene Adsorption onto Nanoparticles: A Novel Method for Obtaining Asphaltenes/Resin Isotherms. *Energy & Fuels* **2015,** 30, (1), 264-272.
51. Taborda, E. A.; Franco, C. A.; Ruiz, M. A.; Alvarado, V.; Cortés, F. B., Experimental and Theoretical Study of Viscosity Reduction in Heavy Crude Oils by Addition of Nanoparticles. *Energy & Fuels* **2017**.
52. Bazyleva, A. B.; Hasan, M. A.; Fulem, M.; Becerra, M.; Shaw, J. M., Bitumen and heavy oil rheological properties: Reconciliation with viscosity measurements. *Journal of Chemical & Engineering Data* **2009,** 55, (3), 1389-1397.
53. Tao, R.; Xu, X., Reducing the viscosity of crude oil by pulsed electric or magnetic field. *Energy & fuels* **2006,** 20, (5), 2046-2051.
54. Yen, T. F.; Chilingarian, G. V., *Asphaltenes and asphalts, 2*. Elsevier: 2000; Vol. 40.
55. Mullins, O. C.; Sheu, E. Y.; Hammami, A.; Marshall, A. G., *Asphaltenes, heavy oils, and petroleomics*. Springer Science & Business Media: 2007.
56. Luo, P.; Gu, Y., Effects of asphaltene content on the heavy oil viscosity at different temperatures. *Fuel* **2007,** 86, (7), 1069-1078.
57. Franco, C. A.; Nassar, N. N.; Ruiz, M. A.; Pereira-Almao, P.; Cortés, F. B., Nanoparticles for inhibition of asphaltenes damage: adsorption study and displacement test on porous media. *Energy & Fuels* **2013,** 27, (6), 2899-2907.
58. Retana, I.; BONILLA, J., Transferencia tecnológica sobre las ventajas y desventajas de la utilización del biodiesel. *Trabajo final, Instituto Nacional de Aprendizaje: Núcleo Mecánica de Vehiculos, San José* **2008**.
59. Maples, R. E., *Petroleum refinery process economics*. Pennwell Books: 2000.
60. Ghanavati, M.; Shojaei, M.-J.; SA, A. R., Effects of asphaltene content and temperature on viscosity of Iranian heavy crude oil: experimental and modeling study. *Energy & Fuels* **2013,** 27, (12), 7217-7232.
61. Balat, M., Potential alternatives to edible oils for biodiesel production–A review of current work. *Energy Conversion and Management* **2011,** 52, (2), 1479-1492.
62. Lešnik, L.; Biluš, I., The effect of rapeseed oil biodiesel fuel on combustion, performance, and the emission formation process within a heavy-duty DI diesel engine. *Energy Conversion and Management* **2016,** 109, 140-152.
63. Franco, C.; Cardona, L.; Lopera, S.; Mejía, J.; Cortés, F. In *Heavy Oil Upgrading and Enhanced Recovery in a Continuous Steam Injection Process Assisted by Nanoparticulated Catalysts*, SPE Improved Oil Recovery Conference, 2016; Society of Petroleum Engineers: 2016.
64. Franco, C. A.; Montoya, T.; Nassar, N. N.; Pereira-Almao, P.; Cortés, F. B., Adsorption and subsequent oxidation of colombian asphaltenes onto Nickel and/or Palladium oxide supported on fumed silica nanoparticles. *Energy & Fuels* **2013,** 27, (12), 7336-7347.
65. Alzate, C. A. C., Perspectivas de la producción de biocombustibles en Colombia: contextos latinoamericano y mundial. *Revista de ingeniería* **2009**, (29), 109-120.
66. García, E. *Colombia sube producción y mezcla obligatoria de biocombustibles*; Recuperado 15/03/2015 http://www. reporteenergia. com[Links]: 2013.
67. Madge, D.; Garner, W., Theory of asphaltene precipitation in a hydrocarbon cyclone. *Minerals engineering* **2007,** 20, (4), 387-394.

68. Peng, D.-Y.; Robinson, D. B., A new two-constant equation of state. *Ind. Eng. Chem. Fundam* **1976,** 15, (1), 59-64.
69. Delgado, J. E.; Salgado, J. J.; Perez, R., Prospects of biofuels in Colombia. *Revista Ingenierías Universidad de Medellín* **2015,** 14, (27), 13-28.
70. Orrego Pemberty, M.; Castaño Duque, J. M. Aplicación del modelo Casi Ideal de Demanda al mercado de combustibles en el sector transporte en Colombia. Universidad EAFIT, 2015.
71. Vélez, L., El precio de la electricidad en Colombia y comparación con referentes internacionales 2012-2015. *Recuperado de http://www. andeg. org/sites/default/files/El% 20precio% 20de% 20la% 20electricidad% 20en% 20colombia* **2015**, 202012-2015.

5. Effect of the Nanotechnology on the Heavy Oil Mobility on Porous Media at Reservoir Conditions.

Asphaltenes are refractory molecules with high molecular weight that can impact the different stages of the production system and refining streams.[1] Asphaltenes contain heteroatoms such as O, N and S and metals such as Ni, Fe and V. The presence of heteroatoms and their location in the structure make asphaltenes the most polar molecules present in crude oil, leading to their self-association and further formation of large asphaltic flocs. These flocs also cause an increase in the HO viscosity, which in some cases leads to formation damage[1-4] and precipitation/adsorption problems in production facilities.[2, 5, 6] At high concentration of asphaltene, namely > 40000 mg/L, the increase in viscosity is mostly due to the formation of a viscoelastic network of nanoaggregates.[7, 8] In addition, sulfur can form strong C-S and C=S bonds, which can also contribute to an increase in the crude oil viscosity.[4, 9]

To improve production, transport and refining of HO and EHO, several techniques under reservoir and surface conditions have been used, namely: i) emulsification of oil-in-water (O/W) emulsions[10-12] that can drastically reduce the fluid viscosity and hence improve the crude oil mobility; ii) use of annular flow as a method for reducing the drag forces;[13-16] iii) deasphalting oil using CO2,[17-19] n-alkanes of low[20-22] and high molecular weight;[23, 24] iv) application of thermal processes based on heat injection through steam and other gases[25-29] to reduce oil viscosity; and 5) in-situ upgrading such as the various modes of air injection, e.g. in-situ combustion (ISC,[30, 31]) thermal cracking[4, 32-34] and its catalytic variations.[35-37]

One of the most frequently used techniques for reducing HO and EHO viscosities has been the dilution with solvents and light hydrocarbons such as naphtha,[38-40] toluene,[41] xylene,[39] gasoline,[42] diesel,[43, 44] light oil,[41] or mixtures thereof[45] as well as some chemical compounds based on R=O (butanone type, among others).[45] Several authors have reported on the dilution of HO and EHO[45-48] with different solvents and the changes to the rheological behavior of mixed fluids.[46, 49, 50] Recently, Mortazavi-Manesh and Shaw[51] studied the effect of toluene, n-heptane and a mixture 50/50 vol% of

toluene and butanone on the rheological properties of Maya crude oil as a function of temperature. Their results showed that the mixture of toluene + butanone caused the largest viscosity reduction. Naphtha has been so far the most used diluent.[47, 52, 53] In some instances, mainly in Venezuela and Colombia, the quantity of naphtha used in the upgrading of these crude oil types can reach 20-40 vol%.[48] Adding naphtha can effectively reduce the viscosity and increase the API gravity of HO and EHO.[46, 49, 51] The excessive use of naphtha for diluting crude oil implies an increase in the operational costs,[41] becoming an impractical technology.[41] Dilution with naphtha is an unfriendly technology for humans due to its lower boiling point, 100% volatiles content, and low explosive limits.[41]

Nanoparticles have been used by the oil industry for formation damage inhibition,[54-57] HO and EHO upgrading,[58] enhanced (EOR) and improve oil recovery (IOR) processes,[56, 59] and wastewater remediation.[60] Due to their particle sizes, between 1 and 100 nm, large available surface area, high dispersibility and tunable physicochemical characteristics, nanoparticles are prone to selectively adsorb asphaltenes and inhibit their self-association. [61] In a previous study,[56, 59, 62] our research group focused on using silica, γ-alumina and magnetite nanoparticles to inhibit the aggregation of asphaltenes under varying temperature, solvent ratios and asphaltene concentration.[59] Silica nanoparticles can induce a significant reduction in the asphaltene to mean aggregate size, which could prevent the formation of large viscoelastic networks and reduce the oil viscosity as a result. However, to the best of our knowledge, there are no studies reporting the rheological behavior of crude oil in the presence of nanoparticles and their impact on relative permeability curves and crude oil recovery (%) under flow conditions in porous media at typical reservoir temperature and pressure, based on "huff-n-puff" type estimulations. In this order, the aim of this chapter is to evaluate the effect of nanoparticles on the rheological properties of a Colombian HO at varying conditions of temperature, shear rate and dosage of nanoparticles. In addition to rheological responses, coreflooding tests at reservoir conditions were also performed. The results in this thesis are expected to open a wider landscape on the use of nanoparticles in IOR processes based mainly on "huff & puff" configurations.

5.1 Experimental

5.1.1 Materials

n-Heptane (99%, Sigma-Aldrich, St. Louis, MO), and Toluene (99.5%, Merck KGaA, Germany) were used as received. A Colombian heavy crude oil of 13°API and a viscosity of 1.2 x 10^5 cP at

298 K was used. The elemental analysis of asphaltenes shows a C: 81.4 wt%, H: 7.5 wt%, O: 8.8 wt%, N: 2.3 wt%. A non-ionic surfactant, Tween 80 (Sigma-Aldrich, St. Louis, MO), was used for dispersing the nanoparticles in the water-based nanofluid. The nanofluid was prepared using distilled water with a conductivity of 3 μS/cm. The nanoparticle choose to evaluation according to the results shows in the others chapters of this thesis was unmodified silica (S8).

The carrier fluid used was composed of a mixture of distilled water and 2 wt% surfactant. The procedure followed for the preparation of the nanofluid is described elsewhere,[63, 64] In brief, the nanoparticles and the carrier fluid are stirred at 500 rpm for 20 minutes at room temperature, then subject to ultrasound for 12 hours at 298 K. The nanofluid has a viscosity of 8.2 cP, a density of 0.96 g/cm3 and a pH 7.3. The properties of the prepared nanoparticles and heavy oil are summarized in Chapter 1

5.1.2 Methods

- **Evaluation of nanoparticles/nanofluids as viscosity reducers**

Rheological measurements were performed using a Bohlin rotational rheometer C-VOR 200 (Malvern Instruments, Worcestershire - UK), equipped with a Peltier plate for temperature control, with a plate-plate geometry with a diameter of 20 mm and a gap of 150 microns. To analyze the change in viscosity induced by the addition of nanoparticles. The optimal concentration was used. at room temperature at shear rate values 0 – 100 s^{-1}. Each measurement was repeated three times.

A nanofluid prepared with water + 2% v/v of nonionic surfactant and the best-performing nanoparticles in adsorption tests as well as tests of aggregates n-C7 asphaltenes fragmentation. The nanoparticle concentration in the nanofluid was variable ensuring nanoparticles concentrations in heavy oil of 0, 10, 1000, 10000 and 40000 mg/L. A fixed dosage of nanofluid of 4% v/v was added to HO and viscosity measurements were conducted at a constant shear rate of 10 s^{-1}. After this, the optimal concentration was selected to run the complete rheological study between 0 – 100 s^{-1} at a temperature of 298 K.

- **Coreflooding tests**

From the analysis of relative permeability curves and oil recovery, before and after the treatment, the effect of nanoparticles on the mobility of oil at reservoir pressure and temperature conditions can be evaluated.

We anticipate that the penetration of nanoparticles suspended in an aqueous medium will modify the flow behavior of the oil phase once they enter in direct contact with it, increasing its mobility in addition to altering the wettability of the porous medium. The selected core has a length of 25 cm, with a diameter of 3.81 cm and a porosity of 11%. The injection fluid consisted of a synthetic brine of 2 wt% of KCl. The core absolute permeability was estimated as 1.1 Darcy, through the injection of 20 pore volumes (PV) of the prepared brine until reaching steady state. The nanofluid used for performing the test is prepared according to the results of the rheological measurements according to the one that generates greater viscosity reduction. Figure 5.1 presents a schematic representation of the experimental test. During the coreflooding tests, pore and overburden pressures were maintained at 2600 and 3600 psi, respectively. The operating temperature was set at 360 K.

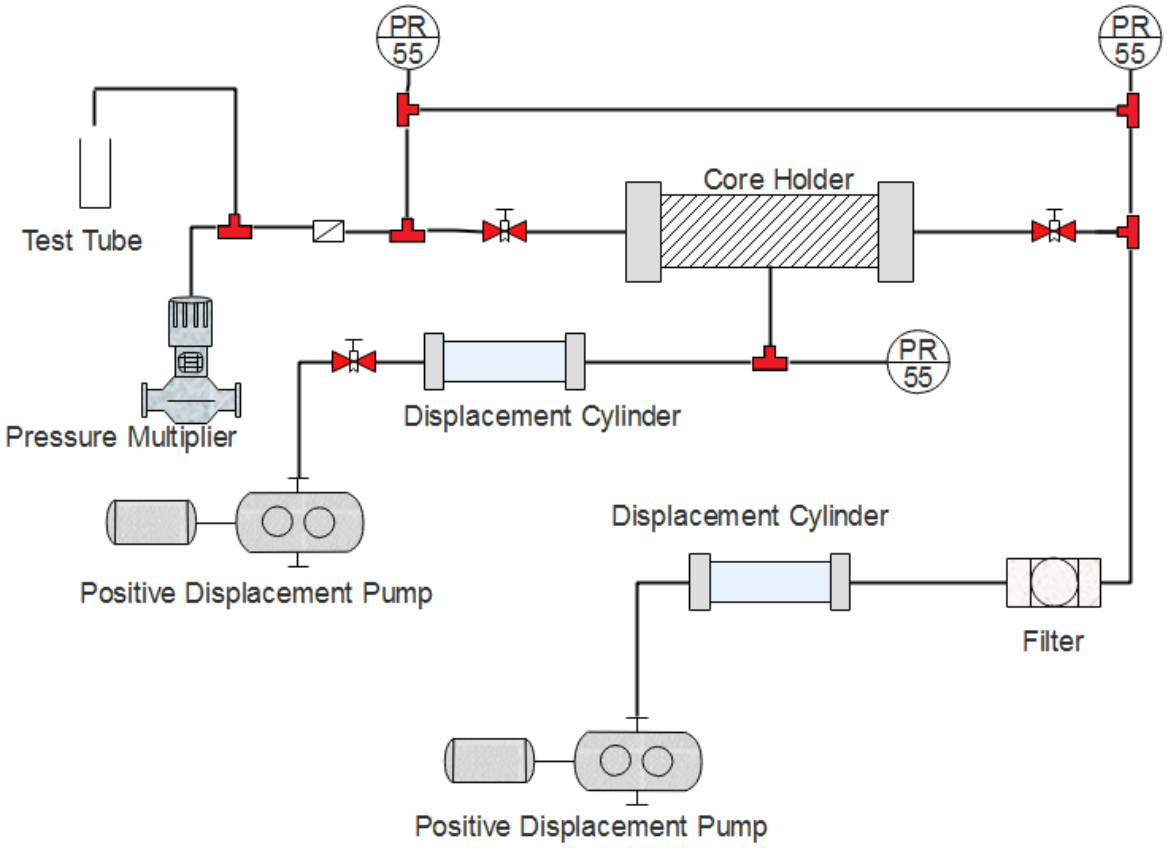

Figure 5.1 Schematic representation of the coreflooding system: 1) core holder, 2) core (Ottawa Sand packing), 3) pore pressure transducer (diaphragm), 4) pump one – positive displacement pump, 5) pump two, 6) displacement cylinder, 7) filter, 8) pressure multiplier, 9) manometer, 10) valve and 11) test tube.

The "base system test" aimed at determining the oil and water relative permeabilities in the absence of nanoparticles. Regardless of the origin and mineralogical composition of the porous media, during the producing life of a reservoir, the reservoir's wettability can vary [38]. For this reason, the "base system test" consisted of subjecting the porous media to a period of aging time needed for wettability restoration

This is achieved by continuous injection of heavy oil for 15 days. Once the system is assumed to have become more oil-wet, oil (ko) and water (kw), corresponding to the end-point effective permeabilities of the oil and water phases, respectively, are measured. This is performed first by injecting 20 PV of water at conditions of residual oil saturation (Sor) followed by 20 PV of oil at conditions of residual water saturation (Swr). Then, oil (kro) and relative water permeability (krw) and oil recovery curves are obtained. Posteriorly, the sample is saturated with oil again, in a secondary drainage process, in order to prepare the core for nanofluid injection. The "post nanoparticles injection" system is obtained by injecting 1 PV in production direction and then letting it soaking for a period of 12 h. Then values of ko, kw, krw, kro and recovery curves are constructed following the aforementioned procedure.

5.2 Modeling

5.2.1 Rheological model

Two rheological models extensively evaluated in the literature, i.e. Cross and Carreau, also known as Power Law rheological models, were used.[65-67] The temperature effect on the flow behavior index (*N* or *m*) was investigated. The flow behavior index relates to the behavior of the fluid, whether it is more or less Newtonian, which for values less than 1 is considered pseudo-plastic [65]. The asymptotic viscosity parameters ($\mu_{0,\gamma}$ and $\mu_{\infty,\gamma}$) indicate the behavior of the fluid when subjected to conditions corresponding to zero and infinite stresses. The characteristic relaxation time (α_c and λ_c) refers to the time required for the fluid to exhibit a response to a perturbation generated by agitation, which for a Newtonian fluid is 0.

In Table 5.1, each model equations with their respective variables are presented.

Table 5.1 Rheological models evaluated

Model	Parameter	Equation
Cross	μ (cP): Viscosity α_c (s): Characteristic relaxation time γ (s^{-1}): Shear Rate m: Constant $\mu_{\infty,\gamma}$ (cP): Viscosity at infinite shear rate $\mu_{0,\gamma}$ (cP): Viscosity at zero shear rate	$\mu = \mu_{\infty,\gamma} + \frac{\mu_{0,\gamma} - \mu_{\infty,\gamma}}{1+(\alpha_c\gamma)^m}$ (4)
Carreau	μ (cP): Viscosity λ_c (s): Characteristic relaxation time γ (s^{-1}): Shear Rate N: Constant $\mu_{\infty,\gamma}$ (cP): Viscosity at infinite shear rate $\mu_{0,\gamma}$ (cP): Viscosity at zero shear rate	$\mu = \mu_{\infty,\gamma} + \frac{\mu_{0,\gamma} - \mu_{\infty,\gamma}}{(1+(\lambda_c\gamma)^2)^N}$ (5)

5.3 Results

Results are divided into two sections: i) rheology measurements of crude oil in absence and presence of nanoparticles/nanofluid and ii) effect of nanofluid on heavy oil mobility under reservoir conditions. Rheology tests were performed for various nanoparticles/nanofluid dosages, temperatures, and shear rates.

5.3.1 Effect of nanofluid on oil viscosity.

It is noticed that the addition of solid nanoparticles to heavy crude oil generates a viscosity reduction, which offers the necessary conditions for optimizing oil mobility. However, for a possible industrial IOR application, nanoparticles have to be suspended in a carrying fluid in order to supply injectivity requirements. Particles in a liquid medium will have greater dispersion thus can come into contact

with as much fluid as compared to the case if solid nanoparticles are added. The performance of a nanofluid formed by the mixture water-surfactant-nanoparticles was evaluated. Five nanofluids with different contents of nanoparticles, i.e. 10, 100, 1000, 10000 and 40000 mg/L, were mixed individually with HO at percentages of 4 and 96% v/v, respectively. The viscosity of the mixtures was measured at 298 K and a fixed shear rate of 10 s^{-1}, along with the degree of viscosity reduction (DVR, Eq. 6) [49]

$$DVR\% = \frac{\left(\mu_{ref} - \mu_{nanof}\right)}{\mu_{ref}} \times 100 \quad (6)$$

where, μ_{ref} and μ_{nanof} are the reference and the after-nanofluid-inclusion viscosity values, measured at 10 s^{-1}, respectively.

Figure 5.2 shows the viscosity reduction produced by the addition of the prepared nanofluids. Again, it is seen that as the concentration of nanoparticles increases in the nanofluid, the mixture viscosity decreases. The optimum point is at a concentration of 1000 mg/L, as we seen in previous chapter, where a maximum DVR is obtained. However, with increasing concentration of nanoparticles up to 10000 and 40000 mg/L, the DVR is much lower (33%), which is possibly due to aggregation of the solid particles in the nanofluid, hence reducing interaction with asphaltenes present in crude oil.

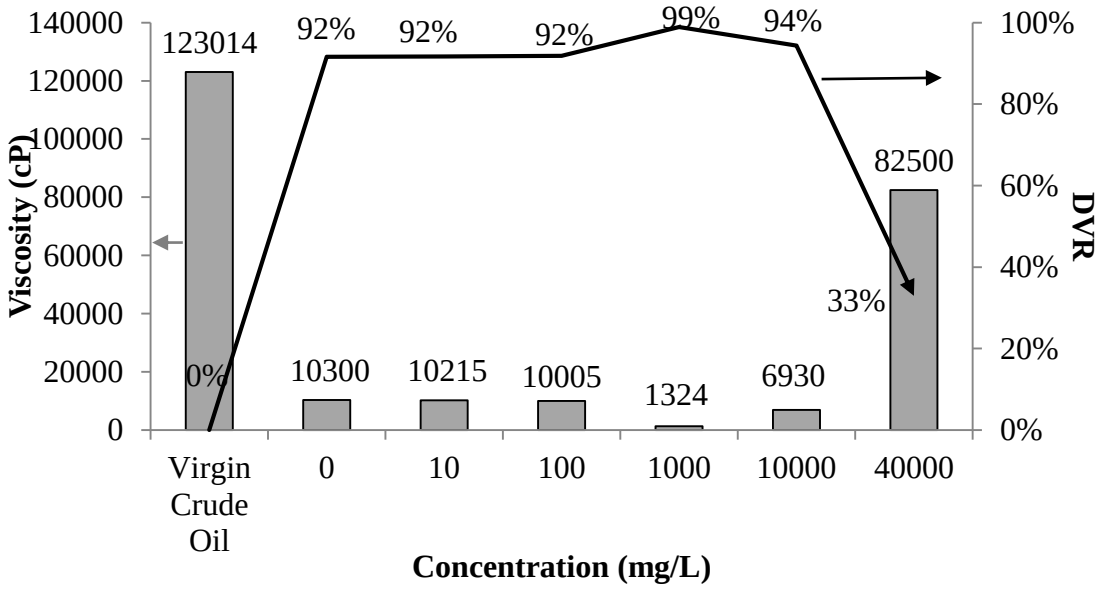

Figure 5.2 Viscosity of crude oil in absence and presence of nanofluid with different concentrations of nanoparticles at 298 K and a shear rate of 10 s^{-1}.

In order to analyze the effect of nanofluid designed to reduce the oil viscosity, rheological tests as a function of shear rate were conducted with silica nanoparticles and the carrier fluid alone to discern the individual effect of each component. A concentration of 1000 mg/L of S8 nanoparticles and 4% v/v of the prepared carrier fluid were selected. Figure 5.3 show the viscosity as a function of shear rate for the crude oil in absence and presence of the prepared carrier fluid at 4% v/v, S8 nanoparticles at 1000 mg/L the selected nanofluid. It is observed that the treated samples followed the same trend as the untreated sample but has lower values due to the addition of the nanofluid. As can be seen in Figure 5.3, there is a high impact in reducing oil viscosity by adding only the carrier fluid medium (nanofluid without nanoparticles). The maximum viscosity change occurs at low shear rate values. The effect yielded on the sample by the nanofluid can be seen even at low agitation conditions. It can be noticed that under these conditions, the slope is greater, showing high viscosity DVR. When evaluating the DVR as a sum of the effect generated by the addition of nanoparticles plus the effect generated by the addition of the carrier fluid separately, an approximate 94% reduction is obtained. However, to directly evaluate nanoparticles dispersed in fluid, a DVR of 99% is obtained. However, it is necessary to analyze these reductions in viscosity as changes in orders of magnitude, when added separately nanoparticles and carrier fluid, the viscosity reduction is about one order of magnitude, whereas when the nanofluid is added with the dispersed nanoparticles, the reduction is about two orders of magnitude, and here lies the importance of using nanofluid with nanoparticles dispersed in it. By using the nanofluid, a synergistic effect is observed that reduces the viscosity more than when the carrier fluid and nanoparticles are used separately. In effect, the addition of a liquid medium to transport the nanoparticles is favorable for reducing viscosity, which could be due to two main reasons: 1) the liquid medium serves as a partial extender of oil, and 2) the nanoparticles are scattered in the medium and when mixed with oil they can occupy more space and foster greater contact with the asphaltenes present in crude in comparison to the case when they are mixed in solid form [62].

However the viscosity change generated only by the addition of nanofluid compared with the addition of either solid nanoparticles or only the carrier fluid, is larger than the untreated crude oil or adding solid nanoparticles, concluding that the nanoparticle interaction with asphaltene has a greater impact on the viscosity reduction over the dilution phenomenon that can generate the amount of surfactant added to nanofluid.

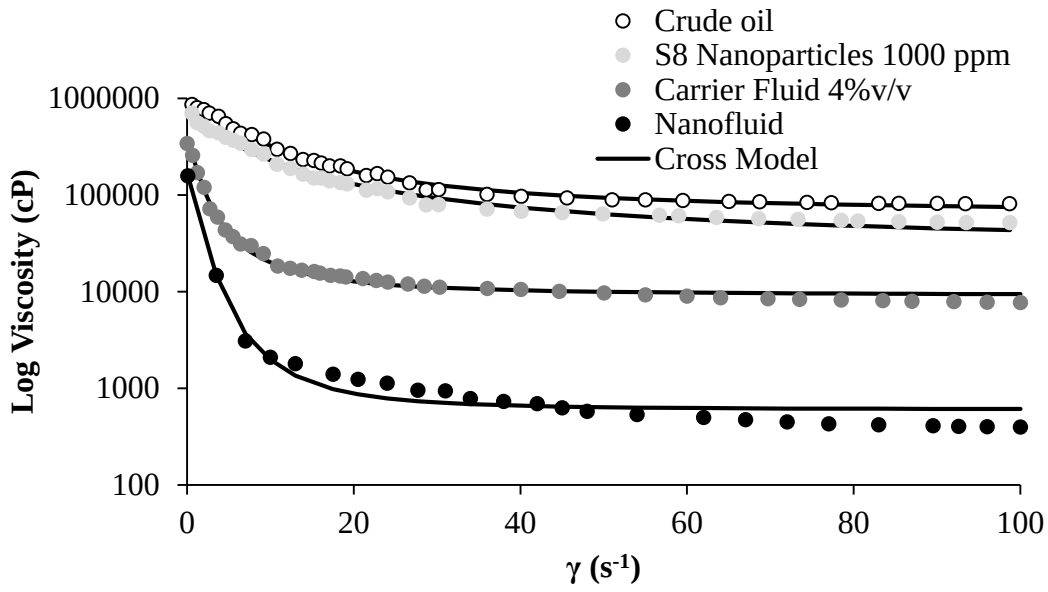

Figure 5.3 Viscosity as a function of shear rate for crude in absence and presence of the prepared carrier fluid at 4% v/v, S8 nanoparticles at 10000 mg/L the selected nanofluid.

In Table 5.2, the parameters of all models evaluated for mixtures between HO matrix and nanoparticles/nanofluids are presented. The model that best fits the experimental data of mixtures of oil with nanoparticles/nanofluid is the Cross model. The data follow a sensible trend for curves that have a viscosity reduction at all shear rates evaluated.

Parameters related to the viscosity at zero and infinity shear rates, are consistent with the experimental data following a well-defined trend as the content of nanoparticles/nanofluid in the HO matrix is increased. The constant m, related to the flow index, suggests that fluids exhibit non-Newtonian behavior, but tending to increase up to 1, and this can occur because the fluid in the presence of nanoparticles/nanofluids reaches a more Newtonian behavior at lower rate shear compared to the untreated crude oil. Several authors have modeled the rheological behavior of heavy crudes based on the content of asphaltene[4, 68, 69] and the consistency of the sample. Ghanavati et al.[4] define the constant of solvation as the ratio of the volume of the solvated asphaltene particles after dispersion to the volume of the dry asphaltene particles before dispersion, and this value is directly proportional to viscosity, i.e. if the viscosity decreases, also the constant of solvation decreases. If we consider that the viscosity of the fluid decreases in the presence of nanofluid, possibly due to a change in the structure of asphaltene, more specifically the relationship between the size before and after the addition of nanofluid. The parameter related to the relaxation time increases as the

concentration of nanoparticles/nanofluids in the medium is increased. Therefore, the system presents a greater delay in reaching equilibrium when subjected to a disturbance, which is possibly due to the change in the internal structure of the fluid associated with the presence of nanoparticles.

Table 5.2 Parameters of rheological models for crude oil on presence of S8 nanoparticles, carrier fluid and the selected nanofluid at 298 K

Model	Parameters	Condition			
		Crude oil	10000 mg/L of nanoparticles	Carrier fluid	Nanofluid with 10000 mg/L of nanoparticles
Cross	m	1.58	1.25	1.63	2.29
	$\mu_{\infty,\gamma}$x10^3 (cP)	65.45	27.5	9.18	0.6
	$\mu_{0,\gamma}$ x10^3 (cP)	874	698	342	159
	α_c (s)	0.16	0.196	0.77	0.78
	RSME	2.75	2.41	4.06	8.88
Carreau	N	0.62	0.46	0.66	0.97
	$\mu_{\infty,\gamma}$x10^3 (cP)	69.3	33	4.8	4.02
	$\mu_{0,\gamma}$ x10^3 (cP)	851	642	340	158
	λ_c (s)	0.45	0.31	1.84	1.87
	RSME	5.15	8.05	8.12	7.55

5.3.2 Coreflooding test

The nanofluid yielding the best results as a modifying agent of oil flow properties is used. According to rheological measurements, S8 nanofluid was used in corefloods. Figure 5.4 shows the relative permeability curves for each scenario evaluated. For the construction of relative permeability curves in heavy oil, a drawback occurs because the water/oil viscosity ratio is very low, making it difficult to observe the contrast of the two curves as the curve relative water permeability lies well below the oil. For the construction of relative permeability curves, the absolute permeability is used as a reference permeability to reduce uncertainties. Relative permeability curves are constructed according to the analytical model developed development by Buckley and Leverett,[70] and expanded by Johnson, Bossler, and Naumann (JBN technique).[71] The JBN technique is frequently used to derive the relative permeability experiments in transient or unsteady-state conditions. K_o values for the base and the after nanoparticles systems were 453 and 1017 mD, respectively.

It can be observed in Figure 5.4 that the K_{ro} curve for the treated system is higher than that for the base system, indicating that the treatment is effective in increasing the relative permeability of oil. The mobility of crude oil depends on two main factors, the viscosity and the relative permeability, which in turn depends on the system's wettability.[56, 72] Hence, it could be inferred from the results of the static tests, that the nanofluid inclusion reduces the oil viscosity and therefore increases the mobility of oil in the porous medium. In addition, wettability changes are apparent as residual saturations of water and oil reflect a change in the wetting state of the system after injecting the nanofluid. Table 5.3 shows the effective permeabilities at residual fluid saturations obtained in the core-flooding tests and the state of saturations for each system. Comparing the results before and after the injection of nanofluid, it is possible to determine changes from 5.6 to 12.8% in the case of S_{wr} and from 23.1 to 10.4% for S_{or} from the systems before and after nanofluid inclusion, respectively. In addition, the point where the relative permeabilities of water and oil are equal (crossover point), switches to the right from 45 to 86% for the system before and after nanofluid, respectively, which according to Craig's rules of thumb,[73] indicates a change in the wetting condition of the system as the crossover point can be found at a S_w value higher than 50%.[74] This is due to increasing S_{wr} and reduced S_{or} due to the alteration of the wettability of the medium as nanoparticles get retained by the rock and act as a coating agent at nanoscale.[62, 72, 73]

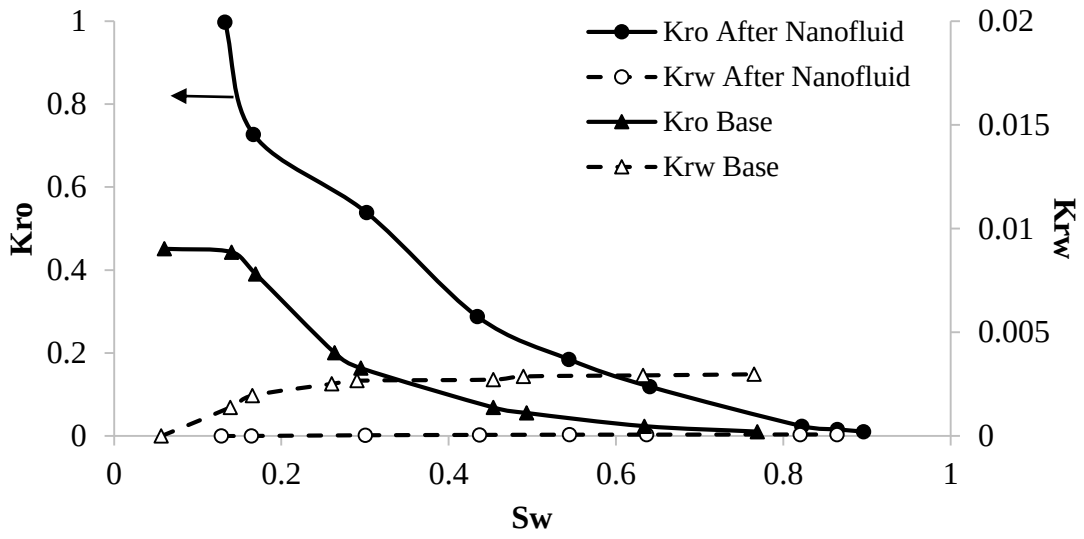

Figure 5.4 The relative permeability curves for the base, the core with crude oil-wet and the treated system after nanofluid injection in their respective formation plug. The relative permeability curves oil (K_{ro}) and the relative permeability curves water (K_{rw}).

While these results are suggestive of wettability changes and should not be taken at face value, additional wettability analysis (not shown) turned out consistent with these observations.

Table 5.3 Effective permeabilities at residual fluid saturations before and after SiO_2 (S8) nanofluid injection.

	Moment	
Property	**Before Nanofluid Injection**	**After Nanofluid Injection**
K_o at S_{wr} (mD)	453	1017
K_w at S_{or} (mD)	248	81
S_{or} (%)	23.1	10.4
S_{wr} (%)	5.6	12.8

Oil recovery curves are obtained by making a record in a time of the volume of oil recovered as the crude oil is displaced with water. These curves are constructed using the maximum volume of mobile crude oil recovered throughout the test, which in this case is that after the injection of the nanofluid. Figure 5.5 shows that for an 81% oil recovery obtained for the base system and after injection of nanofluid, 97% of recovery is obtained, i.e., the system increases its oil production capacity by 16%, reflecting the importance and impact of the proposed technology as optimizer agent mobility heavy oil. This is especially important in IOR processes with huff-n-puff configurations where a soaking time is required.

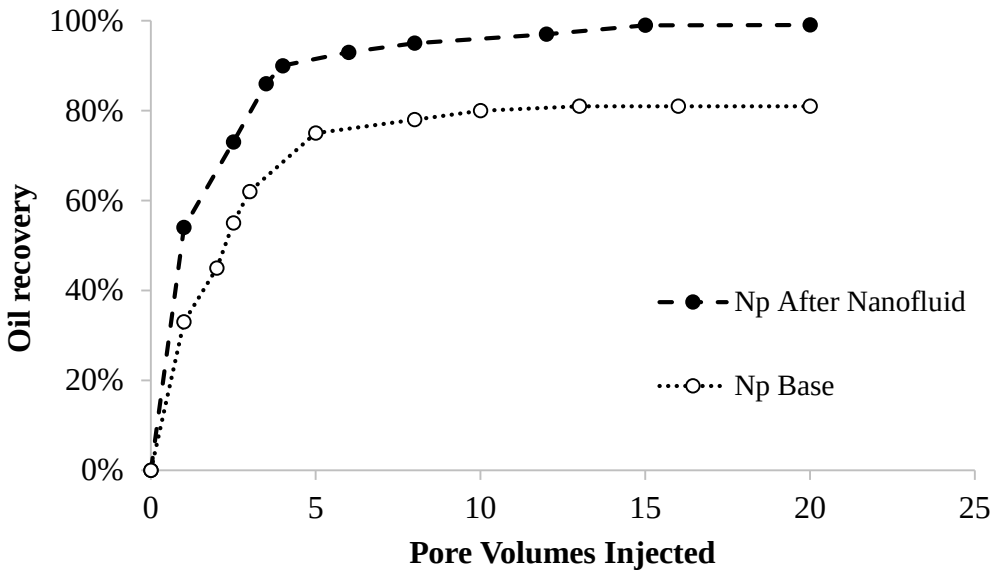

Figure 5.5 Recovery curves for the base and the after nanofluid injection system**.**

5.4 Partial conclusions

- The systematic addition of a nanofluid with active component S8 nanoparticles to a heavy crude oil generates reductions of more than 90% of viscosity in heavy oil.
- In addition, it was observed that as the concentration of nanofluid in the mixture is increased, greater degrees of viscosity reduction are obtained, which evidences that nanoparticles dispersed in a carrier fluid cause a synergistic effect when comparing the effect of individual components. An optimal amount of nanoparticles was shown to exist.
- At typical reservoir conditions of pressure and temperature, nanofluids were able to positively affect the crude oil mobility through the reduction of oil viscosity and the alteration of the porous media wettability.
- The goal of this research has been achieved by demonstrating that nanotechnology exhibits a great and rich potential as an optimizer of heavy oil transport properties. It is expected that this study will open a better landscape abouonthe use of nanofluids in IOR and EOR processes for enhancing the production of heavy and extra heavy oils.

5.5 References

1. Groenzin, H.; Mullins, O. C., Asphaltene molecular size and structure. *The Journal of Physical Chemistry A* **1999,** 103, (50), 11237-11245.
2. Adams, J. J., Asphaltene adsorption, a literature review. *Energy & Fuels* **2014,** 28, (5), 2831-2856.
3. Chavan, S.; Kini, H.; Ghosal, R., Process for Sulfur Reduction from High Viscosity Petroleum Oils. *International Journal of Environmental Science and Development* **2012,** 3, (3), 228.
4. Ghanavati, M.; Shojaei, M.-J.; SA, A. R., Effects of asphaltene content and temperature on viscosity of Iranian heavy crude oil: experimental and modeling study. *Energy & Fuels* **2013,** 27, (12), 7217-7232.
5. Mullins, O. C., The asphaltenes. *Annual Review of Analytical Chemistry* **2011,** 4, 393-418.
6. Mullins, O. C.; Sheu, E. Y.; Hammami, A.; Marshall, A. G., *Asphaltenes, heavy oils, and petroleomics*. Springer Science & Business Media: 2007.
7. Mullins, O. C.; Betancourt, S. S.; Cribbs, M. E.; Dubost, F. X.; Creek, J. L.; Andrews, A. B.; Venkataramanan, L., The colloidal structure of crude oil and the structure of oil reservoirs. *Energy & Fuels* **2007,** 21, (5), 2785-2794.
8. Yudin, I. K.; Anisimov, M. A., Dynamic light scattering monitoring of asphaltene aggregation in crude oils and hydrocarbon solutions. In *Asphaltenes, Heavy Oils, and Petroleomics*, Springer: 2007; pp 439-468.
9. Chuan, W.; Guang-Lun, L.; YAO, C.-j.; SUN, K.-j.; Gai, P.-y.; CAO, Y.-b., Mechanism for reducing the viscosity of extra-heavy oil by aquathermolysis with an amphiphilic catalyst. *Journal of Fuel Chemistry and Technology* **2010,** 38, (6), 684-690.
10. Farah, M. A.; Oliveira, R. C.; Caldas, J. N.; Rajagopal, K., Viscosity of water-in-oil emulsions: Variation with temperature and water volume fraction. *Journal of Petroleum Science and Engineering* **2005,** 48, (3), 169-184.
11. Langevin, D.; Argillier, J.-F., Interfacial behavior of asphaltenes. *Advances in colloid and interface science* **2015**.
12. Maia Filho, D. C.; Ramalho, J. B.; Spinelli, L. S.; Lucas, E. F., Aging of water-in-crude oil emulsions: Effect on water content, droplet size distribution, dynamic viscosity and stability. *Colloids and Surfaces A: Physicochemical and Engineering Aspects* **2012,** 396, 208-212.
13. Joseph, D. D.; Bai, R.; Chen, K.; Renardy, Y. Y., Core-annular flows. *Annual Review of Fluid Mechanics* **1997,** 29, (1), 65-90.
14. Joseph, D. D.; Bai, R.; Mata, C.; Sury, K.; Grant, C., Self-lubricated transport of bitumen froth. *Journal of fluid mechanics* **1999,** 386, 127-148.
15. Saniere, A.; Hénaut, I.; Argillier, J., Pipeline transportation of heavy oils, a strategic, economic and technological challenge. *Oil & Gas Science and Technology* **2004,** 59, (5), 455-466.
16. Wylde, J.; Leinweber, D.; Low, D.; Botthof, G.; Oliveira, A.; Royle, C.; Kayser, C. In *Heavy oil transportation: advances in water-continuous emulsion methods*, Proceedings of the world heavy oil congress, Aberdeen, 2012; 2012.
17. Khelifa, T.; Maini, B. B. In *Evaluation of CO2 based Vapex process for the recovery of bitumen from tar sand reservoirs*, SPE international improved oil recovery conference in Asia Pacific, 2003; Society of Petroleum Engineers: 2003.
18. Schucker, R. C., Heavy oil upgrading process. In Google Patents: 2003.
19. Upreti, S.; Lohi, A.; Kapadia, R.; El-Haj, R., Vapor extraction of heavy oil and bitumen: A review. *Energy & Fuels* **2007,** 21, (3), 1562-1574.
20. Das, S. K.; Butler, R. M., Mechanism of the vapor extraction process for heavy oil and bitumen. *Journal of Petroleum Science and Engineering* **1998,** 21, (1), 43-59.

21. Mokrys, I.; Butler, R. In *In-situ upgrading of heavy oils and bitumen by propane deasphalting: the VAPEX process*, SPE Production Operations Symposium, 1993; Society of Petroleum Engineers: 1993.
22. Zosel, K., Separation with supercritical gases: practical applications. *Angewandte Chemie International Edition in English* **1978,** 17, (10), 702-709.
23. Al-Sahhaf, T. A.; Fahim, M. A.; Elkilani, A. S., Retardation of asphaltene precipitation by addition of toluene, resins, deasphalted oil and surfactants. *Fluid phase equilibria* **2002,** 194, 1045-1057.
24. Schucker, R., Heavy oil feed is thermally cracked using visbreaking or hydrovisbreaking technology to produce product that is lower in molecular weight and boiling point than feed, product is deasphalted using alkane solvent and two stage membrane system. In Google Patents: 2002.
25. Clark, P.; Hyne, J., Studies on the chemical reactions of heavy oils under steam stimulation condition. *Aostra J Res* **1990,** 29, (6), 29-39.
26. Clark, P. D.; Clarke, R. A.; Hyne, J. B.; Lesage, K. L., Studies on the effect of metal species on oil sands undergoing steam treatments. *Aostra J Res* **1990,** 6, (1), 53-64.
27. Hassanzadeh, H.; Galarraga, C.; Abedi, J.; Scott, C.; Chen, Z.; Pereira-Almao, P. In *Modelling of bitumen ultradispersed catalytic upgrading experiments in a batch reactor*, Canadian International Petroleum Conference, 2009; Petroleum Society of Canada: 2009.
28. Hongfu, F.; Yongjian, L.; Liying, Z.; Xiaofei, Z., The study on composition changes of heavy oils during steam stimulation processes. *Fuel* **2002,** 81, (13), 1733-1738.
29. Loria, H.; Trujillo-Ferrer, G.; Sosa-Stull, C.; Pereira-Almao, P., Kinetic modeling of bitumen hydroprocessing at in-reservoir conditions employing ultradispersed catalysts. *Energy & Fuels* **2011,** 25, (4), 1364-1372.
30. Greaves, M.; Xia, T. In *CAPRI-Downhole Catalytic Process for Upgrading Heavy Oil: Produced Oil Properties and Composition*, Canadian International Petroleum Conference, 2001; Petroleum Society of Canada: 2001.
31. Xia, T.; Greaves, M. In *3-D physical model studies of downhole catalytic upgrading of Wolf Lake heavy oil using THAI*, Canadian International Petroleum Conference, 2001; Petroleum Society of Canada: 2001.
32. Chen, Y.; Wang, Y.; Lu, J.; Wu, C., The viscosity reduction of nano-keggin-K 3 PMo 12 O 40 in catalytic aquathermolysis of heavy oil. *Fuel* **2009,** 88, (8), 1426-1434.
33. Hashemi, R.; Nassar, N. N.; Pereira Almao, P., Enhanced heavy oil recovery by in situ prepared ultradispersed multimetallic nanoparticles: A study of hot fluid flooding for Athabasca bitumen recovery. *Energy & Fuels* **2013,** 27, (4), 2194-2201.
34. Yi, Y.; Li, S.; Ding, F.; Yu, H., Change of asphaltene and resin properties after catalytic aquathermolysis. *Petroleum Science* **2009,** 6, (2), 194-200.
35. Adam, J.; Antonakou, E.; Lappas, A.; Stöcker, M.; Nilsen, M. H.; Bouzga, A.; Hustad, J. E.; Øye, G., In situ catalytic upgrading of biomass derived fast pyrolysis vapours in a fixed bed reactor using mesoporous materials. *Microporous and Mesoporous Materials* **2006,** 96, (1), 93-101.
36. Graue, D. J., Upgrading and recovery of heavy crude oils and natural bitumens by in situ hydrovisbreaking. In Google Patents: 2001.
37. Patel, M. A.; Baldanza, M.; da Silva, V. T.; Bridgwater, A., In situ catalytic upgrading of bio-oil using supported molybdenum carbide. *Applied catalysis A: general* **2013,** 458, 48-54.
38. Al-Maamari, R. S.; Buckley, J. S., Asphaltene precipitation and alteration of wetting: the potential for wettability changes during oil production. *SPE Reservoir Evaluation & Engineering* **2003,** 6, (04), 210-214.
39. Gharfeh, S.; Yen, A.; Asomaning, S.; Blumer, D., Asphaltene flocculation onset determinations for heavy crude oil and its implications. *Petroleum science and technology* **2004,** 22, (7-8), 1055-1072.
40. Oskui, G.; Reza, P.; Jumaa, M. A.; Folad, E. G.; Rashed, A.; Patil, S. In *Systematic Approach for Prevention and Remediation of Asphaltene Problems During CO2/Hydrocarbon Injection*

Project, The Twenty-first International Offshore and Polar Engineering Conference, 2011; International Society of Offshore and Polar Engineers: 2011.
41. Urquhart, R., Heavy oil transportation-present and future. *Journal of Canadian Petroleum Technology* **1986,** 25, (02).
42. Hart, A., A review of technologies for transporting heavy crude oil and bitumen via pipelines. *Journal of Petroleum Exploration and Production Technology* **2014,** 4, (3), 327-336.
43. Heim, W.; Wolf, F. J.; Savery, W. T., Heavy oil recovering. In Google Patents: 1984.
44. McMillen, J. M., Enhanced oil recovery; producing a solvent-crude mixture. In Google Patents: 1985.
45. Gateau, P.; Hénaut, I.; Barré, L.; Argillier, J., Heavy oil dilution. *Oil & gas science and technology* **2004,** 59, (5), 503-509.
46. Alvarez, G.; Poteau, S.; Argillier, J.-F.; Langevin, D.; Salager, J.-L., Heavy oil− water interfacial properties and emulsion stability: Influence of dilution. *Energy & Fuels* **2008,** 23, (1), 294-299.
47. Argillier, J.; Barre, L.; Brucy, F.; Dournaux, J.; Henaut, I.; Bouchard, R. In *Influence of asphaltenes content and dilution on heavy oil rheology*, SPE International Thermal Operations and Heavy Oil Symposium, 2001; Society of Petroleum Engineers: 2001.
48. Martínez-Palou, R.; de Lourdes Mosqueira, M.; Zapata-Rendón, B.; Mar-Juárez, E.; Bernal-Huicochea, C.; de la Cruz Clavel-López, J.; Aburto, J., Transportation of heavy and extra-heavy crude oil by pipeline: A review. *Journal of Petroleum Science and Engineering* **2011,** 75, (3), 274-282.
49. Hasan, S. W.; Ghannam, M. T.; Esmail, N., Heavy crude oil viscosity reduction and rheology for pipeline transportation. *Fuel* **2010,** 89, (5), 1095-1100.
50. Pierre, C.; Barré, L.; Pina, A.; Moan, M., Composition and heavy oil rheology. *Oil & Gas Science and Technology* **2004,** 59, (5), 489-501.
51. Mortazavi-Manesh, S.; Shaw, J. M., Thixotropic rheological behavior of Maya crude oil. *Energy & Fuels* **2014,** 28, (2), 972-979.
52. McCants, M. T., Method for production of hydrocarbon diluent from heavy crude oil. In Google Patents: 1992.
53. Tipman, R. N.; Sankey, B. M., Process for separation of hydrocarbon from tar sands froth. In Google Patents: 1993.
54. Amanullah, M.; Al-Tahini, A. M. In *Nano-technology-its significance in smart fluid development for oil and gas field application*, SPE Saudi Arabia Section Technical Symposium, 2009; Society of Petroleum Engineers: 2009.
55. Franco, C.; Patiño, E.; Benjumea, P.; Ruiz, M. A.; Cortés, F. B., Kinetic and thermodynamic equilibrium of asphaltenes sorption onto nanoparticles of nickel oxide supported on nanoparticulated alumina. *Fuel* **2013,** 105, 408-414.
56. Franco, C. A.; Nassar, N. N.; Ruiz, M. A.; Pereira-Almao, P.; Cortés, F. B., Nanoparticles for inhibition of asphaltenes damage: adsorption study and displacement test on porous media. *Energy & Fuels* **2013,** 27, (6), 2899-2907.
57. Mohammadi, M.; Akbari, M.; Fakhroueian, Z.; Bahramian, A.; Azin, R.; Arya, S., Inhibition of asphaltene precipitation by TiO2, SiO2, and ZrO2 nanofluids. *Energy & Fuels* **2011,** 25, (7), 3150-3156.
58. Franco, C. A.; Montoya, T.; Nassar, N. N.; Pereira-Almao, P.; Cortés, F. B., Adsorption and subsequent oxidation of colombian asphaltenes onto Nickel and/or Palladium oxide supported on fumed silica nanoparticles. *Energy & Fuels* **2013,** 27, (12), 7336-7347.
59. Nassar, N. N.; Betancur, S.; Acevedo, S.; Franco, C. A.; Cortés, F. B., Development of a Population Balance Model to Describe the Influence of Shear and Nanoparticles on the Aggregation and Fragmentation of Asphaltene Aggregates. *Industrial & Engineering Chemistry Research* **2015,** 54, (33), 8201-8211.

60. Franco, C. A.; Martínez, M.; Benjumea, P.; Patiño, E.; Cortés, F. B., Water remediation based on oil adsorption using nanosilicates functionalized with a petroleum vacuum residue. *Adsorption Science & Technology* **2014,** 32, (2-3), 197-207.
61. Nassar, N. N.; Hassan, A.; Pereira-Almao, P., Effect of the particle size on asphaltene adsorption and catalytic oxidation onto alumina particles. *Energy & Fuels* **2011,** 25, (9), 3961-3965.
62. Zabala. R, F. C. A., Cortes. F.B., Application of Nanofluids for Improving Oil Mobility in Heavy Oil and Extra-Heavy Oil: A Field Test. *Society of Petroleum Engineers Journal* **2016**, 14.
63. Haddad, Z.; Abid, C.; Oztop, H. F.; Mataoui, A., A review on how the researchers prepare their nanofluids. *International Journal of Thermal Sciences* **2014,** 76, 168-189.
64. Sidik, N. A. C.; Mohammed, H.; Alawi, O. A.; Samion, S., A review on preparation methods and challenges of nanofluids. *International Communications in Heat and Mass Transfer* **2014,** 54, 115-125.
65. Nik, W. W.; Ani, F.; Masjuki, H.; Giap, S. E., Rheology of bio-edible oils according to several rheological models and its potential as hydraulic fluid. *Industrial Crops and Products* **2005,** 22, (3), 249-255.
66. Sarpkaya, T., Flow of non-Newtonian fluids in a magnetic field. *AIChE Journal* **1961,** 7, (2), 324-328.
67. Shao, S.; Lo, E. Y., Incompressible SPH method for simulating Newtonian and non-Newtonian flows with a free surface. *Advances in water resources* **2003,** 26, (7), 787-800.
68. Luo, P.; Gu, Y., Effects of asphaltene content on the heavy oil viscosity at different temperatures. *Fuel* **2007,** 86, (7), 1069-1078.
69. Zirrahi, M.; Hassanzadeh, H.; Abedi, J., Modelling of Bitumen-and-Solvent-Mixture Viscosity Data Using Thermodynamic Perturbation Theory. *Journal of Canadian Petroleum Technology* **2014,** 53, (01), 48-54.
70. Buckley, S. E.; Leverett, M., Mechanism of fluid displacement in sands. *Transactions of the AIME* **1942,** 146, (01), 107-116.
71. Johnson, E.; Bossler, D.; Bossler, V., Calculation of relative permeability from displacement experiments. **1959**.
72. Giraldo, J.; Benjumea, P.; Lopera, S.; Cortés, F. B.; Ruiz, M. A., Wettability alteration of sandstone cores by alumina-based nanofluids. *Energy & Fuels* **2013,** 27, (7), 3659-3665.
73. Craig, F. F., *The reservoir engineering aspects of waterflooding*. Society of Petroleum Engineers: 1971; Vol. 3.
74. Anderson, W. G., Wettability literature survey part 5: the effects of wettability on relative permeability. *Journal of Petroleum Technology* **1987,** 39, (11), 1,453-1,468.

6. Conclusions and Recommendations

6.1 Conclusions

This study provides an important insight about nano-sized particles that can reduce the viscosity of heavy and extra heavy crude oil and the impact on mobility on porous media at reservoir conditions, and also at surface conditions. Several materials were characterized by particle size and surface area. Commercial Silica, Alumina and Magnetite nanoparticles were purchased and also characterized by particle size and surface area, the nanoparticles resulted in mean particle diameters in the nanoscale. The trend followed by the surface area of the nanoparticles was S8 > S8A > S11 > S8B > Al35 > F97 > S97 > S285. Adsorption isotherms were constructed by extracting asphaltenes from two different sources (Ho and EHO), which were dissolved in toluene to obtain the solution models. All nanoparticles have the ability to adsorb asphaltenes, from highest to lowest the trend was: S8A > S8 > S11 > S8B > S97 > Al35 > S285 > F97, this is mainly due to the interaction between polar groups of the asphaltene and the silanol group of the silica nanoparticles. The addition of nanoparticles of different chemical natures to heavy and extra heavy oil produces a viscosity reduction at low particle concentration contrary to expectations based on the behavior described through Einstein's theory on hydrodynamic viscosity. Subsequently, the first mathematical approach to calculating the viscosity as a function of the concentration of nanoparticles is presented, expressed as a function of volume fraction based on a modification to the model Pal and Rhodes for suspensions viscosity. The model fits the experimental data well, for volume fractions between 0 and 3.7×10^{-4}. The solvation constant K and the form factor V follow a trend as a function of the shear rates evaluated and are consistent with the oil shear-thinning behavior. The effect of SiO_2 nanoparticles with mean particle size of 8 nm on the rheological properties of heavy oil was studied through viscosimetry test at steady state as well as dynamic oscillometry. Heavy oil viscosity reduces as shear rate increases following a shear thinning non-Newtonian behavior. The addition of nanoparticles at a concentration of 1000 mg/L reduces the viscosity of heavy oil 12 to 45%, for shear rates between 0 - 100 s^{-1} and temperatures of 288, 298 and 313 K. It was viscoelastic

moduli values indicate that samples fluid flow is governed dominated by viscous dissipation at all strain and frequencies evaluated. This leads to the conclusion that asphaltenes overlap acts like a transient network of fractal aggregates. The shear thinning behavior is so-attributed to the arrangement of overlapped asphaltenes under shear. However, at 313 K and higher frequencies (> 30 rad/s), the value of the storage modulus exceeds the value of the loss modulus, which considerably decreases, just as the phase angle decreases to a value of approximately 38°. Therefore, we can say that under conditions of temperature and these frequency values, the heavy oil in the absence of nanoparticles behaves more like a solid than as a liquid. The effect of fumed silica nanofluids synthesized on the rheological properties of heavy and extra heavy crude was evaluated through rheological tests at steady-state conditions and in dynamic flow tests through a small-scale pipeline, mixing crude oil, nanofluid, and naphtha. Using dynamic tests of flow in a pipeline, the pressure differential during the flow of 1000 ml of the mixture was measured. It was found that the blend of extra-heavy crude with 10% nanofluid and 27% naphtha needs the same pressure differential as the blend composed of extra-heavy crude and 63% of naphtha, and for the blend of heavy crude with 10% nanofluid and 13% naphtha needs the same pressure differential as the blend composed of heavy crude and 27% of naphtha. At typical reservoir conditions of pressure and temperature, nanofluids were able to positively affect the crude oil mobility through the reduction of oil viscosity and the alteration of the porous media wettability.

By means of a simplified economic analysis based on a conventional mass balance, savings of roughly 50% can be obtained in comparison with the habitual consumptions, equivalent to more than USD $2.5 million per day. Also, there is a potential for energy savings in the pumping of heavy and extra-heavy crude oils, the required power and capacity of use of the pipeline is lower when using nanofluids, which generates savings close to 37%, generating savings of more than USD $2 million per year, and the possibility of increasing the volumes of production using the same infrastructure. Additionally, a discussion is presented from the environmental point of view, and the advantages of reducing naphtha consumption showed potential environmental benefits through risk mitigation. In this way, the performance of nanofluid is verified as an optimizing agent for the transport conditions of heavy and extra-heavy crude oils, and it opens a promising technique to generate savings in the energy and fuel consumptions of the oil and gas industry. The goal of this research has been achieved by demonstrating that nanotechnology exhibits a great and rich potential as an optimizer of heavy oil transport properties. It is expected that this study will open a better landscape abouonthe use of nanofluids in IOR and EOR processes for enhancing the production of heavy and extra heavy oils.

6.2 Recommendations

According to the results obtained, the following recommendations are proposed:

- To explore different materials, and different combination with fluids.
- To evaluate different types of heavy crude not only Colombian, but of different origins worldwide
- To determine the effect of resins on the rheology of heavy crude oil, and how it affects the presence of nanoparticles / nanofluids, said effect
- To determine which is the most important property of the asphaltenes in the interaction with nanoparticles able to reduce the viscosity.
- Carry out a more detailed study evaluating many more concentrations of nanoparticles, thus allowing an optimum concentration in which the performance of the nanoparticles generates the greatest reduction of viscosity possible.
- Carry out an analysis of the durability of the proposed treatments by applying nanofluids to the heavy crude
- To determine the effect of nanotechnology on the rheology of W / O emulsions, since many heavy crude deposits tend to form emulsions
- Conduct a traceability study of the nanoparticles to determine the effects they have on subsequent refinery and final disposal processes.

7. Publications and awards

As scientific contribution of this Ph.D. Thesis, the following documents have been published:

7.1 Scientific papers

- **Published**

- **Taborda E.,** Franco C.A., Ruiz M.A., Alvarado V., and Cortés F.B. *Experimental and Theoretical Study of Viscosity Reduction in Heavy Crude Oils by Addition of Nanoparticles.* Energy & Fuels. 2017

- **Taborda E.,** Franco C.A., Ruiz M.A., Alvarado V., and Cortés F.B. *Anomalous Heavy-oil Rheological Thinning Behavior upon Addition of Nanoparticles: Departure from Einstein's Theory.* Chemical Engineering Communications. 2017

- **Taborda E.,** Alvarado V., Franco C.A., and Cortés F.B. *Rheological demonstration of alteration in the heavy crude oil fluid structure upon addition of nanoparticles*. Fuel 189. 322-333. 2017.

- **Taborda E.,** Franco C.A., Lopera S., Alvarado V., and Cortés F.B. *Effect of Nanoparticles/Nanofluids on the Rheology of Heavy Crude Oil and Its Mobility on Porous Media at Reservoir Conditions.* Fuel 184. 222-232. 2016.

- **Taborda E.,** Montoya L.T., Zabala R.D., Osorio R., Ospina N, and Cortés F.B. *Optimización del trasporte de crudo pesado y extrapesado mediante la adición de*

nanofluidos. XVI Congreso Colombiano Petróleo y Gas 2015. ACIPET. Bogotá Colombia, 2105.

- **In Review**

- **Taborda E.,** Franco C.A., Ruiz M.A., Alvarado V., and Cortés F.B. *Striking Behavior of the Rheology in Heavy Crude Oils by Adding Nanoparticles*. Adsorption Science and Technology. 2017.

- **Taborda E.,** Alvarado V., and Cortés F.B. *Effect of SiO2-Based Nanofluids in the Reduction of Naphtha Consumption for Heavy and Extra-Heavy Oils Transport: Economic Impacts on the Colombian Market***.** Energy Conversion and Management, 2017

7.2 Oral Presentations

- *Nanotechnology Effect in Heavy oil Rheology and its Productivity Impact. V Escuela de verano* Retos tecnológicos para la productividad de yacimiento en momentos de crisis. Mayo, 2016. Medellín, Colombia.

- *Optimización del trasporte de crudo pesado y extrapesado mediante la adición de nanofluidos.* XVI Congreso Colombiano Petróleo y Gas 2015. ACIPET. Bogotá Colombia, 2105.

- *Nanotechnology Effect in Heavy oil Rheology and its Productivity Impact.* Encuentro Internacional de Educación en Ingeniería ACOFI. Innovación en las facultades de ingeniería: El cambio para la competitividad y la sostenibilidad. Octubre 4 – 7 de 2016. Cartagena, Colombia.

7.3 Poster Presentations

- *Nanotechnology Effect in Heavy oil Rheology and its Productivity Impact.* Encuentro Internacional de Educación en Ingeniería ACOFI. Innovación en las facultades de ngeniería: El cambio para la competitividad y la sostenibilidad. Octubre 4 – 7 de 2016. Cartagena, Colombia.
- *Nananotechnology effect on the rheology of heavy crude oil and its mobility on porous media at reservoir conditions*. III Workshop on Adsorption, Catalyst and Porous Materials. Univerisdad de los Andes. 29-31 de Agosto de 2016. Botogá, Colombia

7.4 Awards

- **ACIPET price: The Best Work on modality Transport and Refining of Hydrocarbons**. *Optimización del trasporte de crudo pesado y extrapesado mediante la adición de nanofluidos.* XVI Congreso Colombiano Petróleo y Gas 2015. ACIPET. Bogotá Colombia, 2105.

- **III Workshop on adsorption, catalysis and porous materials – The Best Work: Poster Mode**: *Nananotechnology effect on the rheology of heavy crude oil and its mobility on porous media at reservoir conditions.* III Workshop on Adsorption, Catalyst and Porous Materials. Univerisdad de los Andes. 29-31 de Agosto de 2016. Botogá, Colombia